

SIGNIFICANCE OF SIDESCAN SONAR DATA IN MORPHODYNAMICS
INVESTIGATIONS ON SHELF SEAS -
CASE STUDIES ON SUBAQUEOUS DUNES MIGRATION,
REFILLING OF EXTRACTION PITS
AND SORTED BEDFORMS STABILITY



Dissertation
zur Erlangung des Doktorgrades
der Mathematisch-Naturwissenschaftlichen Fakultät
der Christian-Albrechts-Universität
Kiel

vorgelegt von
Adam Kubicki

Kiel 2007

Referent: Professor Dr. Karl Stattegger
Koreferent: Professor Dr. Burghard W. Flemming,
Wilhelmshaven

Tag der mündlichen Prüfung: 13.11.2007
Zum Druck genehmigt: 14.11.2007

gez. J. GROTEMEYER
Dekan

Acknowledgements

This PhD thesis was accomplished within the project STA401/10-1,2 financed by Deutsche Forschungsgemeinschaft – German Science Foundation, which is greatly acknowledged for giving me amazing research opportunities and comfortable environment for living, working and studies.

There are no appropriate words which could describe my gratitude to two great men Prof. Dr. Karl Stattegger and Dr. Klaus Schwarzer, who chose me from thousands, trusted my judgements, let me fulfil my own ideas, gave me the precious research space, who supervised me carefully, but supported immediately when the push was needed. Karl, Klaus, thank you extremely much.

I am deeply thankful to Prof. Dr. Burghard Flemming, who appeared to be the invisible external reviewer of most of the material presented in this thesis. It is actually him, who shaped my research and made my chaotic thoughts understandable.

Many people contributed directly in this research and many more indirectly. I was trying to express my gratitude each time the publication was ready, but many of you deserve repetitive acknowledgements.

Dr. Markus Diesing, thank you for your friendship, never-ending help on shortest notice and calm voice in the moments of panic. Thank you for your input in my projects and for letting me include your fantastic paper in this thesis.

Dr. Tino Manso, thank you for inviting me to EUMARSAND project and for the fruitful cooperation on our paper.

I would like to acknowledge Dr. Friedrich Werner, the guardian and main collector of a huge archive of analogue marine data. Thank you for your hints, suggestions and above all enthusiasm.

I wish to thank also the rest of my Sedimentology family Patrycja, Sabine, Fabiana, Max, Alex, Daniel, you are truly the best. It was a great feeling to work with you all.

My fellow researchers and friends from Corelab, Poznan, Hanoi, Nha Trang, Hamburg and Bremen are warmly thanked for the perfect cooperation and most valuable discussions.

Thank you my Kiel friends, colleagues, teachers. It's amazing how many of you, I had pleasure to meet. I'm glad that I found you on my life path. Thank you for the good times, the overcome bad times and unforgettable experiences.

Summary

A side-looking sonar was constructed for military purposes during World War II as a development of forward-search sonars used for detection of foe submarines hiding motionless on a seabed. An unexpected career of sidescan sonars began with their implementation in marine geology. A sonar ability to recognise sediment roughness and consequently grain size allowed significant opportunities for sediment mapping, which were spatially more precise than the ones performed by sediment sampling. In addition, an acoustic shadow caused by close-seabed scanning over troughs and ridges allowed easier interpretation of the bottom morphology. These revolutionary features opened new ways of underwater exploration. Some multi-disciplinary applications of sonographs on continental shelves are presented in the introduction of this work after a technical description of a sidescan sonar system, and sonograph processing issues.

The main objective of this work is to discuss three case studies on sidescan sonar applications in seabed dynamics research. Each of the study was constructed as a separate research paper qualified for prestigious journals and thus, the introductory part of this work is a descriptive supplement of information enclosed in the presented manuscripts.

A case study from the southern Vietnamese shelf is focused on sand dunes mapping on the basis of not mosaicked sonographs. It was the first investigation on bedforms from this area; however it contains data only from the end of the winter monsoon. The shelf area was divided into five zones grouping dunes of similar size, shape and orientation. All located sand dunes higher than 1.5 m were described, summarized in a scatter plot of height/length ratio and thus compared to dunes observed on other shelves. The dunes orientation corresponded to the overall South China Sea circulation pattern during the winter monsoon. Therefore, the possibility of dunes mobilisation was investigated with the help of empirical equations predicting sediment transport. Depth-integrated velocities necessary to put sediment forming dunes in motion were calculated for distinguished zones. The results were discussed with hydrodynamic *in-situ* measurements of other authors and it was concluded that most of the investigated dunes were likely to migrate actively following the monsoon circulation.

A case study from the Baltic Sea is a rare example of an investigation focused on changes in the morphology of pits created by anchor hopper dredging of marine sand and

gravel aggregates. By means of sidescan sonar and multi-beam echosounder data, a six-year evolution of four pits was presented. In the case of three pits dredged in a sandy seabed faster smoothing of edges and infilling rates larger than in the case of a pit dredged in gravel were clearly observed. The edges of the gravel pit were expanding due to collapsing of the side-walls. The infilling of the pit was investigated based on approximations of pit depth by single- and multi-beam echosoundings, as well as acoustic shade length in the sonographs. Earlier studies of other authors on this pit allowed plotting a curve of infilling rate over six years of pit evolution. The filling clearly slowed down over time and the reasons for that are discussed in this paper. The sand screened in the dredging process surrounded the investigated pit and its backscatter values in sonographs clearly separate it from the gravel seabed. The area covered by the screened sand fraction was monitored and appeared to be decreasing in time. Hydrological data showed the possibility of frequent mobilisation of this fraction and therefore indicated it as the main source for pit infilling.

A case study from the North Sea presents a unique approach of conversion analogue sidescan sonar data into digital, geo-referenced form in order to present morphological stability and birth of sorted bedforms. The analogue mosaic was geo-coded in a DECCA navigation system in 1977. DECCA system technology was described thoroughly and a study of the spatial errors was presented for accurate geo-referencing of the mosaic. Image warping by rubber-sheeting method was performed to compare old sonographs of a sorted bedform with sonographs from 2002. A continuation study of Dr. Markus Diesing et al. additionally contains a multi-beam backscatter mosaic from 2003 as a comparison data-set. The morphological stability of the bedforms over time was discussed in the paper and compared to worldwide examples. Hydrodynamic conditions influencing the bedforms were presented and a significant role of the tidal currents in shaping the sorted bedforms was demonstrated. An asymmetry of a newly appeared sorted bedform, however, was probably related rather to high energy storm events.

Even though the sidescan sonar data were collected from three different seas for three different case studies in three different scales, sonographs proved to be a valuable tool in each of the cases. Minor limitations of sidescan sonar systems and options for applying other devices for the same types of investigations are discussed in the end of this work.

Zusammenfassung

Während des Zweiten Weltkrieges wurde für militärische Zwecke zum Aufspüren feindlicher Unterseeboote, die die sich bewegungslos auf dem Meeresgrund versteckten, ein seitwärts schauendes Sonar als Fortentwicklung des vorwärts schauenden Sonars gebaut. Eine unerwartete Karriere dieses Seitensicht-Sonars begann mit seiner Einführung in der Marinen Geologie. Die Fähigkeit des Sonars, die Sedimenttrauhigkeit und infolgedessen die Korngröße zu erkennen, eröffnete bedeutende Möglichkeiten in der Sedimentkartierung mit einer räumlich besseren Auflösung als sie durch Probennahmen zu erreichen ist. Zusätzlich erlaubt ein akustischer Schatten, der durch bodennahes Überfahren von Vertiefungen und Erhebungen verursacht wird, eine einfachere Interpretation der Morphologie des Meeresgrundes. Diese revolutionären Eigenschaften öffneten neue Wege der Unterwasserforschung. Einige multidisziplinäre Anwendungen von Sonographen auf Kontinentalsöckeln werden in der Einleitung zu dieser Arbeit neben technischen Besonderheiten des Seitensicht-Sonar-Systems und Implikationen bei der Verarbeitung von Sonographie-Daten beschrieben.

Die Hauptzielsetzung dieser Arbeit ist es, drei Fallstudien der Anwendung eines Seitensicht-Sonars in Meeresgrunddynamikstudien darzustellen. Jede der Studien wurde für anerkannte Journale verfasst oder angenommen, der einleitende Teil dieser Arbeit ist eine beschreibende Ergänzung der Informationen in den vorgestellten Veröffentlichungen.

Eine Fallstudie am Südvietnamesischen Kontinentalsöckel ist auf die Kartierung der Sanddünen auf der Basis nicht zusammengesetzter Sonographie-Daten ausgerichtet. Es ist die erste Untersuchung von Bodenformen in diesem Gebiet, enthält jedoch nur Daten vom Ende des Wintermonsuns. Der Schelfbereich wurde in fünf Zonen eingeteilt, um Dünen ähnlicher Größe, Form und Orientierung zu gruppieren. Alle lokalisierten Sanddünen mit einer Höhe größer als 1.5 m wurden beschrieben und in ihrem höhen/längen Verhältnis in einem Scatterplot dargestellt, und auf diese Weise mit Dünen auf anderen Schelfen verglichen. Die Düneorientierung entspricht dem allgemeinen Zirkulationsschema der Südchinesischen See während des Wintermonsuns. Die Möglichkeit der Dünenmobilisierung wurde mit Hilfe empirischer Sedimenttransportgleichungen untersucht. Tiefengemittelte Strömungsgeschwindigkeiten, notwendig um Sedimente zur Bildung von Dünen in Bewegung zu setzen

wurden berechnet. Die errechneten Ergebnisse wurden mit hydrodynamischen In-Situ Messungen anderer Autoren verglichen und es wurde gefolgert, dass die meisten untersuchten Dünen aktiv entsprechend der Monsunzirkulation wandern.

Eine Fallstudie in der Ostsee ist ein seltenes Beispiel einer Untersuchung von Änderungen in der Morphologie von Gruben, die durch Nassbaggern von Marinen Sanden und Kiesen entstandenen sind. Mittels Seitensicht-Sonar und Fächerecholot-Daten wurde die Entwicklung von vier Gruben über sechs Jahre dargestellt. Im Falle dreier Gruben in sandigem Untergrund konnte eine deutlich höhere Abrundungsrate der Kanten und Sedimentation in den Gruben beobachtet werden als dies bei der Grube im Kiesbett der Fall war. Die Ränder der Grube im Kies änderten sich durch Abrutschen der Seitenwände. Sedimentation in den Gruben wurde basierend auf Näherungswerten der Grubentiefe durch Single-Beam-Echolot und Fächerecholot-Messungen, sowie akustische Schattenlänge in den Sonographie-Daten untersucht. Frühere Studien anderer Autoren an diesen Gruben ermöglichten es, die Sedimentationsrate über sechs Jahre darzustellen. Die Sedimentationsrate verlangsamte sich mit der Zeit deutlich, die Gründe hierfür werden in diesem Paper dargestellt. Der Sand, der während des Nassbaggerns ausgesiebt wurde, konnte im Umkreis der untersuchten Grube nachgewiesen werden, das Echo in den Sonographie-Daten war deutlich von dem des kiesigen Meeresgrundes zu unterscheiden. Der Bereich, der durch die ausgesiebte Sandfraktion bedeckt wurde, wurde beobachtet und verringerte sich mit der Zeit. Hydrologische Daten zeigen die Möglichkeit einer häufigen Mobilisierung dieser Sandfraktion, wodurch diese als hauptsächliche verantwortliche Quelle für die Sedimentation in den Gruben ausgemacht werden kann.

Eine Fallstudie in der Nordsee stellt einen einmaligen Ansatz der Umwandlung von analogen Seitensicht-Sonar-Daten in digitale, georeferenzierte Form dar, um die morphologische Stabilität und die Entstehung von sortierten Bodenformen darzustellen. Das analoge Mosaik wurde 1977 im DECCA Navigationssystem geo-kodiert. Die DECCA System Technologie wurde gänzlich beschrieben und für die genaue Georeferenzierung des Mosaiks wurde eine Studie der räumlichen Fehler präsentiert. Eine Anpassung des Bildes wurde per "rubber – sheeting" Methode durchgeführt um historische Sonographie-Daten sortierter Bodenformen mit neuen Sonographie-Daten von 2002 zu vergleichen. Eine nachfolgende Studie von Dr. Markus Diesing *et al.* enthält zusätzlich ein "multi-beam backscattering"

Mosaik von 2003 als vergleichendes Material. Die morphologische Stabilität der Bodenformen über die Zeit wird in dem Paper besprochen und mit weltweiten Beispielen verglichen. Die hydrodynamischen Umgebungsbedingungen der Bodenformen wurden dargestellt und eine bedeutende Rolle der Gezeiten-Strömungen auf diese festgestellt. Eine Asymmetrie neu entstandener sortierter Bodenformen hing vermutlich mit Sturmereignissen hoher Energie zusammen.

Obwohl die Seitensicht-Sonar-Daten in drei unterschiedlichen Meeren für drei unterschiedliche Untersuchungen und in drei unterschiedlichen Maßstäben gesammelt wurden, waren die Sonographie-Daten in jedem der Fälle ein wertvolles Hilfsmittel. Die kleineren Beschränkungen von Seitensicht-Sonar-Systemen und die Möglichkeit der Anwendung anderer Systemen für die gleichen Studien werden im Ende dieser Arbeit diskutiert.

Contents

Summary	i
Zusammenfassung	iii
Contents	vi
List of figures	ix
List of tables	xii
I GENERAL INTRODUCTION	1
<i>I.1 Sidescan sonar system description</i>	<i>1</i>
<i>I.2 Sonographs processing</i>	<i>3</i>
I.2.1 Geometric correction	3
I.2.2 Acoustic correction	5
I.2.3 Mapping and image classification.....	6
<i>I.3. Sidescan sonar technology modifications</i>	<i>6</i>
<i>I.4 Basic applications of sonographs</i>	<i>7</i>
I.4.1 Bedforms and sediment mapping.....	7
I.4.2 Benthic habitat mapping	9
I.4.3 Target recognition applications.....	9
<i>I.5. Applications of sonographs in morphodynamics</i>	<i>10</i>
I.5.1 Sand bodies migration.....	10
I.5.2 Post-dredging seabed recovery	12
I.5.3 Rippled scour depressions, sorted bed forms appearance	13
II CASE STUDY ON SAND DUNES - INDICATORS FOR MIGRATION OF LARGE TO VERY LARGE SUBAQUEOUS DUNES INDUCED BY WINTER MONSOON CIRCULATION ON SOUTHERN VIETNAMESE SHELF, SOUTH CHINA SEA	16
<i>II.1 Abstract</i>	<i>16</i>
<i>II.2 Introduction</i>	<i>16</i>
<i>II.3 Setting</i>	<i>18</i>
<i>II.4 Materials and Methods</i>	<i>20</i>
<i>II.5 Results</i>	<i>23</i>
II.5.1 Surficial sediments	23
II.5.2 Dunes parameters	24
<i>II.6 Discussion</i>	<i>26</i>
II.6.1 Dunes parameters	26
II.6.2 Dunes migration	27
<i>II.7 Conclusions</i>	<i>29</i>
III CASE STUDY ON EXTRACTION PITS - MORPHOLOGICAL EVOLUTION OF GRAVEL AND SAND EXTRACTION PITS, TROMPER WIEK, BALTIC SEA	31
<i>III.1. Abstract</i>	<i>31</i>
<i>III.2. Introduction</i>	<i>31</i>

<i>III.3. Setting</i>	33
<i>III.4. Materials and methods</i>	35
III.4.1 Sidescan sonar	36
III.4.2 Multibeam	38
III.4.3 Grab samples	39
<i>III.5 Results</i>	39
III.5.1 Gravel extraction site	39
III.5.2 Sand extraction site	43
<i>III.6 Discussion</i>	44
III.6.1 Refilling of the gravel pit	44
III.6.2 Refilling of the sand pits	47
III.6.3 Efficiency of monitoring	47
<i>III.7 Conclusions</i>	48
IV CASE STUDY ON SORTED BEDFORMS	51
IV.1 CAN OLD ANALOGUE SIDESCAN SONAR DATA STILL BE USEFUL? AN EXAMPLE OF A SONOGRAPH MOSAIC GEO-CODED BY THE DECCA NAVIGATION SYSTEM	51
<i>IV.1.1 Abstract</i>	51
<i>IV.1.2 Introduction</i>	52
<i>IV.1.3 Study area</i>	52
<i>IV.1.4 Methods</i>	53
IV.1.4.1 Analogue profile description.....	53
IV.1.4.2 The DECCA Navigation System	54
IV.1.4.3 Analogue data processing	56
IV.1.4.4 Geo-referencing procedure.....	57
<i>IV.1.5 Results</i>	59
<i>IV.1.6 Discussion</i>	61
<i>IV.1.7 Conclusions</i>	64
IV.2 DECADAL SCALE STABILITY OF SORTED BEDFORMS, GERMAN BIGHT, SOUTH-EASTERN NORTH SEA	67
<i>IV.2.1 Abstract</i>	67
<i>IV.2.2 Introduction</i>	67
<i>IV.2.3 Setting</i>	70
<i>IV.2.4 Methods</i>	71
IV.2.4.1 Recent surveys	72
IV.2.4.2 Archived data from past surveys	73
IV.2.4.3 Grain-size analysis	74
IV.2.4.4 Shear stress calculations.....	75
<i>IV.2.5 Results</i>	77
IV.2.5.1 Surficial geology	77
IV.2.5.2 Re-mobilisation of surficial sediments.....	81
IV.2.5.3 Temporal variability of sediment distribution patterns	82
<i>IV.2.6 Discussion</i>	85
<i>IV.2.7 Conclusions</i>	88

V GENERAL DISCUSSION AND CONCLUSIONS90

VI LITERATURE CITED93

ABOUT THE AUTHOR107

List of figures

Figure I.1. Sidescan sonar functioning scheme (modified after Newton et al, 1973). A piece of seabed is presented together with its backscatter representation and sonograph examples of: S- sandwaves in both channels; F1 and F2 – fish in water column (source: www.marinesonic.com); P-pit in right channel; B-boulders in left channel.....	2
Figure I.2. Method for computing objects height based on towfish altitude, lengths of an acoustic shadow and range to the end of the shadow. Sonograph example of a sunken ship recorded in left channel (source: www.engin.umich.edu).....	2
Figure I.3. Example of a ship-wreck recorded simultaneously in 100 and 500 kHz. (source: www.l-3klein.com). ...	3
Figure I.4. Example of manual water column removal. Note an imperfect effect in the right-hand side of the figure due to a trough in bottom morphology (WERNER AND NEWTON, 1975).	4
Figure I.5. Sonograph representation of a sorted bedform off a coast of North Carolina, USA, and two geological cross-section (modified after MURRAY AND THIELER, 2004).	14
Figure II.1. Location, bathymetry and available data in the study area. Bold lines represent sidescan sonar transects interpreted in this paper. Circles refer to sediment stations from this study and other authors. Numbers 1 to 5 mark distinguished zones and characteristic dunes examples (see Fig.II.4). The bar-graphs show grain size distributions in grab samples. Note that only sediment samples from locations shown in Fig.II.4 are presented. In addition, areas with larger weight of silt and clay ($\text{PHI} > 4$) are outlined.	17
Figure II.2. Results of the HAMSOM (Hamburg Shelf Ocean Model) model showing flow directions and velocities, integrated over depth and time at locations A-D, Fig.II.3. (courtesy of Hartmut Hein, University of Hamburg). The vectors are geographically aligned and the time frame of the VG-5 measuring campaign is marked. Note the difference in flow direction during the summer and winter monsoon seasons.	19
Figure II.3. Orientation of single dunes, or averaged for dune fields. HAMSOM model nodes (A-D) and in-situ current measurements stations (a-f) are marked with points. Winter and summer water circulation patterns of SCS are presented for overview (Fang and Fang, 1998).	21
Figure II.4. Plot of the dune height (H) vs. dune length (L) observed in the study area. Dunes are grouped into identified five spatial zones. Mean as well as maximum parameters of subaqueous bedforms (FLEMMING, 1988) are plotted for comparison. Note smaller heights and flatter profiles of dunes on southern Vietnamese shelf comparing to world data.	22
Figure II.5. Example of determining dune parameters based on sonograph and cross section of profile 22040501 in Zone '2'.....	23
Figure II.6. a) Scatter diagram of dune height (H) against dune length (L) observed in the study area. Dunes are grouped into identified five spatial zones. Average as well as maximum parameters of subaqueous bedforms are plotted after Flemming (1988) for comparison. Note smaller heights and flatter profiles of dunes on southern Vietnamese shelf comparing to world data; b) diagram of lee slope angle against stoss slope angle determined for investigated dunes. Average asymmetry ratios may be found in the text.	25
Figure III.1. Location of Tromper Wiek Bay and the pits selected for the study in a) the gravel extraction area (sonograph from December 2003) and b) the sand extraction area (sonograph from December 2000). The histograms show the percentage of different sediment fractions in grab samples. Sonographs are geographically aligned.	33
Figure III.2. Significant wave heights and wind speeds from the 0-90° quadrant in Tromper Wiek. Sediment mobilisation lines are drawn according to KLEIN (2003). The measurement campaigns are marked with vertical bold lines.	34

Figure III.3. Series of sidescan sonar images from a) the gravel extraction area and b) the sand extraction area. Each figure is presented together with an interpretation of the sonographs and it is geographically aligned.....	37
Figure III.4. Spatial comparison of the gravel pit size reconstructed on the basis of individual sonographs.....	41
Figure III.5. Comparison of two sets of multibeam measurements. a) Plan-view and b) cross-sections from the gravel-extraction site. c) Plan-view and d) cross-sections from the sand-extraction site.....	42
Figure III.6. Summary of the mean refilling rates estimated for the gravel pit (position 54.6292°N; 13.42041°E). The mean refilling rate appears to be slowing down with time.....	45
Figure IV.1. Sidescan sonar mosaic showing the area of interest. Coarse sediment strips (dark) occur together with fine sand areas (light). The mosaic was obtained from data collected in 2002. Contour lines represent water depth.....	53
Figure IV.2. Dependence of the positioning error of the 'red' DECCA beacon on distance from the transmitting station and the time of the measurements (ANON, 1976). The most accurate measurements are obtained during summer days, the least accurate ones during winter nights.....	55
Figure IV.3. Geo-referencing procedure scheme: (a) GCPs selection 1- ship's path, 2-edge of the range, 3-first bottom reflection; (b) result of geo-referencing by the Rubber Sheeting method. Length of x and y correspond to 100 m in each case.....	58
Figure IV.4. Slant-range correction. (a) Channels before correction; (b) proper correction; (c) simplified stretching.....	59
Figure IV.5. Comparison of sediment patterns on selected profile sections from 1977 and 2002. Contour lines represent water depth.....	60
Figure IV.6. Results of a search for high contrast borders between sediment types in 1977 and 2002 images. An impression of the change in grayscale is a result of different qualities of the images processed by the same tool. In 1977 greater detail caused by roll and pitch artefacts was recorded in the 'northern' A type sediment, whereas in 2002 this influence was more prominent in the 'southern' B type sediment (see original sonographs examples).....	61
Figure IV.7. Ten analogue sidescan sonar profiles from 1977 were processed in this study. The resultant mosaic contains some blank areas indicating a lack of data, but the overall sediment pattern is clearly visible.....	62
Figure IV.8. Positioning errors with and without layback application during eastward and westward measurements. Grid lines are given in metres and the axes are geographically aligned.....	63
Figure IV.9. Overview of parts of the German Bight west of the North Frisian Islands. Location of the research area and wave gauge NSB II is indicated.....	70
Figure IV.10. Geo-referencing procedure scheme: (a) Selection of ground control points: 1—sidescan sonar path, 2—edge of the range, 3—first bottom reflection and (b) result of geo-referencing with rubber sheeting method. Length of x and y is 100 m.....	73
Figure IV.11. Water-level amplitudes of station Helgoland in the German Bight. Shown are results for the eight main tidal components as analysed from gauge records and numerical model simulations.....	77
Figure IV.12. Overview of the research area showing relationships between surficial sediments indicated by sidescan sonar backscatter strength and bathymetry. View is from southwest. Vertical exaggeration: 75-fold.....	78
Figure IV.13. Sediment types within the research area. Interpretation is based on sidescan sonar backscatter strength and ground-truth sediment grab sample data. Positions of grab sampling stations are indicated.....	79
Figure IV.14. Representative grain-size distributions for fine sand (UR-04), coarse sediment (UR-34) and transitional sediment (UR-09).....	80

Figure IV.15. Current- and wave-induced shear stresses in relation to critical shear stresses for the remobilisation of seabed sediment at the fine sand station (UR-33, $d_{50} = 141 \mu\text{m}$, water depth 34.5 m). 81

Figure IV.16. Current- and wave-induced shear stresses in relation to critical shear stresses for the remobilisation of seabed sediment at the coarse sediment station (UR-05, $d_{50} = 2.46 \text{ mm}$, water depth 34 m). 82

Figure IV.17. Multibeam backscatter map from May 2003. Outline of fine sand/coarse sediment boundary derived from data obtained in May 2002 is indicated by black line. White boxes indicate locations of close-ups shown in Fig.IV.18. 83

Figure IV.18. Comparison of sidescan sonar backscatter records from individual profile lines gathered in 1977 and 2002. A high level of seafloor morphologic stability is apparent. 84

Figure IV.19. Reconstructed mosaic of geo-referenced analogue sidescan sonar backscatter data from 1977. Outline of fine sand/coarse sediment boundary derived from data obtained in May 2002 is indicated by black line. 85

List of tables

Table II.1. Observation date, total depth d , depth integrated velocity \bar{u} , observation depth d_o , maximum velocity V_{max} , average velocity V_{av} , and average flow direction A in current measurement stations on SVS collected by Lanh and Hoan, (2002) (see Fig.II.5. for location).....	20
Table II.2. Number of interpreted dunes N_d , number of available sediment samples N_s , average grain size d_{50} , depth d , dune length L , dune height H , asymmetry ratio L_{STOSS}/L and depth integrated velocity generating dunes \bar{u} calculated from Eq. (II.1) in distinguished zones (see Fig.II.1. for locations).	24
Table III.1. Data sets interpreted in this study.	38
Table III.2. Quantitative estimates of the extent of the pit and screened sand in the gravel-extraction area.	41
Table III.3. Refilling rate of the pits existing in different sediment between 2003 and 2005.	43
Table IV.1. Standard deviation values of the DECCA positioning error for all transmission stations in the geometric centre of the study area ($\varphi = 54^\circ 45.95'$; $\lambda = 7^\circ 4.63'$) calculated from equations IV.1, IV.2, and IV.3.	56
Table IV.2. Possible sources of inaccuracy, magnitude of their error and error direction.....	64
Table IV.3. Grain-size statistical measures of samples from ground-truth stations.	78

I GENERAL INTRODUCTION

I.1 Sidescan sonar system description

A sidescan sonar system typically consists of a towfish containing active sonar, and a computer system registering backscatter on board of a towing vessel. The towed sonar emits acoustic waves simultaneously from both sides of a fish and receives backscatter from a seabed stripe (ping) directly beneath the sonar, perpendicular to fish axis (Fig.I.1).

A backscatter spectrum is typically registered in an 8-bit greyscale palette. In this work highest backscatter values are presented in dark to black tones and a lack of backscatter is projected in white, except in chapter IV.2, where this scale is reversed. The backscatter value corresponds to the amount of energy coming back to sonar from individual footprints, which are recorded as separate pixels. Since footprints of longer wavelengths are larger, small ripples can be registered as plain coarse sand even at 100 kHz frequency of scanning (e.g. WRIGHT ET AL., 1987). Lack of backscatter from any footprint is usually a result of obstacles limiting acoustic wave propagation behind them. Since sidescan sonar is normally towed at about 10-m altitude over seabed and it scans a range of 50-75 m, waves propagation can be limited even by larger boulders. Thus an acoustic shadow appears on sonographs (Fig.I.1-P,B,R). Geometrical analysis of acoustic shadow can lead to approximation of obstacles height assuming flat seabed as shows Fig.I.2.

A towfish altitude is visible in the sonograph as a width between the middle axis and the first bottom return signal ('h' in Fig.I.1). This blank fragment of the sonograph represents a record of backscatter from the water column and can therefore contain suspended sediment matter, or fish ('F₁' in Fig.I.1).

A lateral extent (range) of a ping depends primarily on frequency of an acoustic wave. At lower frequencies acoustic wavelengths are longer and therefore travel larger distances in the same time than waves at higher frequencies. Shorter waves, on the other hand, resolve object roughness more accurate, what results in a sharper image (Fig.I.3), but shorter range. A system called GLORIA (Geological LOng Range Inclined Asdic) scanning with frequency close to 7 kHz was used for deep-sea bottom mapping (e.g. BELDERSON ET AL., 1970), whereas on the shelf areas working frequency of about 100 kHz proved to be most efficient (see models comparison in FLEMMING, 1982) at the initial stage of seabed exploration.

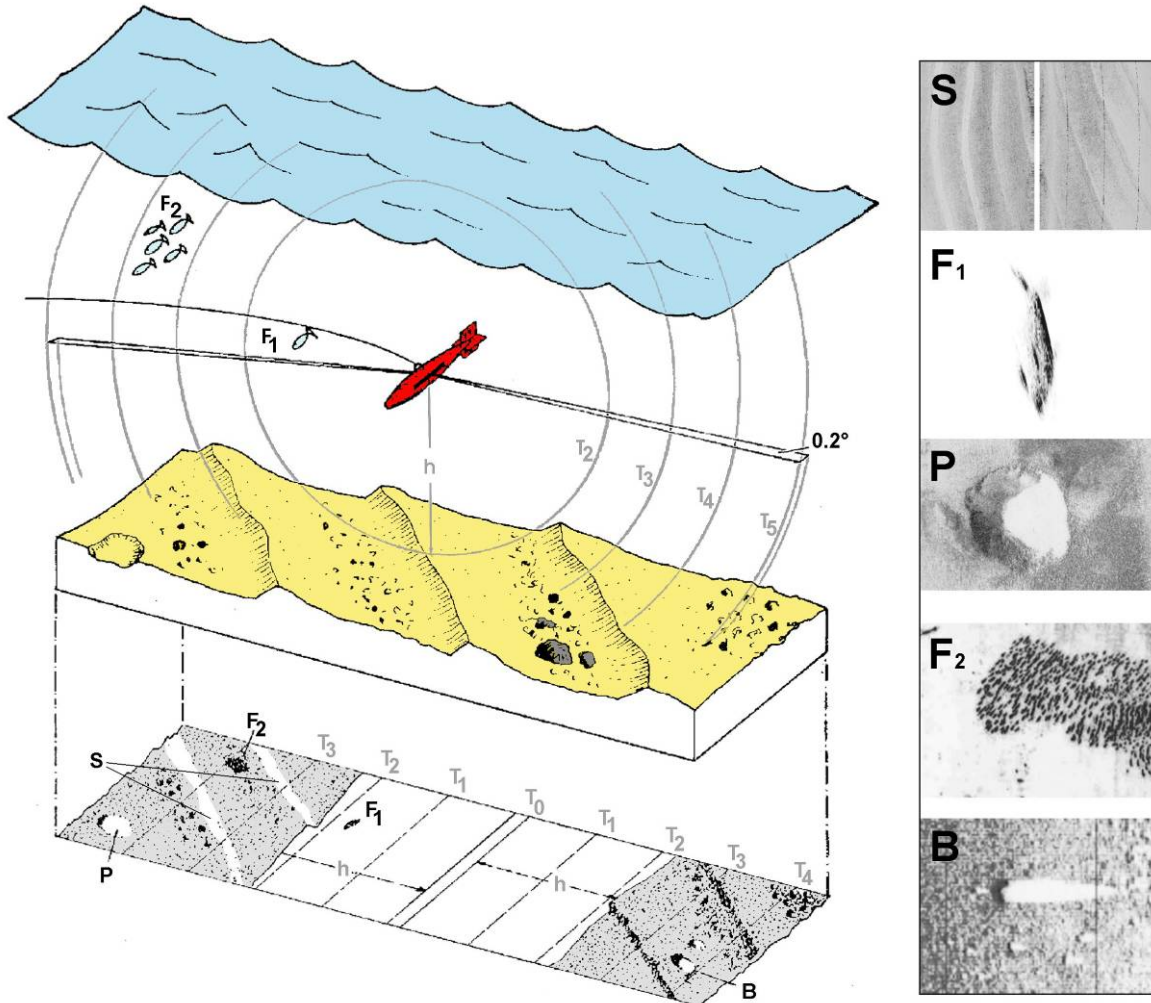


Figure I.1. Sidescan sonar functioning scheme (modified after NEWTON ET AL, 1973). A piece of seabed is presented together with its backscatter representation and sonograph examples of: S- sandwaves in both channels; F1 and F2 – fish in water column (source: www.marinesonic.com); P-pit in right channel; B-boulders in left channel

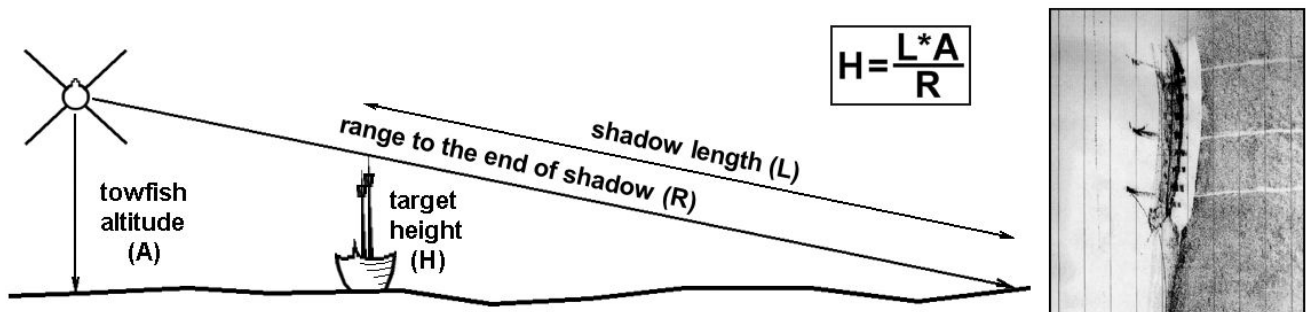


Figure I.2. Method for computing objects height based on towfish altitude, lengths of an acoustic shadow and range to the end of the shadow. Sonograph example of a sunken ship recorded in left channel (source: www.engin.umich.edu).

Scanning of sequential pings along a predetermined survey path results in a linear image of a seabed backscatter. Every shake of the towfish causes different alignment of one ping in respect to another and consequently distortions are recorded in the sonograph. Scanning along long paths appeared to be the best way to minimise this problem. In order to map a part of seabed wider than the operative swath, a mosaic of neighbouring, overlapping profiles had to be executed. Otherwise areas between the scanning paths were blank and mapping through geometrical interpolation was necessary.

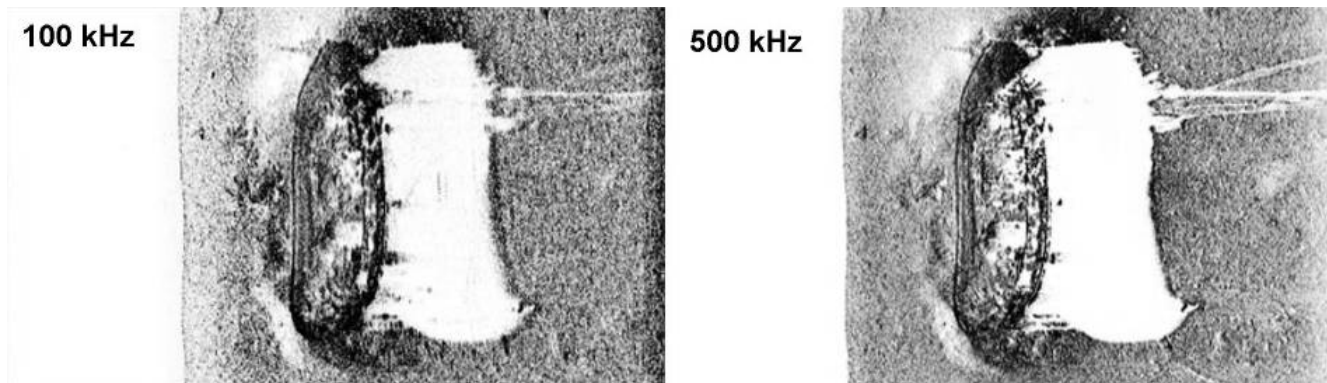


Figure I.3. Example of a ship-wreck recorded simultaneously in 100 and 500 kHz. (source: www.l-3klein.com).

I.2 Sonographs processing

I.2.1 Geometric correction

The most crucial element of sidescan sonar data processing is nowadays georeferencing, during which each recorded footprint is being assigned real-world co-ordinates. In case of early analogue sonographs collection, a special care was focused on correct imagining x-axis (perpendicular to survey path) to y-axis (along-path) ratio, since contemporary positioning technology was not accurate enough (e.g. [KARL ET AL., 1994](#) faced the problem of 200-400 m offset).

A number of procedures, called in general a geometric correction, needed to be performed in order to place each pixel correctly. Except the mentioned unpredictable distortions caused by yawing, rolling and pitching of a towfish, there exist also predictable consequences of survey parameters

Sonograph geometry along the x-axis is thus controlled by the angle between a towfish altitude and a propagation of backscattering signals. Each footprint, starting from a nadir point to the furthest range, was recorded in the same pixel-size. For small angles however, i.e. in the near-range, actual footprints were denser than in the far-range. Consequently, true distances were gradually more compressed in the near-range parts of sonographs (FLEMMING, 1982). In addition, footprints from expected near-nadir parts are recorded despite a lack of backscatter from a water column. A slant-range correction has to be therefore applied to stretch the sonograph along the x-axis and thus remove the water column. The latter was relatively easy for flat seabeds (e.g. WERNER AND NEWTON, 1975; Fig.I.4), however a proper slant-range correction was hardly possible without a microprocessor analysing and correcting slant-ranges during a data collection (KLEIN, 1982).



Figure I.4. Example of manual water column removal. Note an imperfect effect in the right-hand side of the figure due to a trough in bottom morphology (WERNER AND NEWTON, 1975).

Distortions along the y-axis used to be related to variable speed of a vessel compared to a rate of feeding paper while printing sonographs. Some methods were introduced to overcome this problem (e.g. WALKER, 1978), but in general, an accelerating vessel was causing compressing of the sonograph along the y-axis if the feeding rate remained constant. This affected angles of features orientation in the sonographs. A graphical solution of angular distortion ellipse was used to present true angles (FLEMMING, 1982; Fig.I.4), which was mathematically described by VOULGARIS AND COLLINS (1991).

Another issue affecting accuracy of geo-referencing was poor control over a layback of towed sidescan sonar. A method for layback calculation based on cable-out length and possible towing angle at a certain vessel speed used to be a major approximation of towfish

position in the water. Accounting for different layback values was simpler while mosaicking seabed with path-parallel long morphological forms (e.g. transverse sand dunes), when matching shapes in neighbouring sonographs was available. Nevertheless, a towfish was not necessarily towed behind a vessel along the y-axis. Residual currents were also pushing sidescan sonar as well along the x-axis which additionally complicated sonograph positioning. Modern sidescan sonar systems use transponders, i.e. extra sonar system locating towfish in respect to the vessel. Surveys are controlled by a differential Global Positioning System (GPS), which assures accuracy of few meters in any world basin. Software for sidescan sonar data collection and processing controls geo-referencing of every ping basing on GPS and transponders readings. Towfish pitching and rolling is controlled by an installed gyro and according to its readings, sonographs geometry is updated. Correction of water-column offset and slat-range correction can be as well solved in the real-time and thus, a powerful computer system can nowadays perform geometry correction already during a data collection process (CHAVEZ ET AL., 2002).

1.2.2 Acoustic correction

A backscatter value of each pixel also needs to be updated due to spreading and absorption of acoustic waves, noise in a water column, or failures of devices during data acquisition. These procedures are called an acoustic (radiometric) correction and include in practise an application of various algorithms for correction of pixels intensity. They are therefore possible only for digital form of sonographs although time-varying gain settings were applied also during analogue sonograph printing (KLEIN, 1982). Even though analogue sonographs can be converted to digital form by office scanners, there appears a certain loss of pixel intensity and spatial information, which needs to be corrected initially (WHIPP AND HORNE, 1976).

Acoustic correction is performed mostly along the x-axis, i.e. along waves propagation direction. A fading of signal in the far-range of the sonograph, which results in shading, was corrected by already mentioned gain increase for the far-range. In digital image processing a procedure of strengthening the far-range signal was usually performed with a flat-bed assumption (REED AND HUSSONG, 1989), even though seabottom morphology was

recognised to affect strongly backscatter intensity (KEETON AND SEARLE, 1996). Noise in water column and data acquisition failures result in regularly distributed speckles or striping. These can be removed only after the sonograph is acquired due to application of high-pass filters, which correct the pixel intensity in respect to neighbouring pixels (CHAVEZ ET AL., 2002)

I.2.3 Mapping and image classification

A well-designed path of the survey and proper geometric and acoustic corrections applied to individual sonographs simplify significantly a mapping process. Creating maps used to be a laborious activity of manual depicting sediment patterns, or objects location, which nowadays became supported by Geographic Information Systems (GIS). Ability to visualise vast areas and multiple, geographically aligned sonographs on a small screen of a GIS system accelerated the map-making process enormously. Solutions for automatic borders vectorising, or automatic image classification were presented by many authors (e.g. PACE AND GAO, 1988; TAMSETT, 1993; GOFF ET AL., 2000; MIGNOTTE AND COLLET, 2000; TANG AND STEWART, 2000; OJEDA ET AL., 2004; COLLIER AND BROWN, 2005; WIENBERG AND BARTHOLOMÄ, 2005; BARTHOLOMÄ, 2006; ROOPER AND ZIMMERMANN, 2007), however a huge role of human interpretation is still undeniable.

I.3. Sidescan sonar technology modifications

Apart from increasing image quality and spatial data precision several technical modifications have been applied to towed sidescan sonar. Hull-mounted versions were used for deep-water investigations (e.g. FERENTINOS ET AL., 1988, mounted on a surface vessel, or PARSONS ET AL., 2005, on a submarine). Sidescan sonars were installed also on unmanned vehicles for precise morphology mapping in a surf-zone (e.g. THORNTON ET AL., 1998). Earlier developments in sonar applications in surf-zone studies presented GREENWOOD ET AL., 1985 (cited in VINCENT AND OSBORNE, 1993, who installed three acoustic backscatter sensors on a static transducer). HAY AND WILSON (1994) implemented a rotary sonar system scanning with 2.25 MHz frequency surf-zone morphology under storm waves. Authors working in a surf-zone highlighted problem of gas bubbles affecting sonographs. Bubbles originated from

breaking waves affect as well images from synthetic aperture radars and therefore a shallow-towed sidescan sonar study of HENNINGS ET AL. (1993) was addressed to this issue. Inverted sidescan sonar mounted on a sea bottom for scanning bubbles was used earlier by THORPE AND HALL (1983) for better understanding breaking-zone hydrodynamics. Towed, but inverted sidescan sonars were also used for detecting water-surface-oriented fish (e.g. TREVORROW, 2002). EDWARDS ET AL. (2003) presented sonographs from a sidescan sonar mounted on submarine, containing artefacts, and thus images, from the base of the Arctic ice canopy. This all proves unlimited applications of sonar technology in marine sciences.

I.4 Basic applications of sonographs

I.4.1 Bedforms and sediment mapping

A nomenclature of sand bodies used to be rather chaotic (e.g. ALLEN, 1968; DALRYMPLE ET AL. 1978; BOUMA ET AL., 1980; RUBIN AND McCULLOCH, 1980; FIELD ET AL., 1981; SWIFT ET AL., 1983, KUIJPERS ET AL. 1993; also see review in AMOS AND KING 1984) until a proposal of unification earlier classifications was given at 1987 Mid-year Meeting of Society for Sedimentary Geology (ASHLEY, 1990). This classification scheme based on bedforms morphology is currently more or less accepted worldwide, but some authors of later and obviously majority of earlier studies used different names for bedforms being described. Until the publication of ASHLEY (1990) a very successful solution for comparison of global sand bodies appeared to be visualisation of height/length ratio (e.g. FLEMMING, 1978, 1988; AMOS AND KING, 1984; ADAMS ET AL., 1986).

Early published sonographs were the effect of curiosity rather than systematic mapping. KENYON (1970) in British waters and later STUBBLEFIELD ET AL. (1977) in New York Bight presented sonographs together with camera photos of sand waves and sand ribbons. STRIDE AND CHESTERMAN (1973) observed seven meters high sand waves in Skagerrak Straits. MCKINNEY ET AL. (1974) used sidescan sonar for ribbons mapping on New Jersey shelf. WERNER AND NEWTON (1975) observed comet-marks, sand ribbons and sand waves on sonographs from Langeland Belt. FLEMMING (1978, 1980) described bedforms on the South-African shelf on basis of a single 800-km profile. BOUMA ET AL. (1980) presented bedforms distribution in lower Cook Inlet, Alaska and approached their classification. MANN ET AL. (1981)

at Nantucket Shoals, USA, as well as [KNEBEL ET AL. \(1982\)](#) on Rhode Island shelf mapped a distribution of bedforms using both sidescan sonar and echosounder. [KLEIN ET AL. \(1982\)](#) supported similar study with a current meter. [GREEN \(1986\)](#) presented a sand-ridges field in Mid-Atlantic Bight with a help of one of the first mosaics. Many other authors focused exclusively on subaqueous bedforms distribution (e.g. [NEWTON AND STEFANON, 1982](#); [AMOS AND KING, 1984](#); [GOSTIN ET AL., 1984](#); [HARRIS AND COLLINS, 1984](#); [SALGE AND WONG, 1988](#); [GARDNER ET AL., 1989](#); [FENSTER AND FITZGERALD, 1996](#); [REYNAUD ET AL., 1999](#); [DUCK ET AL., 2001](#); [LYKOUSIS, 2001](#); [MASSON ET AL., 2002](#); [MORALES ET AL., 2006](#)), but eventually appeared a need for ground-truthing of sonographs and consequently bottom sediment maps.

One of the first sediment mapping performed with assistance of sidescan sonar presented [KELLAND AND HAILS \(1972\)](#) in Start Bay, England. It was based mostly on sediment samples and sonographs together with sub-bottom seismic profiles had only a supportive role. A sediment map entirely based on sidescan sonar data covered area off Nile Delta ([COLEMAN ET AL., 1981](#)). [HOBBS \(1986\)](#) showed a similar study depicting spatial extent of sandy patches in muddy environment on Chesapeake Bay seabed. [KNEBEL \(1986\)](#) supported the seismic mapping of Holocene sediments of Penobscot Bay with sonographs taken at surface sediment boundary. [WRIGHT ET AL. \(1987\)](#) using a digital sidescan sonar data collection prepared a sediment map of Lower Chesapeake Bay on bases of irregular grid of sidescan sonar profiles and local mosaics. Spatial distribution of sediments derived from spatially irregular grid of sonographs was presented as well by [AUBREY ET AL. \(1982\)](#), [COTTAZ ET AL. \(1989\)](#), [ERGIN ET AL. \(1991\)](#), [KNEBEL \(1993\)](#), [THIELER ET AL. \(1995\)](#), [KNEBEL ET AL. \(1999\)](#), [LEWIS AND BARNES \(1999\)](#), [MANIGHETTI AND CARTER \(1999\)](#), and [HUMBORSTAD ET AL. \(2004\)](#). In the earlier studies [BARRIE ET AL. \(1984\)](#), [DAVIS ET AL. \(1996\)](#) or [WEVER ET AL. \(1997\)](#) prepared sediment mapping from a regular mosaic of analogue sidescan sonar profiles, however the best mapping quality was achieved by digital collection and processing systems used for scanning mosaics over large areas (e.g. [CHAVEZ ET AL., 2002](#); [NITSCHKE ET AL., 2004](#))

In practise, however, sediment and bedforms mapping were performed simultaneously. [COLEMAN ET AL. \(1981\)](#) observed in this way sand ridges topped by sand waves. [HUNTER ET AL. \(1988\)](#) mapped a small piece of Monterey Bay, USA. [HARRIS \(1988a\)](#) supported sediment mapping in Torres Straits with sonographs and aerial photographs updating earlier study. [KUIJPERS ET AL. \(1993\)](#) described both, sediment and bedforms of

Skagerrak Straits. [PARK AND LEE \(1994\)](#) used additionally seismic profiler and current meters to provide information about Korean coast of Yellow Sea. Newer studies contain full sedimentological and morphological interpretation of sonographs mosaics (e.g. [ANTHONY AND LETH, 2002](#); [EITTREIM ET AL., 2002](#); [TWICHELL ET AL. 2003](#)).

I.4.2 Benthic habitat mapping

Benthic ecosystems are strongly associated with sediment type. Application of sidescan sonar for benthic habitat mapping was recognised relatively early ([WARWICK AND DAVIES, 1977](#)). Examples of benthos mapping supported by sonographs can be found in [HOLME AND WILSON \(1985\)](#), [DAVOULT AND CLABAUT \(1988\)](#), [BROWN ET AL. \(2002\)](#). [PASQUALINI ET AL. \(1998\)](#) interpreted sonographs in order to delineate seagrass extent. [COCHRANE AND LAFFERTY \(2002\)](#) classified sonographs mosaic and achieved benthic habitat map without blank areas. [EHRHOLD et al. \(2006\)](#) classified in this way 200 km² of Bay of Concarneau, France. Similar mapping presented [OJEDA ET AL. \(2004\)](#), [BROWN ET AL., \(2005\)](#), [OR LATHROP ET AL. \(2006\)](#). [BIRCHENOUGH ET AL. \(2006\)](#) compared four yearly sonographs mosaics from the same area to present changes in macrobenthos spatial limits. [COLLIER AND HUMBER \(2007\)](#) used a 675-kHz sonar for mapping coral reefs in Seychelles waters.

I.4.3 Target recognition applications

Sidescan sonar appeared to even broader applications for natural or human-made objects location. Possibility to locate submerged cables and pipelines in sonographs was recognised very early ([DE GROOT, 1982](#)). Apart from common industrial applications, [KARL ET AL. \(1994\)](#) tried to locate barrels at disposal sites using 120 kHz channels. Barrels could not be resolved on the sonographs, so authors supported investigation with video images. Scanning in higher frequencies allowed application of sidescan sonar in marine archaeology studies (e.g. sunken frigate in [QUINN ET AL., 2002](#)). [BALLARD ET AL. \(2002\)](#) located beach berm of ancient Black Sea coast at 155 m water depth. Ability to record on sonographs artefacts caused by shallow gas bubbles were also used in a few studies. [WEVER ET AL. \(1998\)](#) used sonographs of Eckernförde Bay, Germany to map muddy seabed with pockmarks, where

shallow gas deposits were expected. [ROGERS ET AL. \(2006\)](#) were looking for pockmarks indicating such deposits in Belfast Bay, USA.

I.5. Applications of sonographs in morphodynamics

Tracking of physical changes in a shelf morphology developed into a broad topic investigated with numerous short- and long-term methods. A series of at least two measurements taken in the same area one after another were sufficient to interpret morphodynamics on the sea bottom. The most cost-efficient methods of bedforms dynamics observation appeared to be applications of optical remote sensing. The use of aerial photographs (e.g. [SCHWARZER ET AL., 2003](#)), or satellite imagery (e.g. [BALOUIN AND HOWA, 2002](#); [NIEDERMEIER ET AL., 2005](#)) was limited only to shallower parts of shelves due to light penetration physics. A long-term morphodynamics study can be performed basing on bathymetrical charts. [BLOTT ET AL. \(2006\)](#) presented in this way morphological changes in Mersey estuary, UK, starting from year 1738 and quantitative comparison from 1912. Similar study for Indus delta showed [GIOSAN ET AL. \(2006\)](#), or [VAN LANCKER ET AL. \(2004\)](#) for Teignmouth, UK. These investigations focused on spatial volume comparison and thus resulted in presentation of areas affected by erosion, or accretion.

For deducing sediment transport pathways having only sediment samples available a McLaren Model was used ([MCLAREN AND BOWLES, 1985](#); example by [DUCK ET AL., 2001](#)), or its development by [GAO AND COLLINS \(1992\)](#) (e.g. [VAN LANCKER ET AL., 2004](#)), which took into consideration spatial grain-size trends. Such studies were, however, spatially large and did not resolve single sand bodies, which appeared to be the best indicator of seabed dynamics.

I.5.1 Sand bodies migration

The first offshore sandwaves were reported by [VAN VEEN \(1935\)](#) and already their similarity to eolian landforms affected theories of underwater migration. The asymmetry of observed sand bodies was interpreted as the indicator for migration normal to the lee-side surface by many authors (e.g. [ALLEN, 1962](#); [STRIDE, 1965](#); [GELLATLY, 1970](#); [MCCAVE 1971](#); [TOIMIL AND REIMNITZ 1979](#); [CASTON, 1981](#); [AUBREY ET AL., 1982](#); [BARRIE ET AL., 1984](#); [HARRIS](#)

AND COLLINS, 1984; PERILLO AND LUDWICK, 1984; GREEN, 1986, HARRIS, 1988B; SALGE AND WONG, 1988; THIELER ET AL., 1995; VAN DER MEENE ET AL., 1996; VIANA ET AL., 1998; DUCK ET AL., 2001; LYKOUSIS, 2001; KNISKERN AND KUELH, 2003). WERNER AND NEWTON (1975), TODD ET AL. (1999), or MASSON (2001) located additionally comet marks indicating water movement. Such migration assumptions were possible to present already on basis of any single series of single-beam echosounder or sidescan sonar profiles.

Repetitive profiles, however, offered better evidence of bedforms migration when only an identification of a studied bedform was possible during the following surveys. LANGHORNE (1973) observed branching of sandwaves crests on basis of sidescan sonar and echosounder material from four campaigns. WERNER AND NEWTON (1975) compared two sonographs from Langeland Belt, Denmark recorded 14 months one after another. FIELD ET AL. (1981) repeated in this way three different sidescan profiles after one year and observed sandwaves migration. LANGHORNE (1981) using echosounder presented morphological change of a sandwave crest due to tidal currents. KLEIN ET AL. (1982) using as well sonographs showed morphological changes of a sand ridge off Korean coast. PERILLO AND LUDWICK (1984) made repetitive soundings of a single sandwave over two years. They assumed its stability, but claimed to have positioning errors of 18.5 m. Monitoring of sandwaves fields on basis of echosounder and sonographs performed as well SHEPHERD AND HAILS (1984), HARRIS AND COLLINS (1984), HARRIS (1989), HENNINGS ET AL. (1993), FENSTER AND FITZGERALD (1996), ANTHONY AND LETH (2002), SCHROTTKE ET AL. (2006). SANTORO ET AL. (2004) compared single echosounder data of sandwaves field with multibeam echosounder data recorder 10 years later. TONNON ET AL. (2007) collected by these means data covering 18 years. All these works focused on changes in monthly or yearly time frames.

Direct proves of a short-term sediment transport in marine conditions were collected by underwater video-cameras (e.g. FIELD ET AL., 1981; KENNY AND REES, 1996). Short periods of time were covered as well in most of morphodynamics studies in a surf-zone (e.g. VINCENT AND OSBORNE, 1993; HAY AND WILSON, 1994; THORNTON ET AL., 1998; STERNBERG AND NOWELL, 1999; GALLAGHER, 2003)

Many authors tried to confirm the sediment migration by associating spatial geological data with measured, or predicted current velocities (e.g. MCCAVE, 1971; RUBIN AND

McCULLOCH, 1980; COLEMAN ET AL., 1981; FIELD ET AL., 1981; AUBREY ET AL., 1982; KLEIN ET AL., 1982; HARRIS AND COLLINS, 1985; ADAMS ET AL., 1986; GARDNER ET AL., 1989; HARRIS, 1989; KNEBEL, 1989, 1993; ERGIN ET AL., 1991, PARK AND LEE, 1994; KNEBEL ET AL., 1999; LEWIS AND BARNES, 1999; REYNAUD ET AL., 1999; TAUBER AND EMEIS, 2005; Basetti et al., 2006). The others approached the prediction of possible current velocities forming bedforms (e.g. FLEMMING, 1978; GARDNER ET AL., 1989; BODUR AND ERGIN, 1992; KUIJPERS ET AL., 1993; HENNINGS ET AL., 2000). Such investigations were possible due to empirical derivations of equations for sediment mobilisation and transport (e.g. by EINSTEIN, 1950; BAGNOLD, 1963; YALIN, 1963; ENGELUND AND HANSEN, 1967; STERNBERG, 1972; ACKERS AND WHITE, 1973; DARLYMPLE ET AL., 1978; GADD ET AL., 1978; VAN RIJN, 1984; BLACK AND HEALY, 1986; or YANG, 1986). Calibrations of these equations led to better approximation of sediment transport and consequently bedforms migration. Increasing computational power of personal computers allowed solving water flow equations together with these for sediment transport. Many of the conceptual models of bedforms origins and migration (e.g. McCAVE, 1971; RUBIN AND McCULLOCH, 1980; FIGUEIREDO ET AL., 1982; HARRIS, 1988a; BEST, 1992) could now be evaluated not only by laboratory experiments (e.g. RUBIN AND McCULLOCH, 1980, or CATANO LOPERA AND GARCIA, 2006), but also by numerical modelling (e.g. HULSCHER, 1996; GERKEMA, 2000; KNAAPEN AND HULSCHER, 2002; NEMETH ET AL., 2002, 2007; BESIO ET AL., 2003; MORELISSSEN ET AL., 2003; MURRAY AND THIELER, 2004; TONNON ET AL., 2006).

1.5.2 Post-dredging seabed recovery

A physical recovery of seabed after dredging activities was quite an unexplored issue even though dredging has surprisingly very long traditions (see dredging in ancient Tyre harbour in MARRINER AND MORHANGE, 2006). It is obvious that after extraction pits or furrows become a new element in seabed morphology, but very little is known on their infilling, or if it actually takes place. The probable reason is that for a very long time there was no tool precise enough to handle such studies although an idea of repetitive monitoring the sites with sidescan sonar appeared relatively early (DE GROOT, 1979).

Much simpler method of biological sampling was applied in many studies to investigate recolonisation of dredged areas and thus biological recovery. Many authors

addressed the issue of benthos disappearing and recovery (e.g. POINER AND KENNEDY, 1984; VAN DER VEER, 1985; BOYD ET AL., 2003; QIAN ET AL., 2003; GILKINSON ET AL., 2005, ROBINSON ET AL., 2005; SIMONINI ET AL., 2005; GUERRA-GARCIA AND GARCIA-GOMEZ, 2006; SZYMELFENIG ET AL., 2006; COOPER ET AL., 2007), as well as consequences of extraction on fisheries (e.g. DE GROOT, 1979; OULASVIRTA AND LETHONEN, 1988; SMITH ET AL., 2006). PINTO ET AL. (1995), or BERGEN ET AL. (2005) presented also studies on toxicity and overall chemistry on post-dredging areas, but pure physical effects of dredging activities (i.e. changing beach profiles) were tracked mostly onshore (e.g. WANG AND GERRITSEN, 1995; BENDER AND DEAN, 2003; THORNTON ET AL., 2006).

Several offshore post-dredging biological studies were supported by sonographs (e.g. KENNY AND REESE, 1996; DESPREZ, 2000). BOYD ET AL. (2005) compared a series of three sonographs to visualise changes in benthos coverage. WIENBERG AND BARTHOLOMÄ (2005) presented results from three simplified sediment mapping by a single-beam echosounder and a QTC seabed classification system. BIRCHENOUGH ET AL. (2006) presented sediment coverage changes on four sonographs recorded over four years. Earlier, GILKINSON ET AL. (2003) monitored furrows being the effect of clam-dredging. Less and less defined edges of furrows were observed in a series of subsequent four sonographs and this was probably the most valuable information about post-dredging morphodynamics within any studied site.

1.5.3 Rippled scour depressions, sorted bed forms appearance

Shore perpendicular depressions filled with coarser sediment usually topped with ripples and thus forming ribbon-like patches in sonographs (Fig.1.5) were reported long before CACCHIONE ET AL. (1984) named them rippled scour depressions (e.g. MCKINNEY ET AL., 1974, COLEMAN ET AL., 1981; KNEBEL ET AL., 1982; NEWTON AND STEFANON, 1982). Later studies (see review of MURRAY AND THIELER, 2004) showed their common location in low-energy and sediment-starved shelves. CACCHIONE ET AL. (1984) related the origins of rippled scour depressions to a cross-shore water movement, however SCHWAB (1997) discussed that their appearance is rather the effect of along-shore currents reworking relict sediments. Already KNEBEL ET AL. (1982), or NEWTON AND STEFANON (1982) speculated that sandy ribbons may

have appeared due to sediment sorting and FLEISCHER ET AL. (1996) actually observed for 20 years an appearance of a new unit due to sediment reworking, transport and redeposition.

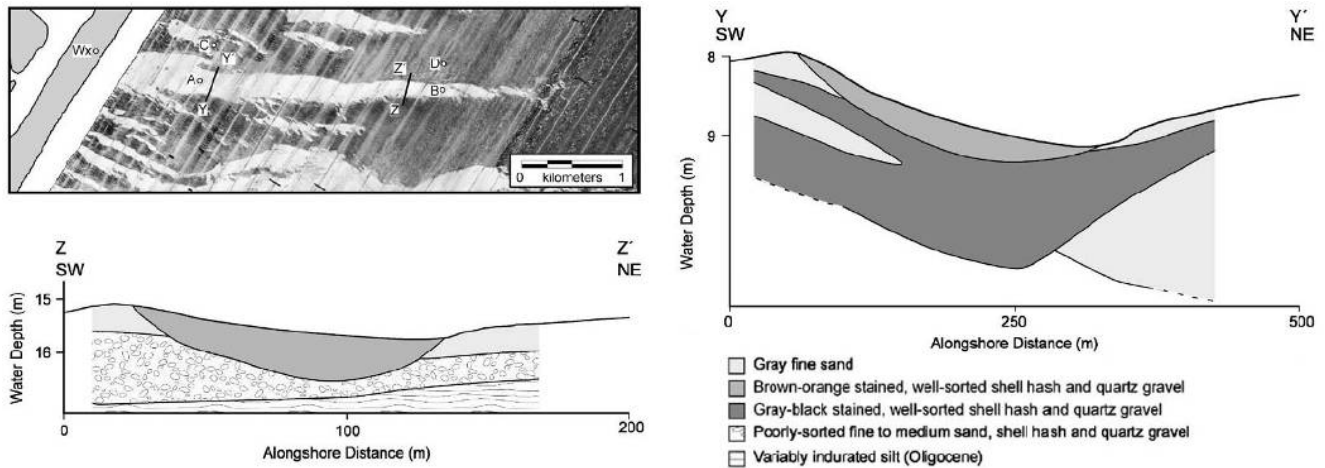


Figure I.5. Sonograph representation of a sorted bedform off a coast of North Carolina, USA, and two geological cross-section (modified after MURRAY AND THIELER, 2004).

The theory of origins due to sediment sorting was summarised by MURRAY AND THIELER (2004), who approached additionally a numerical modelling of rippled scour depression behaviour. They proposed a term 'sorted bedforms' for such depressions, where along-shore water movement is responsible for sediment dynamics. GUTTIERREZ ET AL. (2005), who focused on behaviour of a sorted bedform during 45 days of hydrological monitoring, supported possibility of finer sand advection within the structure. The time necessary to sort a new bedform is unknown at this stage of investigations. GARNAUD ET AL. (2005) observed new depressions present 20 years after earlier mapping. MURRAY AND THIELER (2004) showed the morphological stability of sorted bedforms over three years time, whereas during a seven-month monitoring period of sorted bedforms pattern GOFF ET AL. (2005) observed changes in sediment pattern on order of tens of metres locally.

A. Kubicki

Indicators for migration of large to very large subaqueous dunes induced by winter monsoon circulation on southern Vietnamese Shelf, South China Sea

Journal: Geo-Marine Letters

Received: 23 February 2007

Status of this article: under review

A. Kubicki (✉)
Institute of Geosciences,
Christian Albrechts University,
D-24118, Kiel, Germany
E-mail: akubicki@gpi.uni-kiel.de
Tel: +49 431 8802866
Fax: +49 431 8804432

II CASE STUDY ON SAND DUNES - INDICATORS FOR MIGRATION OF LARGE TO VERY LARGE SUBAQUEOUS DUNES INDUCED BY WINTER MONSOON CIRCULATION ON SOUTHERN VIETNAMESE SHELF, SOUTH CHINA SEA

II.1 Abstract

The southern Vietnamese Shelf (SVS) was studied by sidescan sonar profiling twice at the ends of the winter monsoon seasons 2003 and 2004. Over 1000 km of transects revealed a widespread occurrence of subaqueous dunes from which large to very large dunes (longer than 10 m and higher than 0.75 m) were investigated in details. On the basis of sonographs supported by single-beam echosounder data, dunes parameters were estimated. A variety of dunes were grouped spatially into five zones according to their size, shape, depth of occurrence and orientation. The pattern of the latter corresponded with the directions of the current circulation induced by winter monsoon from NE towards SW and S. Depth-averaged velocities capable of generating investigated dunes were calculated and combined with hydrological observations of other authors in this area. It is concluded that the migration of large and very large dunes on the SVS is likely and the direction of movement is influenced by the monsoon circulation pattern.

II.2 Introduction

Subaqueous dune-like bodies are the most common morphological features on seabeds worldwide. Their role as a significant indicator of local hydrological conditions and sediment balance was recognised very early. It is now well established that major factors controlling dunes dimensions, shapes and migration rates are sediment grain-size, water depth of occurrence and water flow velocity (MAZUMDER, 2003). A number of flume experiments and empirical derivations led gradually to more accurate predictions of sand bodies parameters and mobility in steady-flow conditions. In offshore environment however, the predictions are less reliable due to natural complexity of the system affected by waves and currents influence, dynamics of seabed morphology and variable sediment supply.

Within the framework of the project 'Land-ocean-atmospheric interactions in the coastal zone of Southern Vietnam' two sidescan sonar measuring campaigns were executed offshore (Fig.II.1). The objectives were

- 1) to locate and describe dunes on the southern Vietnamese Shelf (SVS),
- 2) to depict possible migration paths and
- 3) to determine the conditions of their mobility.

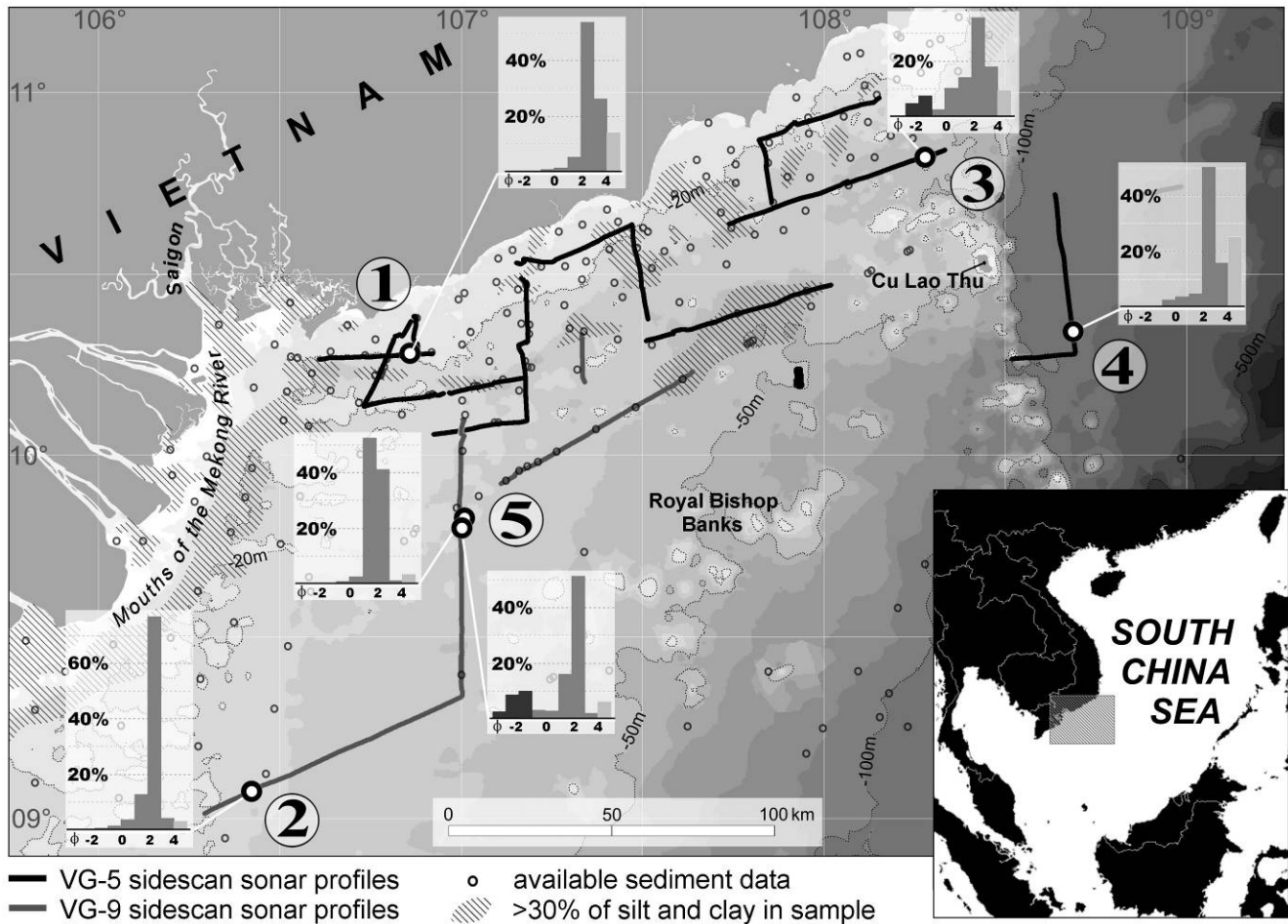


Figure II.1. Location, bathymetry and available data in the study area. Bold lines represent sidescan sonar transects interpreted in this paper. Circles refer to sediment stations from this study and other authors. Numbers 1 to 5 mark distinguished zones and characteristic dunes examples (see Fig.II.4). The bar-graphs show grain size distributions in grab samples. Note that only sediment samples from locations shown in Fig.II.4 are presented. In addition, areas with larger weight of silt and clay ($\text{PHI} > 4$) are outlined.

Very little information is available about the SVS bottom, even though it was extensively studied by the oil industry. Most of the research papers dealing with this region focus on the Mekong Delta, in particular on its geomorphological history (e.g. NGUYEN V.L. ET

AL., 2000) and sediment discharge (e.g. WOLANSKI ET AL., 1996). No subaqueous dunes were reported from this area and thus, in this paper, unique data is presented.

The study is focused on dunes higher than 1.5 m, which are defined by ASHLEY (1990) as large (0.75 – 5 m high, 10 – 100 m long) and very large (higher than 5 m, longer than 100 m). The shelf is divided into zones grouping dunes of similar parameters. Probable directions of dunes migration are presented and water flow velocities necessary to initiate their mobilisation are estimated.

II.3 Setting

The southern Vietnamese Shelf (Fig.II.1), forming the northern part of the Sunda Shelf, was inundated as a result of the Holocene transgression, which had begun about 21 ka ago (HANEUTH ET AL., 2000). The river system of the Paleo-Mekong was here recognised based on fully, or partially filled valleys (SCHIMANSKI AND STATTEGGER, 2005). Modern surface sediments are mostly composed of siliciclastic sands (NGUYEN V.T., 1996), identified as relict sands south of Royal Bishop Banks (deposited during the transgression) and of recent terrigenous origin closer to the Vietnamese mainland (JAGODZINSKI, 2005).

The southern tip of the Mekong Delta is affected by a semidiurnal tide with amplitudes ranging from 1 m and 2 m during neap and spring tide, respectively. The amplitudes increase northwards up to 2 m during neap tide and 4.4 m during spring tide at the Saigon River mouth. From here eastwards, neap and spring tide amplitudes decrease down to 0.5 m and 1.6 m, respectively and the tidal regime changes to diurnal (ANON, 2005).

The hydrodynamics of the SVS is influenced significantly by the tropical monsoon regime (HU ET AL., 2000). Due to winter winds blowing from North and Northeast with an average speed of 8 m/s, a cyclonic gyre forms in the central South China Sea (SCS) (November to April). The reversed summer anti-cyclonic gyre (June to September) is induced by westerly and southwesterly winds blowing with an average speed of 6 m/s (NINH, 2003). Surface currents over the SVS (Fig.II.3) as well as depth-integrated currents (Fig.II.2) follow the general circulation controlled by wind fields.

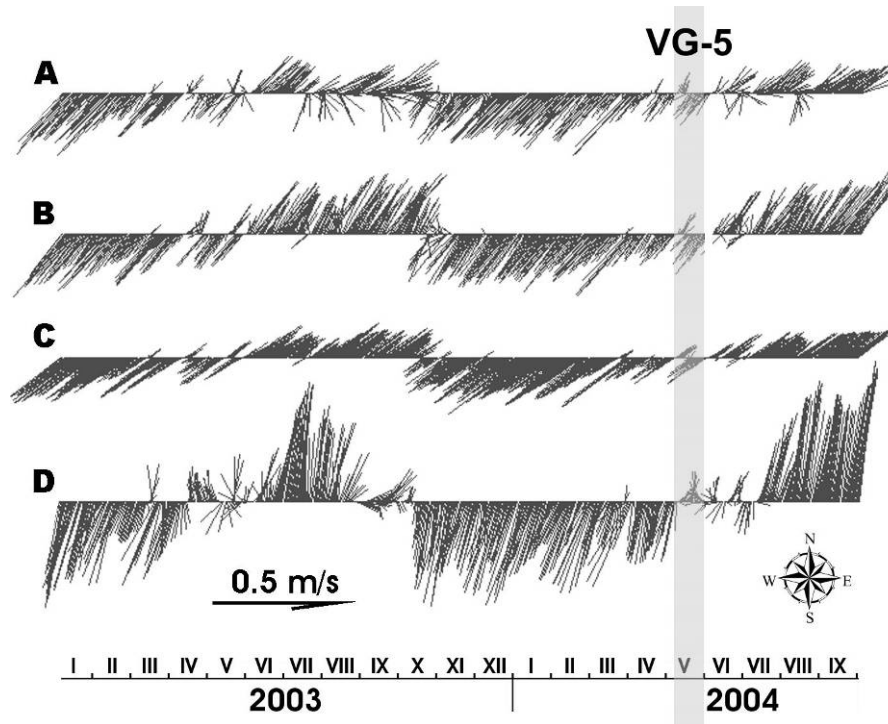


Figure II.2. Results of the HAMSOM (Hamburg Shelf Ocean Model) model showing flow directions and velocities, integrated over depth and time at locations A-D, Fig.II.3. (courtesy of Hartmut Hein, University of Hamburg). The vectors are geographically aligned and the time frame of the VG-5 measuring campaign is marked. Note the difference in flow direction during the summer and winter monsoon seasons.

Very few authors estimated current velocities on the SVS. [LEVITUS \(1982\)](#) gave surface velocity values lower than 0.5 m/s based on ship drifts. [MORIMOTO ET AL., \(2000\)](#) estimated winter surface current velocities of 0.15 – 0.2 m/s, yet considering them as underestimated. Existing numerical models of SCS circulation were focused mainly on eddy-resolving (e.g. [CHERN AND WANG, 2003](#)) and therefore a calibrated model showing absolute values of current velocities is not yet available for the area. Selected uncalibrated results of HAMSOM model (Fig.II.2) suggested depth-integrated velocity values lower than 0.32 m/s at locations A, B and C and lower than 0.55 m/s at the node D (courtesy of Hartmut Hein, University of Hamburg).

In-situ measurements in the central part of the Vietnamese Shelf revealed a southwestern winter current along the central Vietnamese coastline with a depth-averaged velocity of 0.7 m/s ([NINH, 2003](#)). [DIPPNER ET AL. \(2007\)](#) observed it also in July 2003 (velocities up to 1.4 m/s in 60-110 m water depth), but suggested its eastward turn at $\sim 12^{\circ}\text{N}$ due to an upwelling phenomenon taking place further south. The same experiment revealed a northward undercurrent (with local maximum of 1 m/s in 70 m water depth) inside the upwelling zone ([DIPPNER ET AL., 2007](#)) (see Fig.II.3 for location).

From 44 current measurement stations accumulated in LANH AND HOAN (2002) only six were situated on SVS (Tab.II.1, Fig.II.3, stations a-f). The experiments lasting few days between the Cu Lao Thu Island and the mainland revealed maximum velocities of 0.9-1.1 m/s in 5 m water depth and 0.4-0.8 m/s close to the seabed during the summer monsoon season. Station f investigated during winter season showed maximums close to 0.8 m/s in 10 m as well as 90 m water depth (see Tab.II.1 for detailed information).

Table II.1. Observation date, total depth d , depth integrated velocity \bar{u} , observation depth d_o , maximum velocity V_{max} , average velocity V_{av} , and average flow direction A in current measurement stations on SVS collected by LANH AND HOAN, (2002) (see Fig.II.5. for location).

station	date	d [m]	\bar{u} [m]	d_o [m]	V_{max} [m/s]	V_{av} [m/s]	A [°]
a	VIII,1980	22	0.24	5	0.89	0.41	51
				15	0.43	0.20	34
b	VIII,1992	24	0.45	5	0.93	0.70	82
				21	0.38	0.19	50
c	VIII,1993	25	0.31	20	0.66	0.37	60
d	VIII,1992	28	0.42	5	0.88	0.53	64
				24	0.75	0.35	66
e	VIII,1980	50	0.43	5	1.09	0.63	66
				35	0.84	0.41	44
f	I,1995	99	0.40	10	0.82	0.54	278
				90	0.76	0.24	190

II.4 Materials and Methods

More than 1.000 km of sidescan sonar profiles were run across the SVS (Fig.II.1). Both cruises, VG-5 and VG-9, took place in the end of winter monsoon in May 2004 and April 2005, respectively. A measuring campaign plan and local conditions allowed to scan a very irregular pattern of corridors, which resulted merely in an overview of the region. A method of acoustic scanning along hundreds-kilometre lines however, proved to be a successful initial approach when applied to large uncharted seabed regions (e.g. FLEMMING, 1978). Sidescan sonar mapping by mosaicking (e.g. CHAVEZ JR. ET AL., 2002) was applied for a 6 km² piece of a dune field (location '5', fig.II.4).

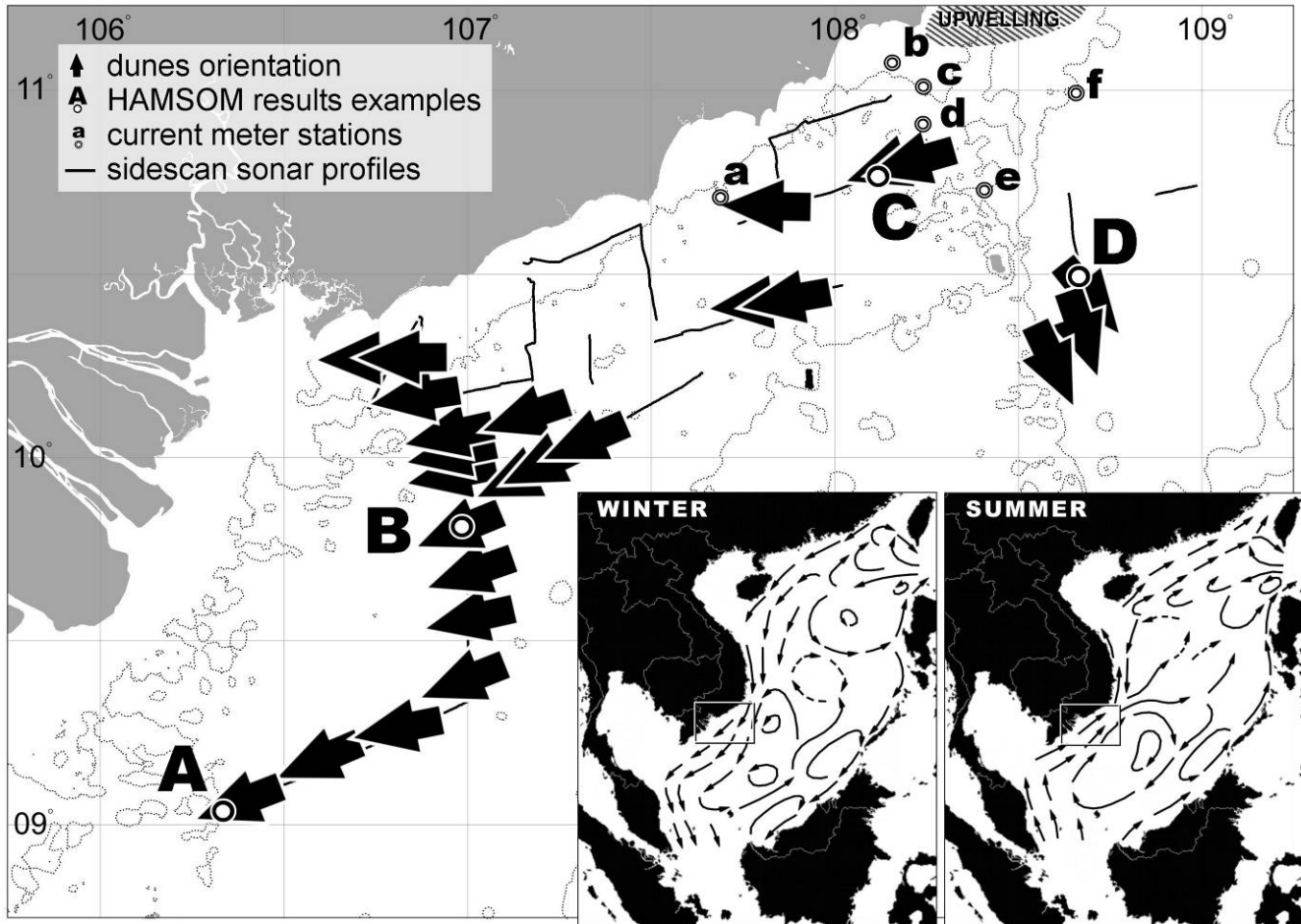


Figure II.3. Orientation of single dunes, or averaged for dune fields. HAMSOM model nodes (A-D) and *in-situ* current measurements stations (a-f) are marked with points. Winter and summer water circulation patterns of SCS are presented for overview (FANG AND FANG, 1998).

A Klein 595 sidescan sonar system was used with a scanning frequency of 385 kHz and a 75-metre range to each side. Data collection and post-processing were performed using the ISIS software (Triton Elics Int.). As no precise towfish position control was available, a positioning error of about 25 m was estimated while accounting for cable-out lengths. They were computed while comparing to GPS readings of a boomer system, which was running simultaneously. This magnitude of error was negligible if weighed against the investigated distances. In the case of the single mosaic, errors smaller than 10 m were estimated.

Seismic surveys were performed simultaneously using EG&G shallow seismic boomer system (0.5–15 kHz). The penetration depth of several tens of metres below the shelf bottom was achieved with a vertical resolution of 0.3 m. The fragments of boomer profiles used in this study were processed by NWC software (Nautic Nord GmbH) to filter frequencies of noise.

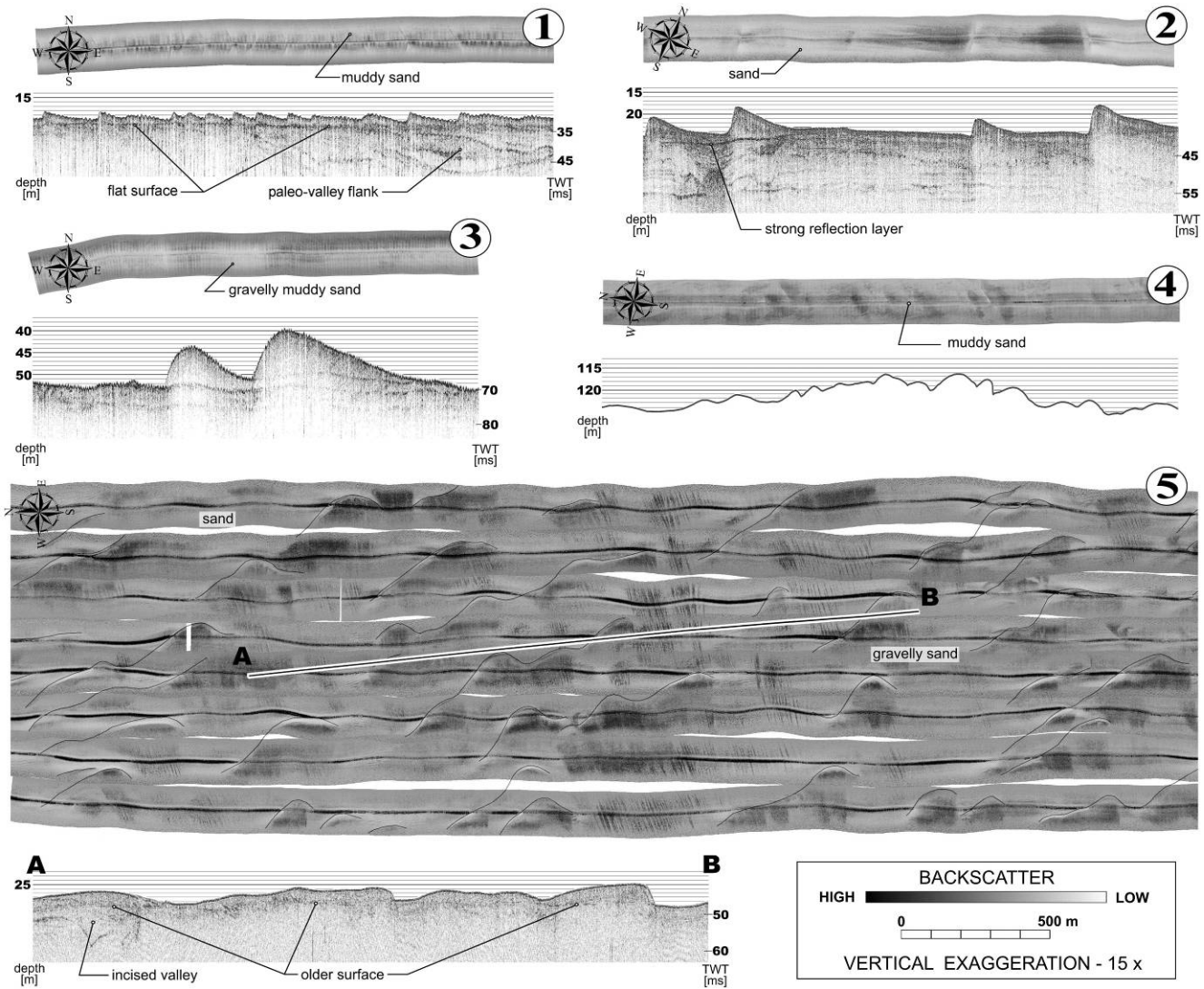


Figure II.4. Sonographs and sub-bottom profiles of dunes (where available) representative for selected zones (see Fig.II.1 for location). Vertical and horizontal scales are the same for each of the images. Note various geographical alignments of sonographs. In example '5' dune crests were delineated in order to highlight dunes shapes.

In order to calibrate sonographs for sediment mapping, during both campaigns, VG-5 and VG-9, in total 59 sediment samples were collected with a HELCOM standard Van Veen grab sampler and a box corer. All samples were treated by grain size analysis following [FOLK \(1954\)](#). This data base, together with results from [NGUYEN V.T. \(1996\)](#) and [NGUYEN B. \(2000\)](#), enabled an accurate identification of sediment types, which form the investigated dunes.

All noticeable subaqueous dunes higher than 1.5 m were identified. Their heights and lengths were computed based on sonographs and data recorded by a single-beam echosounder (Fig.II.5). The orientation of the dunes as a perpendicular to a dune crest line was estimated based on the widths visible within the swath of the sonographs. It should be therefore noted that the results may contain slight inaccuracies since the majority of the sand dune fields were crossed only once.

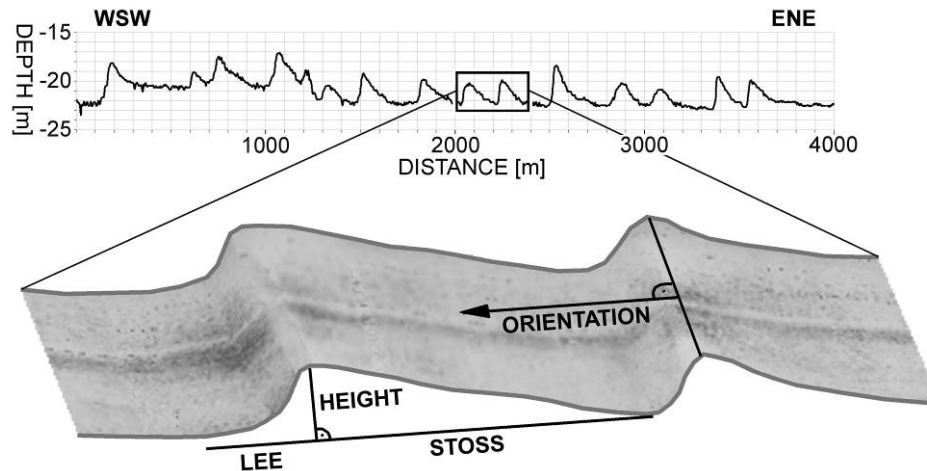


Figure II.5. Example of determining dune parameters based on sonograph and cross section of profile 22040501 in Zone '2'.

II.5 Results

II.5.1 Surficial sediments

The sand fraction (2000-63 μm) dominates the area of investigation, with exception of the vicinity of the Mekong delta and several paleo-valleys, which are filled significantly with silt and clay (< 63 μm) (Fig.II.1). In few samples appears a gravel fraction (up to 20% of sample weight). Such samples were taken mainly close to volcanic rocks protruding from the seabed. The surface layers of all identified dunes were composed mainly of sand (at least 70% in each sample) (Fig.II.1). A median grain size (d_{50}) was obtained typically in a range between 100 and 300 μm what suggested a dominance of medium, fine and very fine sand on the SVS.

II.5.2 Dunes parameters

The study area was divided into five zones (Fig.II.1), taking into account the average parameters of the identified dune fields or single dunes. The parameters for all the zones are summarised in Table II.2. A representative example of collected sonographs for each of the zones is presented together with an image of a seismic profile (when available) (Fig.II.4).

Table II.2. Number of interpreted dunes N_d , number of available sediment samples N_s , average grain size d_{50} , depth d , dune length L , dune height H , asymmetry ratio L_{STOSS}/L , depth integrated velocity generating dunes \bar{u} calculated from Eq. (II.1) and critical velocity mobilising sediment V_{cr} calculated from Eq. (II.5) in distinguished zones (see Fig.II.1. for locations).

	N_d	N_s	Average values					\bar{u} [m/s]	V_{cr} [m/s]
			d_{50} [μm]	d [m]	L [m]	H [m]	L_{stoss}/L		
Zone '1'	17	5	155	19	125	2.1	0.82	0.8	0.14
Zone '2'	23	3	120	27	275	3.4	0.84	1.0	0.14
Zone '3'	10	4	240	43	256	5.4	0.78	1.1	0.24
Zone '4'	11	1	105	119	152	2.8	0.69	0.7	0.23
Zone '5'	24	5	195	29	340	3.3	0.91	0.9	0.19

Zone '1' covers a shallow part (between 15-25 m of water depth) close to the Mekong and Saigon river mouths. In this area the shelf architecture showed a wide paleo-valley (Fig.II.4). It was also evidenced by a depression visible in the bathymetrical charts. The valley was mainly filled with silt and clay (at least 50% of samples). The observed dunes were situated on valley banks and they were composed of muddy sand (following classification of [FOLK, 1954](#)). Their 3-dimensional shapes were mostly barchanoid. They appeared to be the smallest subaqueous dune formations in the region (Fig.II.6a) with heights not exceeding 3 m and lengths smaller than 200 m. Almost all dunes showed an asymmetrical profile (average asymmetry ratio 0.82) with lee slopes oriented towards West (Fig.II.3).

Zone '2' combines dunes identified in the most southwestern part of the investigation area. Here, dunes were observed at water depths from 20 to 35 m. They were typically composed of fine sand (Fig.II.1). Dunes of various dimensions were identified, exceeding a height of 6.4 m and a length of 460 m. This qualified few of them as very large (Fig.II.6a). Dunes in this zone were generally 2-dimensional, all asymmetric (average ratio 0.85), with lee slopes exposed towards WSW. Several incised valleys were visible in a sub-bottom profile.

They were filled with sediment and on top a strong reflectance horizon can be observed, which built a clear boundary between surficial sediments and the sub-bottom (Fig.II.4).

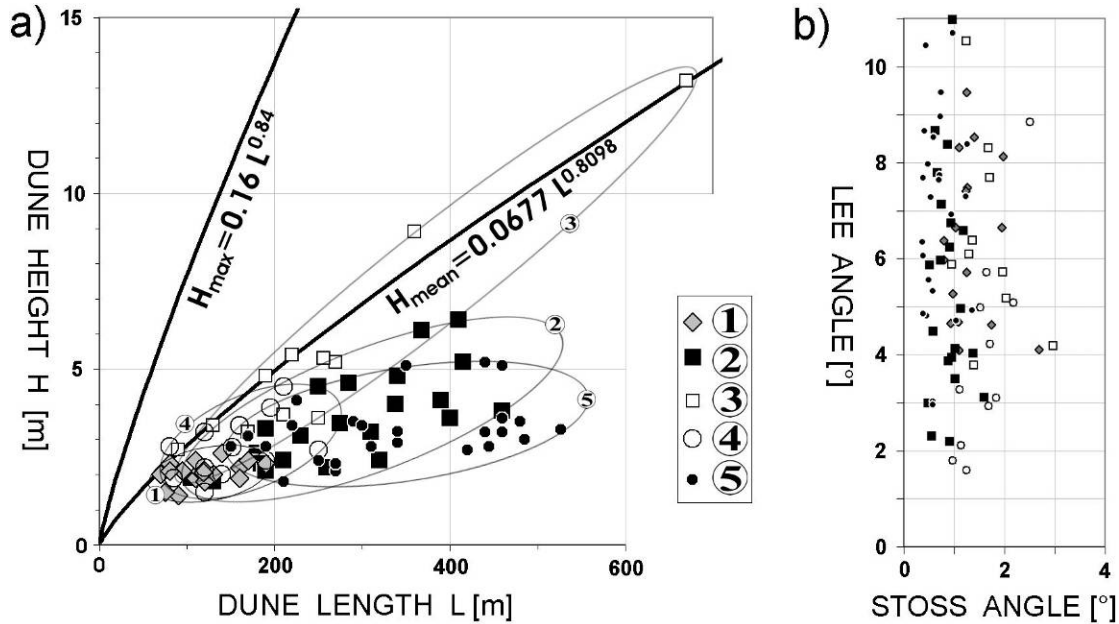


Figure II.6. a) Scatter diagram of dune height (H) against dune length (L) observed in the study area. Dunes are grouped into identified five spatial zones. Average as well as maximum parameters of subaqueous bedforms are plotted after FLEMMING (1988) for comparison. Note smaller heights and flatter profiles of dunes on southern Vietnamese shelf comparing to world data; b) diagram of lee slope angle against stoss slope angle determined for investigated dunes. Average asymmetry ratios may be found in the text.

In zone '3' the largest two dunes (about 9 and 13 m high) of SVS were discovered (Fig.II.4). The heights of other dunes in this zone were between 3 and 6 m and their lengths were smaller than 300 m. All dunes were asymmetric (average ratio 0.78), with lee slopes exposed towards W-WSW. Both 2- and 3-dimensional shapes were recorded. Dunes were composed of slightly gravely and gravely muddy sand (Fig.II.1). No large dune in this area was observed at depths less than 30 m. It is crucial to note that the largest two dunes influence average dune parameters in this zone (Tab.II.2).

Dunes grouped in zone '4' were located where the SVS deepens into a terrace-like wide step, between 100 and 150 m water-depth (Fig.II.1). Due to technical issues neither sub-bottom profiling nor grab sampling took place in the vicinity of dunes. Sidescan sonar backscatter values suggested however that the observed dunes are formed from muddy sand (Fig.II.1). Dune parameters were not significant in a regional comparison (Fig.II.6a). All of them were identified as large, 2-dimensional and their asymmetrical shape was less obvious

(average asymmetry ratio 0.69) (Fig.II.6b). What distinguished them from all studied sand bodies apart from the depth of occurrence was southern to south-southeastern orientation (Fig.II.3).

Dunes in zone '5' were crossed along their troughs and thus their 3-dimensional shapes were well recorded (Fig.II.4). Their shape rather than dimensions distinguished these dunes from those in zone '2' (Fig.II.6a). Here dunes were mainly large with a few examples being very large, but not exceeding 6 m in height and 550 m in length. All observed dunes were asymmetric (average ratio 0.91) and appeared at depths between 25-35 m. They were composed of sand with locally some minor percentage of gravel (Fig.II.1). The sub-bottom profiles revealed completely filled valleys and a flat surface of stronger reflectance underneath the sand bodies.

II.6 Discussion

II.6.1 Dunes parameters

Single dunes heights and lengths were compared to the global average sizes collected by FLEMMING (1988) (Fig.II.6a). Dimensions of dunes of SVS fall within the worldwide scatter-band, but the plot revealed their smaller dimensions and flatter profiles than the average values. This feature might be caused by smaller sediment grain sizes, or lower energy of the enclosed SCS comparing to exposed oceanic shelves. It can be also speculated that dunes are reshaped relict features. The relict origin is likely for the two largest dunes of SVS. Assuming similar geological and hydrological conditions in Zone '3', the two dunes must have been generated otherwise.

The majority of asymmetric dunes plotted on a map showing the orientation of the dunes (Fig.II.3) suggests the probability of dunes migration across the SVS during the NE monsoon. The lee sides of dunes situated shallower than 100 m are exposed towards SW-W what corresponds to a general winter monsoon circulation over the SVS (see Fig.II.2, A,B,C). Dunes of zone '4' are oriented towards SSE, what may be related to the morphology of this part of the shelf. The underwater ridge, of which the Cu Lao Thu Island is exposed over the sea-surface is a natural barrier for water masses. Winter near-bottom currents along the central Vietnamese coast are likely to continue moving southwards along the visible contour

of 100 m depth. This theory is supported by in-situ measurements (Tab.II.1, station 'f') and numerical modelling results (Fig.II.2, station D).

The discontinuity surfaces visible in boomer profiles (Fig.II.4, locations '1', '2', '5') directly below the dune fields support the migration theory. Such a sedimentological layout indicates that the top layer can be originating from elsewhere (KOMAR, 1976) and dunes were migrating into this area after the Paleo-Mekong valleys had been filled up with modern sediment

Precise morphodynamics studies like performed ERNSTSEN ET AL. (2006) using series of precisely positioned multi-beam soundings, or KNAAPEN ET AL. (2005) additionally supported with fixed markers, could not be carried out. Such studies would be very difficult to perform over wide areas of the SVS and therefore no direct evidence for dunes migration exists.

II.6.2 Dunes migration

Based on average parameters of the identified dunes (Tab.II.2), depth-averaged current velocities, which are necessary to generate observed dunes were estimated for each of the five zones. Out of many empirical formulae, the approach of YALIN (1964) was chosen as the most commonly used, even though it was developed for steady uni-directional flows in non-marine conditions (SOULSBY, 1997). Yalin estimated a height of a dune as

$$H = \frac{d}{6} \cdot \left(1 - \frac{\tau_{cr}}{\tau_{0s}} \right) \quad (II.1)$$

Where d -water depth, τ_{cr} - critical bed shear-stress and τ_{0s} - bed shear-stress due to skin friction. This equation can be applied for $\tau_{cr} \leq \tau_{0s} < 17.6 \tau_{cr}$, because otherwise the water flow does not initiate bedforms (YALIN, 1964).

The critical shear stress τ_{cr} is defined as

$$\tau_{cr} = \theta_{cr} \cdot g \cdot (\rho_s - \rho) \cdot d_{50} \quad (II.2)$$

where g -gravitational acceleration, ρ_s -density of bed sediment, ρ -density of sea water, d_{50} - median grain size and θ_{cr} – critical Shield's parameter defined by SOULSBY AND WHITEHOUSE (1997) as

$$\theta_{cr} = \frac{0.3}{1 + 1.2 \cdot D_*} + 0.055 \cdot [1 - \exp(-0.02 \cdot D_*)] \quad (II.3)$$

where $D_* = \left[\frac{(\rho_s / \rho - 1) \cdot g}{\nu^2} \right]^{1/3} \cdot d_{50}$, and ν is the kinematic viscosity.

The bed shear-stress due to skin friction τ_{0s} is denoted by

$$\tau_{0s} = \left[\frac{\bar{u}}{7} \cdot \left(\frac{d_{50}}{d} \right)^{1/7} \right]^2 \cdot \rho \quad (II.4)$$

where \bar{u} is the depth-integrated current velocity capable of generating dunes of height H .

Thus obtained depth-integrated velocities in a range between 0.7 to 1.1 m/s (see Tab.II.2) appear to be higher than velocities reported for this region. LANH AND HOAN (2002) collected mean velocity values of 0.24 to 0.45 m/s in zones '3' and '4'. The HAMSON model results suggested similar flow velocities in other parts of the SVS. The southward winter current reported by NINH (2003) did exceed 0.7 m/s along the central Vietnamese shelf. There exist, however, no winter measurement data confirming that it enters the SVS undisturbed. In terms of the available data, it is therefore not clear how the dunes were generated and how their heights prevail.

The hydraulic data seems to be also insufficient to validate theory on mobilisation of sediment forming dunes. According to VAN RIJN (1984) critical velocity needed to transport grain sizes smaller than 500 μm can be estimated from empirical equation

$$V_{cr} = 0.19 \cdot (d_{50})^{0.1} \log(4d / d_{90}) \quad (II.5)$$

where d_{90} is approximately $d_{50} \cdot 1.5$. The calculated mean grain sizes can be put in motion by flow velocities of 0.14 to 0.24 m/s (see Tab.II.2). The measurement executed closest to seabed was elevated 3 m over the bottom (LANH AND HOAN, 2002) and showed the maximum velocity of 0.38 m/s (Tab.II.1,'b'). The local seabed morphology at point 'b' remained unknown, but if 3-metre high dunes were present in the area, the recorded water flow would be able to mobilise at least the tops of their crests. Any sediment transport computations, however, remain speculative without more accurate hydrological data covering at least one monsoon cycle in few locations on SVS.

II.7 Conclusions

Sidescan sonar data collected on the SVS at the end of winter monsoon period revealed the dominance of asymmetrical sand dunes, oriented generally towards the Southwest at depths shallower than 60 m and towards the South in the deeper, eastern part of the SVS. These azimuths show a relationship with winter water circulation directions as evidenced by *in-situ* measurements and numerical models results.

The investigated large and very large dunes on the SVS are of smaller dimensions compared to dunes from other parts of the world collected by FLEMMING (1988), what may indicate lower energy environment on SVS, or simply smaller grain-sizes of sediment building dunes.

Material forming some of the dune fields was probably of external origin, what suggested strong reflectance horizons beneath dunes visible in seismic profiles.

The dunes generation and prevailing is expected to occur at depth-integrated velocities ranging from 0.7 to 1.1 m/s, which are estimated for average parameters of sand dune fields (i.e. dunes height, mean grain size and depth of occurrence). *In-situ* current velocity measurements performed by other authors yielded values below the calculated thresholds. It should be stressed however, that the computations were based on the formulae of YALIN (1964), which were derived for steady-flow conditions.

. Reported near-bottom maximum velocities suggest that the occurrence of conditions allowing mobilisation of average particle sizes is likely. The data set however, lacks comparable material at the chosen locations during the yearly monsoon cycle.

It is concluded that the observed large and very large dunes on SVS could be either active geomorphological bedforms whose migration paths are induced by the monsoon water circulation, or relict features whose crests are only reshaped by the monsoon cycle.

Acknowledgements

This work was funded by the Deutsche Forschungsgemeinschaft (DFG) (grant code: STA401/10-1,2). The author also wishes to thank the captain and crew of R/V *Nghien Cuu Bien* as well as the shipboard scientific party and irreplaceable technicians Helmut Beese and Eric Steen. Chief scientists Karl Stattegger and Nguyen Tien Hai are greatly acknowledged for making impossible arrangements happen. Hartmut Hein, Robert Jagodzinski, Alex Schimanski, Witold Szczucinski, Jort Wilkens, Christian Winter and above all Klaus Schwarzer are deeply thanked for valuable critics, hints and precious comments on early versions of the manuscript. Last but not least Patrycja Czerniak and Bui Viet Dung are acknowledged for enormous help in a multilingual literature study.



Morphological evolution of gravel and sand extraction pits, Tromper Wiek, Baltic Sea

Adam Kubicki ^{a,*}, Faustino Manso ^b, Markus Diesing ^a

^a *Institute of Geosciences, Christian-Albrechts-University, D-24118 Kiel, Germany*

^b *Geological Survey of Denmark and Greenland, Øster Voldgade 10, DK-1350 Copenhagen K, Denmark*

Received 7 June 2006; accepted 19 September 2006

Available online 7 November 2006

Abstract

The growing demand for marine mineral resources introduces anthropogenic impacts in the coastal zone, among others also through aggregate dredging. Pits created by anchor hopper dredging may affect local sediment budgets, local hydrodynamics and biological habitats. In this study we investigate the processes and time-scales of pits refilling at two extraction sites over 6 years following cessation of dredging. We focused on the evolution of a single pit at a gravel extraction site and the development of a group of three pits located at a sand extraction site. In the case of the gravel pit, a series of six sonograph and two multibeam surveys were evaluated. We observed a spatial expansion of the edge of the pit, decreasing availability of screened sand in the neighbourhood of the pit (a possible source of refilling), and a slowing down of the refilling process with time. At the sandy pit site a series of seven sonographs and two multibeam surveys were available. We observed a smoothing of the edges and larger mean refilling rates than in the gravel pit case. We conclude that the most effective method for monitoring of pit evolution is to make measurements every six months by simultaneously deploying sidescan sonar and multibeam devices.

© 2006 Elsevier Ltd. All rights reserved.

Keywords: dredging effects; monitoring; physical regeneration; western Baltic Sea

1. Introduction

In recent years, marine aggregates (sand and gravel) have become an important resource for the construction industry and for coastal protection. On a European scale, the demand for such resources has steadily increased since the 1980s (ICES, 2001).

Offshore sediment extraction, however, can have a negative impact on the marine environment and due to the dynamic nature of the sea, such impacts may not only be restricted to the immediate area of extraction. The size of the impacted area is dependant on factors such as the environmental conditions, the type of the extracted resources, the benthic life within the extraction area, and the method of extraction. Several studies have addressed the issue of dredging impact on the environment

and the recovery of benthic habitats and species (Kenny and Rees, 1994, 1996; Desprez, 2000; van Dalssen et al., 2000; Sarda et al., 2000; van Dalssen and Essink, 2001; Boyd and Rees, 2003; Boyd et al., 2004, 2005; Krause et al., submitted for publication). In addition, dredging close to the shore might cause unwanted impacts on the coastal sediment budget (Nielsen et al., 1991; Hilton and Hesp, 1996; Otay et al., 2002; Work et al., 2003). Therefore, when planning and granting new extraction sites, it is necessary to estimate possible negative influences on the marine environment and coastal stability.

In German waters of the Baltic Sea, two different methods of aggregate extraction are commonly practised. In the case of trailer-suction hopper dredging, extraction is carried out using a moving ship, which leads to the production of shallow linear furrows. On the other hand, anchor hopper dredgers remain stationary over the deposit and mine it by forward suction through a pipe. In this case, dredging usually results in the formation of pits typically up to 10 m in depth below the seafloor and 10–50 m in diameter (HELCOM, 1999; Boyd et al., 2004).

* Corresponding author.

E-mail address: akubicki@gpi.uni-kiel.de (A. Kubicki).

III CASE STUDY ON EXTRACTION PITS - MORPHOLOGICAL EVOLUTION OF GRAVEL AND SAND EXTRACTION PITS, TROMPER WIEK, BALTIC SEA

III.1. Abstract

The growing demand for marine mineral resources introduces anthropogenic impacts in the coastal zone, among others also through aggregate dredging. Pits created by anchor hopper dredging may affect local sediment budgets, local hydrodynamics and biological habitats. In this study we investigate the processes and time-scales of pits refilling at two extraction sites over 6 years following cessation of dredging. We focused on the evolution of a single pit at a gravel extraction site and the development of a group of three pits located at a sand extraction site. In the case of the gravel pit, a series of six sonograph and two multibeam surveys were evaluated. We observed a spatial expansion of the edge of the pit, decreasing availability of screened sand in the neighbourhood of the pit (a possible source of refilling), and a slowing down of the refilling process with time. At the sandy pit site a series of seven sonographs and two multibeam surveys were available. We observed a smoothing of the edges and larger mean refilling rates than in the gravel pit case. We conclude that the most effective method for monitoring of pit evolution is to make measurements every six months by simultaneously deploying sidescan sonar and multibeam devices.

III.2. Introduction

In recent years, marine aggregates (sand and gravel) have become an important resource for the construction industry and for coastal protection. On a European scale, the demand for such resources has steadily increased since the 1980s (ICES, 2001).

Offshore sediment extraction, however, can have a negative impact on the marine environment and due to the dynamic nature of the sea, such impacts may not only be restricted to the immediate area of extraction. The size of the impacted area is dependant on factors such as the environmental conditions, the type of the extracted resources, the benthic life within the extraction area, and the method of extraction. Several studies have addressed the issue of dredging impact on the environment and the recovery of benthic habitats and

species (KENNY AND REES, 1994, 1996; DESPREZ, 2000; VAN DALFSEN ET AL., 2000; SARDA ET AL., 2000; VAN DALFSEN AND ESSINK, 2001; BOYD AND REES, 2003; BOYD ET AL., 2004, 2005; KRAUSE ET AL., submitted for publication). In addition, dredging close to the shore might cause unwanted impacts on the coastal sediment budget (NIELSEN ET AL., 1991; HILTON AND HESP, 1996; OTAY ET AL., 2002; WORK ET AL., 2003). Therefore, when planning and granting new extraction sites, it is necessary to estimate possible negative influences on the marine environment and coastal stability.

In German waters of the Baltic Sea, two different methods of aggregate extraction are commonly practised. In the case of trailer-suction hopper dredging, extraction is carried out using a moving ship, which leads to the production of shallow linear furrows. On the other hand, anchor hopper dredgers remain stationary over the deposit and mine it by forward suction through a pipe. In this case, dredging usually results in the formation of pits typically up to 10 m in depth below the seafloor and 10-50 m in diameter (HELCOM, 1999; BOYD ET AL., 2004).

In the Tromper Wiek, the study area discussed in this paper (Fig.III.1), several investigations of sediment extraction effects have been carried out in the past (FIGGE ET AL., 2002; DIESING, 2003; KLEIN, 2003; ZEILER ET AL., 2004; DIESING ET AL., 2006), and short-term changes within dredged areas have been discussed for both offshore gravel and sand extraction sites.

Several monitoring techniques are available for assessing the regeneration of aggregate extraction sites (BOYD, 2002). These include, among others, sidescan sonar and multibeam echo-sounding combined with grab sampling for ground-truthing purposes. Sidescan sonar can provide high-resolution, geo-referenced acoustic images of the seafloor and is, therefore, a useful tool for identifying structures resulting from aggregate extraction. Detailed investigations of small-scale bathymetric features and quantitative assessments of volume changes require the use of multibeam echo sounders together with high-precision positioning systems.

In this paper, we present a unique data set that was collected using the above methods. A six-year period of pit evolution (1999-2005) is interpreted, discussed and compared with previous studies in order to identify the processes and speed associated with natural refilling of pits created by anchor-suction hopper dredging.

III.3. Setting

Two extraction sites, the Tromper Wiek Ost and the Tromper Wiek 1 have been investigated in this study. Both are situated in the southern Baltic Sea (Fig.III.1), a practically non-tidal epicontinental shelf sea in northern Europe. According to the classification of DAVIS AND HAYES (1984), both study sites can be described as wave-dominated environments.

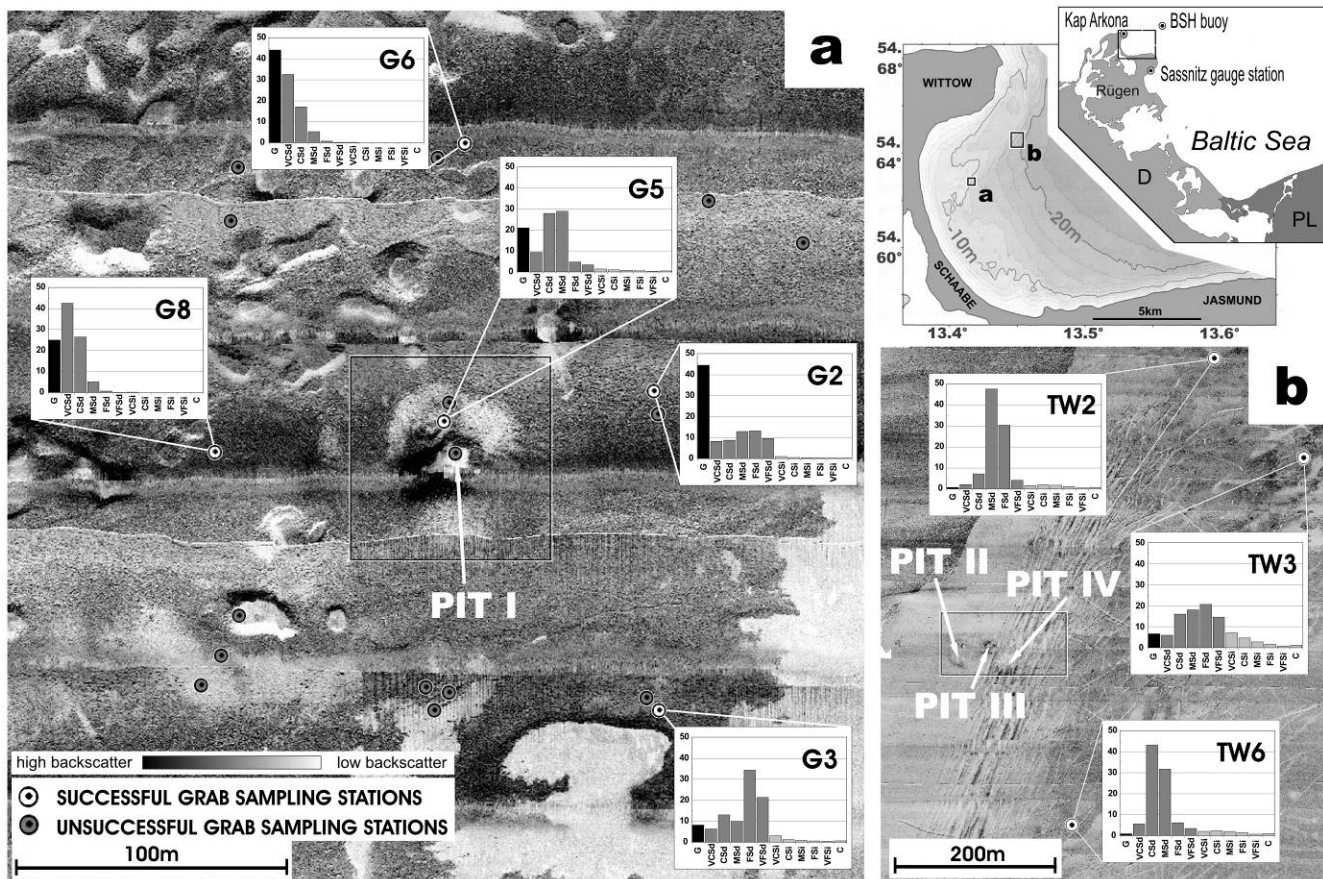


Figure III.1. Location of Tromper Wiek Bay and the pits selected for the study in a) the gravel extraction area (sonograph from December 2003) and b) the sand extraction area (sonograph from December 2000). The histograms show the percentage of different sediment fractions in grab samples. Sonographs are geographically aligned.

The Tromper Wiek is a semi-enclosed bay located in the NE of Rügen Island (Fig.III.1). Two protruding headlands (Jasmund and Wittow) are connected by a dune-topped spit (Schaabe), which developed during the last 6000 years (SCHUMACHER AND BAYERL, 1999). The bay opens towards the northeast. Westerly winds dominate in this area, but due to the coastal configuration, high waves are only generated by easterly winds which are common during

spring. Northerly winds are rare (MOHRHOLZ, 1998). Wave energy measured at a water depth of 25 m between March 2000 and June 2001, is dominated by short-period wind waves with an average significant wave height of 0.48 m and a maximum significant wave height of 3.9 m. Average and maximum zero-crossing periods amount to 3.12 s and 6.6 s, respectively (KLEIN AND MITTELSTAEDT, 2001).

KLEIN (2003) found a high correlation ($r = 0.9$) between the significant wave heights at the location of the gravel extraction site and the speeds of wind blowing only from the quadrant $0-90^\circ$ recorded at Kap Arkona station (see Fig.III.1 for location). He also observed a correlation ($r = 0.94$) between significant wave heights coming from this quadrant and bottom orbital velocities at gravel pit. He estimated that the bottom orbital velocities necessary to exceed the threshold of sediment motion (according to KOMAR, 1976) are as high as 0.43 m/s for gravel (>2 mm) and 0.2 m/s for medium sand (0.25-0.5 mm). The significant wave height required to put sediment into motion was thus calculated to be 3.0 m for gravel and 2.0 m for medium sand, which requires wind speeds of 25 m/s and 20 m/s, respectively.

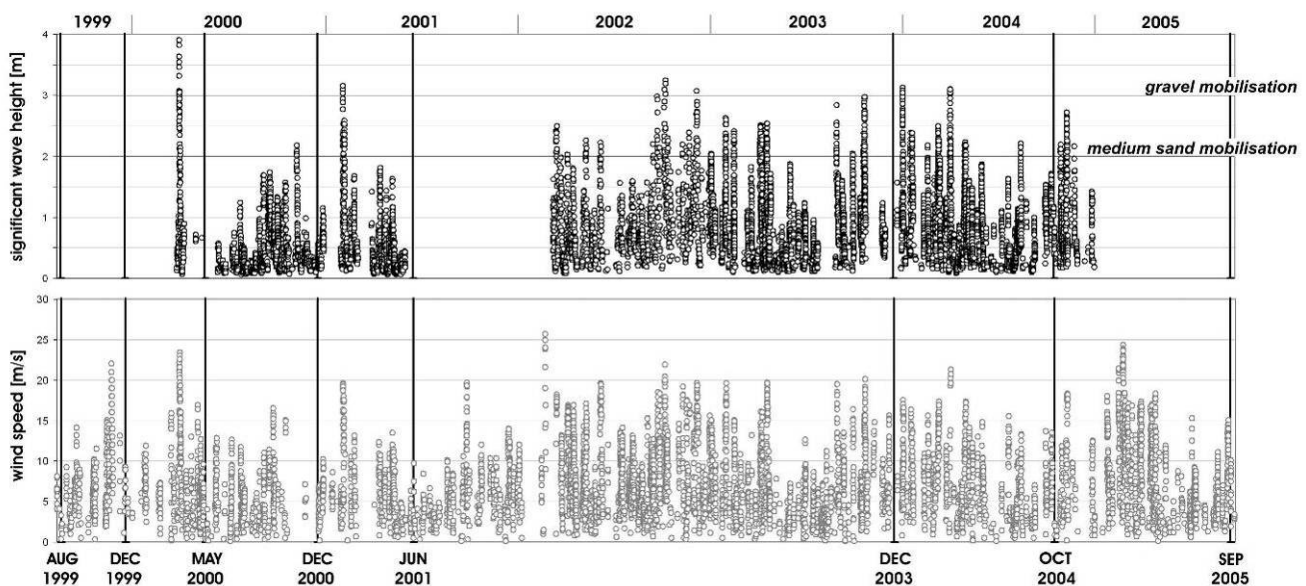


Figure III.2. Significant wave heights and wind speeds from the $0-90^\circ$ quadrant in Tromper Wiek. Sediment mobilisation lines are drawn according to KLEIN (2003). The measurement campaigns are marked with vertical bold lines.

Wind speeds for winds blowing from the sector between 0° and 90° at Kap Arkona are presented in Fig.III.2, covering the entire monitoring period between August 1999 and

September 2005. Significant wave height readings from Acoustic Doppler Current Profilers (ADCPs) deployed in Tromper Wiek and from a BSH (Federal Maritime and Hydrographic Agency) buoy located in the entrance to Tromper Wiek (see [Fig.III.1](#) for location) are also presented in [Fig.III.2](#).

The seafloor at the Tromper Wiek Ost extraction site is characterized by fine sands in water depths between 14 and 21 m. Sand has been extracted on two occasions at this site using trailer-suction dredging: 151,000 m³ in 1989 and 104,000 m³ in 2000 (W. Sorge, Bergamt Stralsund, personal communication).

The Tromper Wiek 1 extraction site is situated at water depths between 9 and 14 m. Here, the seafloor is covered by sandy gravel forming prominent NE-SW-trending ridges, interpreted as the relicts of a drowned beach-ridge system dating back to the Late Pleistocene ([SCHWARZER ET AL., 2000](#)). The sediment is extracted by anchor hopper dredging. After extraction, the material is screened on board so that sediments with grain sizes less than 2 mm are sorted out and returned to the sea (screened sand fraction). Between 1988 and 2000, approximately 460,000 m³ of sediment were extracted, approximately 50% of which was rejected after screening (K. Brauckhoff, Müsing GmbH, personal communication).

III.4. Materials and methods

Pits within marine gravel and sand areas were monitored by seven sidescan sonar surveys in August 1999, December 1999, May 2000, December 2000, June 2001, December 2003, and October 2004. Several grab-sampling stations were used for ground-truthing of the sonographs. In addition, multibeam bathymetry surveys were performed in December 2003 and September 2005. The centre of the selected gravel pit (Pit I) is located at 54.62920° N; 13.42041° E. At the sand extraction site, a group of three pits was selected for investigation. The individual pits are labelled in ascending order from the western-most (Pit II) to the eastern-most (Pit IV). The most recent position determined for the centre of the middle pit (Pit III) is 54.64675° N; 13.45118° E (see [Fig.III.1](#) for pit locations).

III.4.1 Sidescan sonar

For sea-bed mapping, a Klein 595 sidescan sonar was used with a scanning frequency of 385 kHz and a range of 50 m along each profile line. Data collection and post-processing were performed using the ISIS software (Triton Elics). Seven surveys were carried out within a six-year period (Tab.III.1). Sea-states varied from survey to survey, October 2004 survey being particularly negatively affected. The sidescan sonar was towed behind the research vessel with different cable lengths during different cruises. To account for these different lengths, a layback correction was applied. However, even though the application of this correction improved the position of bottom features, a considerable local spatial error remained. For more precise matching of different sets of sonographs a polynomial based geo-referencing procedure was applied using the ERDAS Imagine software. Polynomial equations are used to convert co-ordinates of the pixels in an image into rectified ones. A geometric correction using a first-degree polynomial equation results in a linear change of pixel position (ERDAS, 1997). The correction can be executed after selecting three Ground Control Points (GCPs), which should be selected as vertices (apexes) of triangles covering the area of interest. Within the gravel extraction site, three groups of boulders visible on all sonographs were selected as stable GCPs. This procedure resulted in a positioning accuracy of better than 2 m. At the sand extraction site there is a lack of stable reference points. Pit bottoms were therefore selected as the least changeable targets that could serve as GCPs for polynomial fitting. In this case, the spatial accuracy of fitting was 10 m at best.

The backscatter values from the area around the edges of the pits usually differ, slopes having higher backscatter intensities than the flat seabed nearby. This is caused by slope exposure rather than different sediment grain sizes. Furthermore, due to the depth of the pits, the pit bottoms are in the acoustic shadow zone at the survey geometry of the sonographs (Fig.III.3a, e.g. images from December 1999 or December 2000). The backscatter from the pit edges contrasts strongly with the lack of backscatter within the acoustic shadow zone. This all allowed a good definition of the rim morphology of the pits.

To better understand collapse processes of the pit walls in the gravel extraction area, the maximum extent of slumps was drawn for every series, as were the inner edges. In addition, a flat pit bottom was delineated for purposes of investigating the geometry of the pit.

Furthermore, the spatial cover of the sand fraction screened during dredging was determined to allow an assessment of the amount of refill material available near the rim of the pit.

Different qualities of sonographs resulted in different backscatter values for the same screened sand fraction. It was therefore not always possible to select the same pixel signatures for all of the images. As a result, the spatial extent of the screened sand was obtained using an unsupervised classification of the pixels comprising the sonograph fragments. During this digital process, all pixel reflection signatures were divided into four equally distributed classes.

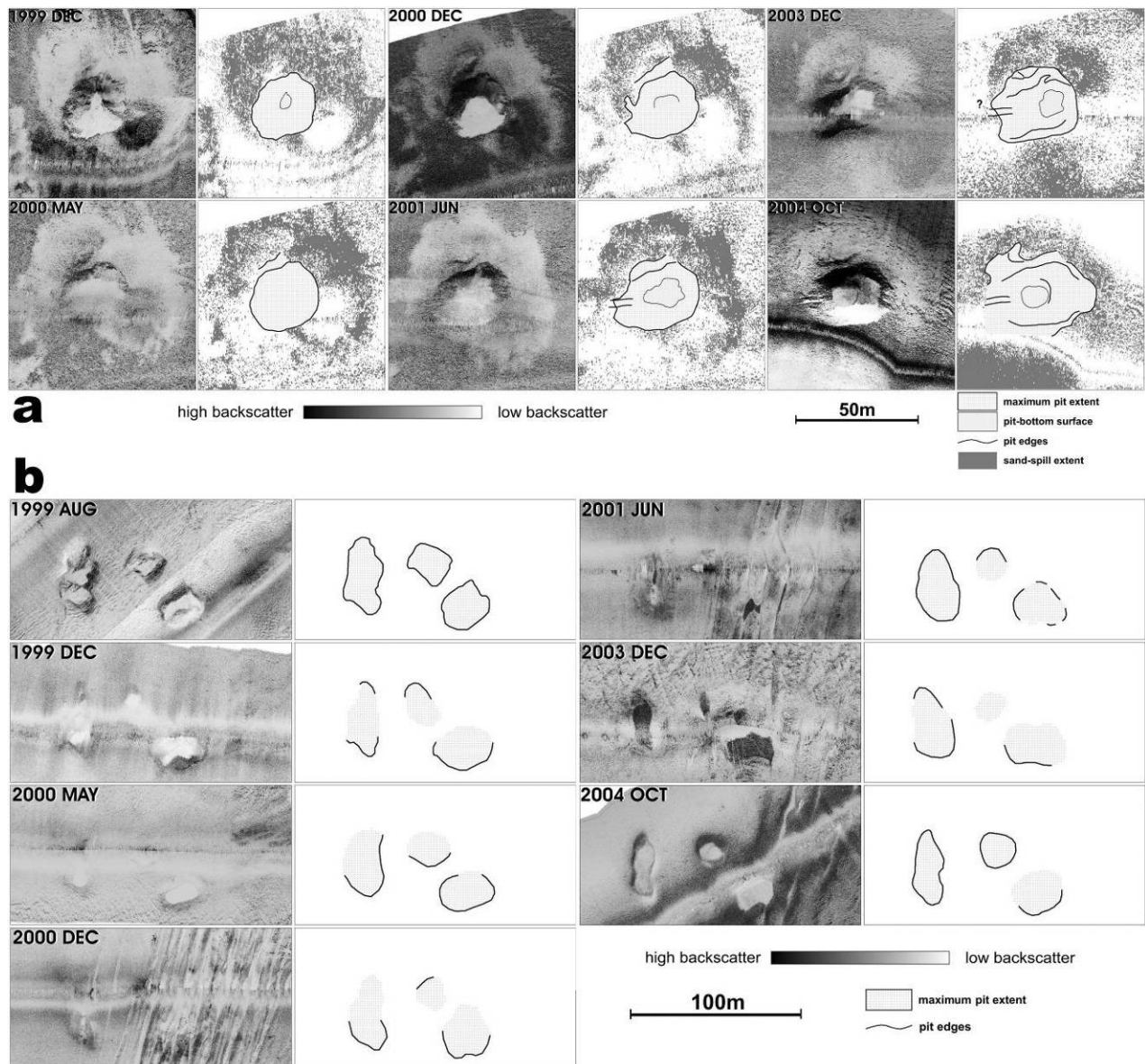


Figure III.3. Series of sidescan sonar images from a) the gravel extraction area and b) the sand extraction area. Each figure is presented together with an interpretation of the sonographs and it is geographically aligned.

We assumed that the class with the lowest reflection values corresponded to the screened sand fraction. For each separate survey, exactly the same area near the pit was classified according to pixel values. This allowed a quantitative comparison of screened sand areas (Fig.III.3a).

At the sand extraction site it was only possible to delineate the pits on the basis of interpreted edges because the character of the edges in the sand environment differs from that at gravel site due to different angles of repose. In sand, the rims are much smoother, and the difference between the backscatter from the walls and from the surface is less obvious. In most of the sonographs, the pits were crossed at the nadir of the tow-fish where slant-range correction leaves the largest uncertainties. In addition, starting with the December 2000 survey, Pit IV was affected by trailing-hopper dredging which crossed the pit several times along a NNE-SSW axis (Fig.III.3b). Due to these factors and the less accurate georeferencing procedure mentioned earlier, the delineation of edges and, consequently, the calculation of pit areas incorporated a significant spatial error.

Table III.1. Data sets interpreted in this study.

Device	Survey Date
Sidescan sonar	August 1999
	December 1999
	May 2000
	December 2000
	June 2001
	December 2003
	October 2004
Multibeam	December 2003
	September 2005
Grab samples (55 samples)	October 2004

III.4.2 Multibeam

A hull-mounted L3/ELAC Nautik Seabeam 1185 multibeam was used for two bathymetric surveys. Both data sets were corrected with respect to contemporary sea level recorded at the gauge station in Sassnitz, 20 km from the investigated area (see Fig.III.1 for location), with several centimetres of confidence. The multibeam emits 126 beams of 180 kHz pulses over a swath width covering about seven times the water depth. Its accuracy exceeds

the minimum standards for hydrographic surveys proposed by the International Hydrographic Organisation (IHO, 1998). The HydroStar software (Elac Nautic) was used for data collection, and HDP Edit and HDP Post software (Elac Nautic) for data processing. The outer 10% of beams, which have the largest error, were excluded from the bathymetric mapping. For each data set, the same area of the gravel and sand extraction sites was examined using the ArcView software (ESRI) to allow spatial comparisons to be made. In addition, vertical cross-sections through the sites were examined to monitor the geometrical shape of the pits and the refilling rate (Fig.III.3).

III.4.3 Grab samples

During the October 2004 survey, a total number of 55 sampling stations were selected at the two extraction sites. The grab samples were obtained using an 80 kg HELCOM-standard Van Veen sampler. Due to direct hits on boulders, most of the grab samples were not successful in the gravel area (Fig.III.1). Sediment from 24 successful samples was analysed by combining dry sieving of the coarser fraction ($>2000\ \mu\text{m}$) with the results Beckman Coulter LS 13320 laser diffraction particle analyses for the fraction 2000-0.4 μm .

III.5 Results

III.5.1 Gravel extraction site

Five successful samples were collected in the vicinity of Pit I (Fig.III.1a). They revealed that the high acoustic reflection was caused by boulders and gravel ($>2\ \text{mm}$) (samples G8, G6, and G2). In the south-eastern part of the area, low backscatter was associated with fine and very fine sand (0.063e0.25 mm) (sample G3). A sample from the screened sand area (sample G5) showed that after screening mostly medium and coarse sand (0.25-1 mm) remained in the area.

Pit I was first detected during the December 1999 survey, no evidence of mineral extraction having been observed in August 1999 at this site. In December 1999, both the edge and the flat bottom of the pit had an almost circular shape, suggesting a cone-like pit geometry (Fig.III.3a). Using trigonometry, we estimated the depth of the pit at 9.3 m on the

basis of the length of the acoustic shadow. This was the best depth estimate at this early stage. The sand screened during the dredging process surrounded the pit in an oval shaped drape. In March 2000, 9 weeks before the next measurement campaign, a major storm occurred during which maximum orbital velocities were able to move gravel-sized particles (Fig.III.2). In the May 2000 sonograph, an acoustic shadow covers the pit interior and bottom (Fig.III.3a) and a slump scar is evident along the northern part of the pit. The coverage of screened sand, as well as the overall shape of the pit edge, were not significantly different from December 1999 survey. In the period before the next sidescan sonar survey, one event with waves higher than 2 m was recorded during which the mobilisation of sand particles should have been possible. However, in the December 2000 sonograph, new edges were observed along the western wall and the northern slump scar was more clearly visible. Although an acoustic shadow partly obscures the pit bottom, enough of the bottom was visible to suggest that its area had more than doubled in the course of 1 year. A depth of 6.5 m from the pit bottom to rim was calculated using the acoustic shadow length. In February 2001, stormy conditions with waves higher than 3 m could have mobilised gravel. The June 2001 sonograph shows that the geometry of the pit edge and bottom became more oval-shaped at its western end. Two parallel morphological ridges cut the western wall. These are interpreted as probably being of anthropogenic origin. Outside the pit, the distribution of screened sand appeared to be very similar to that of December 1999, whereas it clearly differs in the image of December 2003 where the eastern part of the cover seems to have disappeared. Since no sidescan sonar surveys were carried out during the 30 months from June 2001 onward it is not clear when this change took place. There were no wave data available for the period up to February 2002, but wind data and wave data collected in the entrance of the bay suggest that several events occurred at Pit I which were able to move sand and gravel. In December 2003, the sidescan sonar profile crossed the pit at the nadir, but the slant-range correction evidently overstretched the near-range area of the sonograph so that this part cannot be treated as being free of errors. Also, the two parallel ridges identified in the western part of the previous sonograph were no longer visible in December 2003. The image of October 2004, however, suggests that these features actually existed in 2003 (Fig.III.3a). On the image of December 2003 new slumps can be observed along the northern and western walls. After that survey, two strong storms (with significant wave heights greater than 3 m) influenced the

hydrodynamics of the Tromper Wiek. In October 2004 slumping along the eastern wall is evident for the first time. This sonograph was affected by rough seas so that the acoustic reflection values may not be reliable. The screened sand is also not clearly visible.

Table III.2. Quantitative estimates of the extent of the pit and screened sand in the gravel-extraction area.

Date	Pit area [m ²]	Mean Rate Per month [%/month]	Screened sand area [m ²]	Mean Rate Per month [%/month]
December 1999	541.15	0,00	1658.30	0.00
May 2000	612.81	+ 1.89	1561.59	0.83
December 2000	600.99	+ 1.84	1457.68	2.02
June 2001	787.71	+ 2.53	1405.53	0.85
December 2003	853.28	+ 5.77	1381.64 ?	1.67
October 2004	1282.68	+ 13.7	1300.37 ?	2.16

Comparing all the available sonographs, it is evident that the perimeter of the upper rim of Pit I grew with time (Fig.III.4). The largest changes are observed along the western wall, whereas slumping along the relatively stable eastern wall has begun 5 years after the excavation. Tab.III.2 gives values for the pit area and spatial coverage of screened sand. It shows that the pit area expanded at an accelerating rate and that the area of screened sand reduced at variable rates.

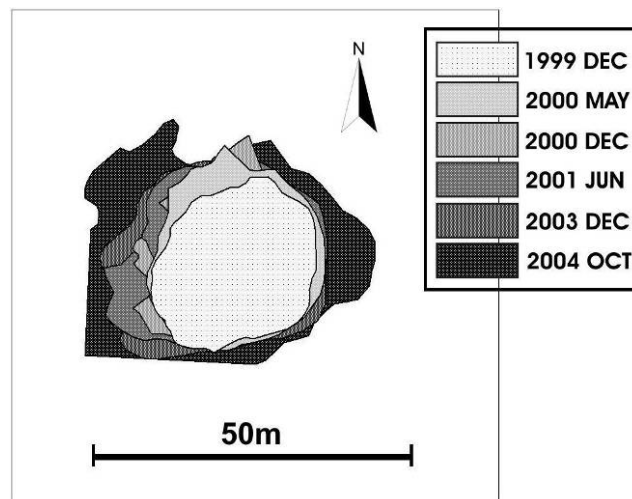


Figure III.4. Spatial comparison of the gravel pit size reconstructed on the basis of individual sonographs.

The multibeam bathymetric map of December 2003 (Fig.III.5a) confirms that the rim of the pit was oval-shaped and elongated in an ENE-WSW direction, as already observed on the

sidescan sonar image. A comparison of the images obtained by the two survey methods suggests that the collapse of the walls identified on the sonographs must have involved a thin sediment layer close to the 12 m depth contour. The deeper contours are almost undisturbed, which suggests that no major slumps occurred in the lower part of the pit. The pit edges, as well as the two parallel ridges in the western wall identified on the sonographs, cannot be seen in the multibeam data due to insufficient resolution. The pit itself is situated in a shallow (less than 50 cm deep) depression, but it is not clear whether the depression is natural or whether it was formed by dredging. The depth of the pit was less than 4 m in 2003, the lowest point of the pit exceeding a water depth of 15.71 m.

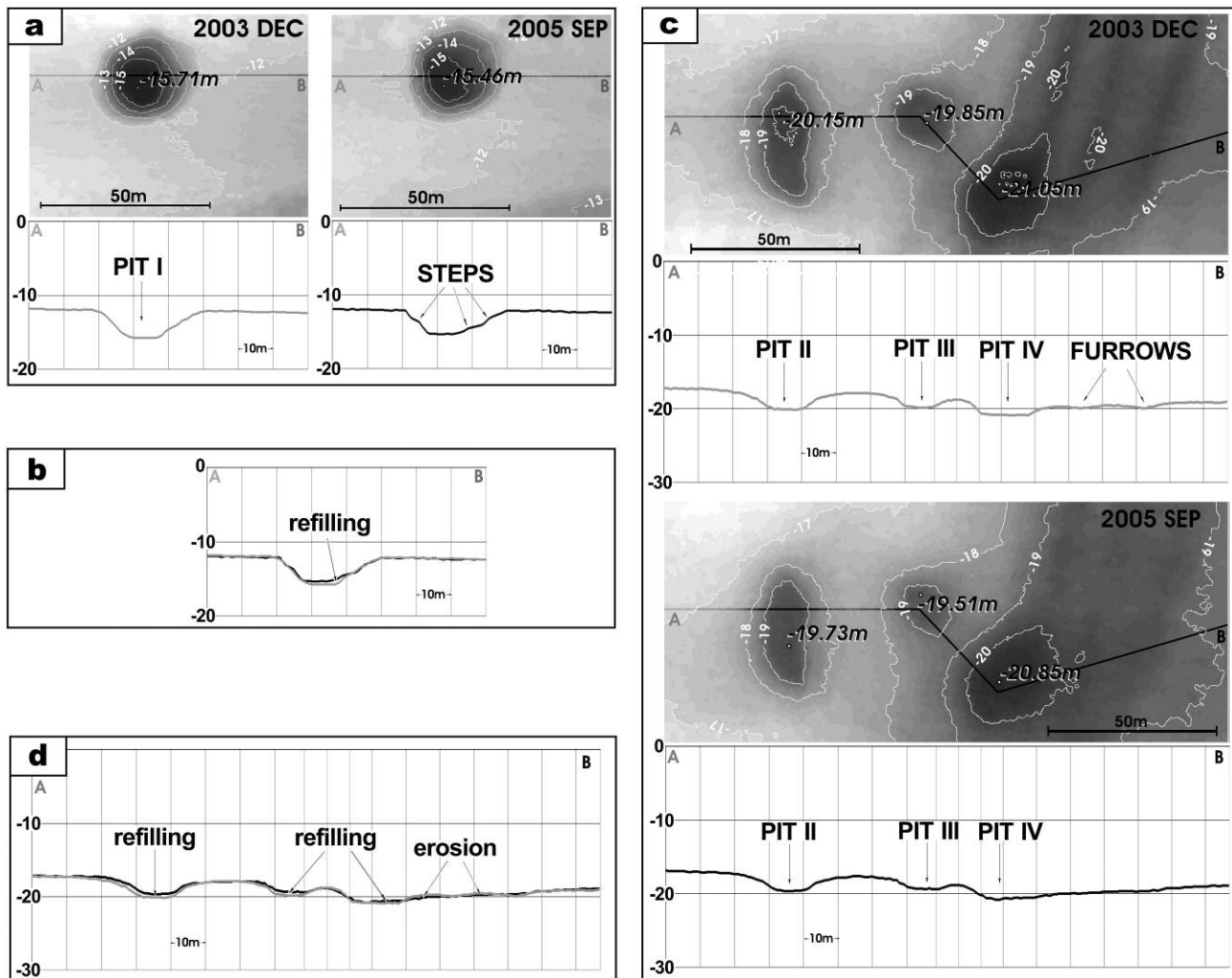


Figure III.5. Comparison of two sets of multibeam measurements. a) Plan-view and b) cross-sections from the gravel-extraction site. c) Plan-view and d) cross-sections from the sand-extraction site.

On the image of September 2005 (Fig.III.5a), the pit architecture had changed markedly. As a result of major slumping, the slope of the eastern wall became more gentle. Comparing the 2005 cross-section with the one of 2003, it surmised that sediment from the edge of the eastern wall had slid into the pit, creating the two terrace-like steps visible in the cross-section (Fig.III.5a). A similar step was developed in the western wall. The maximum depth recorded inside the pit was 15.46 m, which indicated a refilling of 25 cm with respect to the 2003 survey (Tab.III.3). The mean refilling rate of gravel Pit I was thus about 1.2 cm per month in the period between the two multibeam surveys. A comparison of the 2003 and 2005 cross-sections shows that refilling was largest along the eastern wall (Fig.III.5b).

Table III.3. Refilling rate of the pits existing in different sediment between 2003 and 2005.

Pit name	Depth DEC 2003	Depth SEP 2005	Difference	Mean Refilling Rate [cm/month]
Pit I	15.71 m	15.46 m	-25 cm	1.2
Pit II	20.15 m	19.73 m	-42 cm	2.0
Pit III	19.85 m	19.51 m	-34 cm	1.6
Pit IV	21.05 m	20.85 m	-20 cm	0.95

III.5.2 Sand extraction site

No samples were recovered near the selected pits at the sand extraction site. The three nearest samples show that medium and coarse sand (0.25-1 mm) are the dominant size fractions in the area (Fig.III.1b).

In August 1999, the three pits were already present in the area, which means that they are older than gravel Pit I (Fig.III.3b). By December 2000, the rims became smoother and their maximum perimeter increased slightly. Pit IV had a W-E elongated axis in May 2000. The hydrodynamic data for this period are very poor, but the wind data suggest that at least two major events mobilised material in the vicinity of the pits. In December 2000, numerous furrows created by trailing-suction hopper dredgers crossed the pits in the eastern part of the survey area (Fig.III.3b). Pit IV, which was heavily affected by trailing dredgers, changed its shape to become elongated along its N-S axis. The June 2001 sonograph also shows how the trailer dredging changed the inner geometry of Pit IV. The outline of its flat bottom implies further deepening of the pit, the fill probably consisting of shell hash. While the number of visible furrows had decreased, they had also become wider. The sediment in the area was

probably reworked during the storm of February 2001 (Fig.III.2). Many similar storm events took place between June 2001 and December 2003, but the poor quality of the sonograph does not allow the quantification of changes. Despite this, the areas of the flat bottoms of Pits II and IV certainly increased. The lack of clearly visible edges around Pit III in December 2003 is the effect of sonograph quality rather than contemporary morphology. Due to the many uncertainties, a quantification of pit areas was not attempted.

All three investigated pits at the sand extraction site lie in an E-W elongated depression at water depths below 17 m (Fig.III.5c). We assume that trailing-hopper suction dredging deepened the depression in the eastern part of the site, but no data on extracted volumes are available. Multibeam results show that, in December 2003, the western pit was 20.15 m deep, the central pit 19.85 m, and the eastern pit had a maximum depth of 21.05 m. In 2005, the depths were 19.73, 19.51 and 20.85 m, respectively (Fig.III.5c). Pit II, which had the greatest depth (around 2 m) and the steepest walls, was refilled by 42 cm in the two years. The smallest pit in the area, Pit III, was refilled by 34 cm and the Pit IV by 20 cm (Tab.III.3). A relationship between wall steepness and refilling rate is evident. Pit II tended to refill faster, whereas the mean refilling rate of the eastern and shallowest pit (Pit IV) was only half as fast. Cross-sections from 2003 and 2005 confirm that greater refilling took place in the western part of the pits (Fig.III.5d). It is also evident that the furrows in the eastern part of the site were refilled along the line of the cross-section after 2 years.

III.6 Discussion

III.6.1 Refilling of the gravel pit

Pit I was first observed on 5 December 1999. A rough estimate of its depth based on the acoustic shadow was 9.3 m below seabed. Sedimentation rates within Pit I were initially calculated on the basis of a vibro-core. The core, taken on 21 March 2000 in the centre of Pit I, showed 270 cm of refilled material over glacial till (DIESING, 2003). The lower 126 cm of the refilled material consisted of sands showing a normal grading (fining-upward). This section is interpreted as consisting of screened sands deposited within the pit immediately after screening. Considering the grain sizes and the corresponding settling velocities, deposition will have taken place within hours. The next depositional section has a thickness of

53 cm and consists of gravel clasts embedded in a sandy matrix. It was most probably derived from slumping processes due to instabilities of the steep flanks of the pit. This is followed by 69 cm of medium sand which resembles the blanket of screened sand surrounding the pit. This material most likely entered the pit by remobilisation and transport during storm events. The upper 22 cm of the core consisted of mud deposited during fair weather periods (DIESING, 2003).

Assuming the pit was excavated in early August 1999, i.e. immediately after the first sidescan sonar survey, the mean refilling rate would be about 36 cm/month. However, if this pit was created just before the December 1999 survey, then the mean refilling rate would be about 76 cm/month (Fig.III.6). If we do not take into account the 126 cm of almost instantaneously deposited screened sand, then the mean sedimentation rates would be 19 and 41 cm/month, respectively.

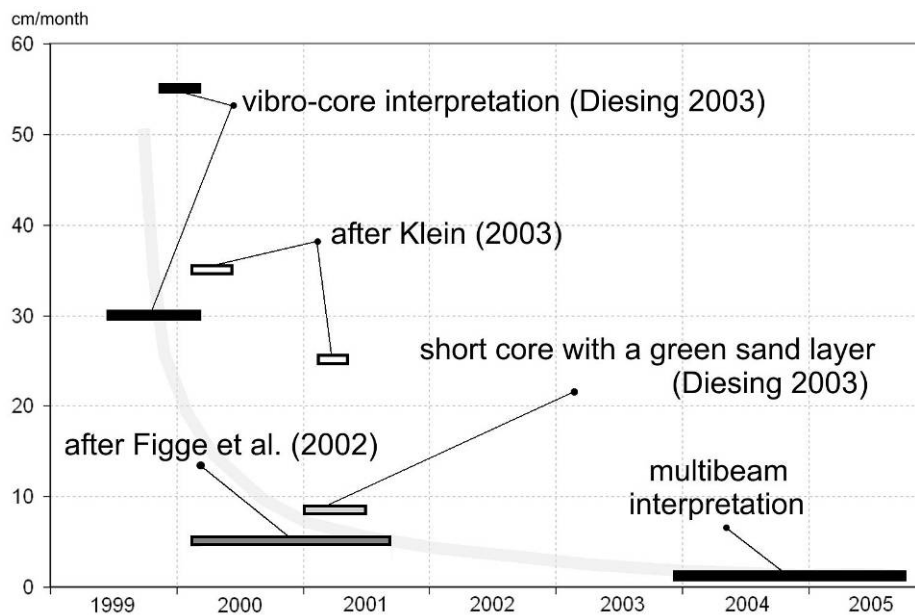


Figure III.6. Summary of the mean refilling rates estimated for the gravel pit (position 54.6292°N; 13.42041°E). The mean refilling rate appears to be slowing down with time.

Observations made by divers when installing the ADCP inside the pit suggest that the refilling rate was about 35 cm/ month between March and June 2000 and about 25 cm/month between March and May 2001 (KLEIN, 2003) (Fig.III.6).

The stratification of the refill sediment consists of cyclic layers of sand and *Mytilus edulis* shells, suggesting that sedimentation inside the pit was episodic rather than continuous (KLEIN, 2003).

In March 2000, a particular point at the bottom of the pit measured by echo-sounder was located at a depth of 17.6 m (DIESING, 2003). Based on the acoustic shadow length observed in the December 2000 sonograph, a relative pit depth of 6.5 m was calculated. Precise multibeam measurements were undertaken in December 2003, i.e. 4 years after dredging. These measurements show that the deepest point of the pit was at 15.71 m below mean sea level. If the echo-sounding measurement made in 2000 were correct, then it can be calculated that the pit accreted by about 1.9 m in 3 years. This is equivalent to the observed amount of sediment that was added by May 2001 (KLEIN, 2003). Between May 2001 and the multibeam measurements in December 2003, however, several storm events took place (Fig.III.2) and some sediment must have fallen into the pit. Therefore, the results of KLEIN (2003) must be treated with some caution.

Tracer experiments performed between January and June 2001 yielded sedimentation values of 34 to 38 cm within 136 days (DIESING, 2003), i.e. a mean refilling rate of ca. 8 cm/month for this period. This differs substantially from the 25 cm/month suggested by KLEIN (2003).

FIGGE ET AL. (2002) calculated that the refill sediment reached a thickness of 94 cm between March 2000 and September 2001, giving a mean refilling rate of 5 cm/month. Assuming that this value is representative for the time between September 2001 and the multibeam survey in December 2003, sediment must have been entering the pit at a mean rate of 3.5 cm/month. We calculated that the mean refilling rate of Pit I was as much as 1.2 cm/month in the period from December 2003 to September 2005. These values suggest a progressive reduction of refilling rates with time (Fig.III.6).

The reduction in refilling rates may be connected with the sediment availability in the neighbourhood of the pit. This study has shown that the surface area covered by screened sand decreased by 1-2% per month. Also, a coarsening of the screened sand was observed between December 2000 and June 2001 (DIESING, 2003). Therefore, thresholds for mobilisation were exceeded less frequently with time. DIESING (2003) suggests that the deceleration may also be related to the geometry of the pit. Due to the cone-like shape of the

pit, the rate of change in the volume of trapped sediment may actually have remained constant, but because of the larger radius of overlying layers, the thickness of the sediment layers decreased.

III.6.2 Refilling of the sand pits

In the case of the sand extraction site, three different stages of pit evolution can be identified. The refilling rate between 2003 and 2005, calculated from two multibeam data sets, was highest for Pit II, which was the deepest of the three pits (mean value of about 2 cm/month). The lack of stable edges and the relatively steep walls, suggest that waves higher than 2 m would be able to move material from the rim to the bottom of the pit. Although this pit is located in much deeper water than the gravel pit (about 17 m), it had a mean refilling that was twice as high as that of the gravel pit in the period from December 2003 to September 2005. Also, Pit III had a higher mean refilling rate than the gravel pit (approximately 1.5 cm/month). Sand remobilisation was mainly directed down-slope towards the east, as revealed by the bathymetric cross-sections ([Fig.III.5](#)). By 2005, Pit IV was almost completely refilled. In comparison to the data from 2003 it became 20 cm shallower and much broader, refilling at a mean rate of less than 1 cm/month. Its disappearance was probably accelerated by trailing-hopper suction dredging which dramatically lowered the pit walls in comparison to what is seen on the sonograph of August 1999.

III.6.3 Efficiency of monitoring

The correct interpretation of sidescan sonar data is the key to understanding horizontal changes at the rims of dredged pits. Minor slumps can only be delineated if the angle of the pit edge is large enough to produce a distinctly different backscatter signal. This is observed in the gravel area where the coarser material has larger angles of natural repose. Due to the lower resolution of multibeam grids, pit edges are almost undetectable by this survey method. In addition, the sidescan sonar images enable the recognition of finer sediment near the rim of the gravel pit because of the different characteristics of the screened sand as compared to the gravel. This feature of the sidescan sonar performance failed in the case of the sand extraction site because of the homogeneity of the sediment. A trigonometric analysis of the

acoustic shadow visible in the sonographs gave a rough estimate of the relative depth of gravel Pit I. It is clear, however, that a precise comparison of pit dimensions at different stages of their evolution can only be performed by multibeam mapping. The multibeam data have superior geo-referencing because we used a hull-mounted device. After proper water level and hull-movement correction, it is possible to track spatial changes at the seabed, including pit interiors, with centimetre precision. Sidescan sonars, on the other hand, are particularly useful in the monitoring of dredged sites when deployed in conjunction with multibeam devices.

In the present case, the monitoring of dredging effects at 6-month intervals (e.g. between August 1999 and June 2001) proved to be sufficient to observe changes in pit shape or sand availability at the gravel site. The 2-year break in data collection between June 2001 and December 2003, on the other hand, was too long to determine precisely the availability of screened sand at the gravel site.

III.7 Conclusions

This study focused on an area of only 20,000 m², allowing the monitoring of natural pit refilling processes and changes in pit shape in two contrasting sediment types. Using sidescan sonar and multibeam data, it was possible to document this evolution and, in the case of the gravel pit, compare the observations with earlier studies. We were able to determine the natural refilling speed of the gravel pit, which slowed during the monitoring period. Earlier studies have shown that this process is not continuous and dependent on storm events. The mean refilling rates of the sand pits, which are located at almost twice the water depth as the gravel pit, were higher over the same monitoring period. Since the finer sediment is mobilized during lower energy events, the changes observed in the sand pit area were more dynamic than at the gravel pit site. The amount of medium sand screened during gravel dredging decreased with time, which suggests that it was either trapped within the pit or transported outside of the study area.

The methods selected for monitoring the pits proved sufficient to determine changes in pit shape and estimate the distribution of screened sand fraction. Precise quantification of spatial changes, however, is only possible when sidescan sonar and multibeam data are

collected simultaneously. Under the hydrodynamic conditions in the Tromper Wiek, 6-monthly measurement campaigns are recommended to monitor pit evolution sufficiently.

Acknowledgements

We would like to acknowledge our colleagues: Klaus Schwarzer for constructive remarks in the early version of the manuscript and Ron Hackney for the entire weekend lost on corrections, and to anonymous reviewers for all the comments improving the quality of the paper. Data older than from the year 2002 was collected in a framework of the project "Regenerierung von Materialentnahmestellen in der Nord- und Ostsee" funded by the Bundesministerium für Bildung und Forschung (grant no. 03KIS008). The newer data were obtained within the project European Sand and Gravel Resources: Evaluation and Environmental Impact of Extraction-EUMARSAND (HPRN-CT-2002-00222).



Can old analogue sidescan sonar data still be useful? An example of a sonograph mosaic geo-coded by the DECCA navigation system

Adam Kubicki*, Markus Diesing

Institute of Geosciences, Christian-Albrechts-University, Olshausenstr. 40, D-24098 Kiel, Germany

Received 18 September 2005; received in revised form 1 June 2006; accepted 12 June 2006
Available online 14 August 2006

Abstract

In the Baltic and the North Sea area the collection of sidescan sonar data began in the early 1970s. Although positioning systems at that time were much less accurate than today, such analogue data archives are a valuable source of comparison for estimating spatial and temporal changes in sediment patterns. This paper describes how geographic information systems (GIS) and remote sensing methods are being applied for more accurate positioning and geometric correction of analogue sidescan sonar profiles geo-referenced by the DECCA navigation system (DNS). A 20 km² area in the North Sea, where even after 25 years a complicated sediment pattern has only changed slightly, was selected for the comparison. Data from two sidescan sonar surveys, one from 1977 and the other from 2002, were available. The 2002 data, acquired with a positioning accuracy of estimated 25 m, were mosaicked using modern digital processing techniques. This dataset was used to estimate positioning errors in the analogue sidescan sonar profiles of 1977. After the application of a geo-referencing method of 'rubber sheeting' based on an irregular network of ground control points to generate a mosaic of the analogue profiles, positioning errors of 211 m in the E–W and 98 m in the N–S directions were obtained. The positioning error of the DNS calculated from equations provided by the DECCAN Navigator Company for this area, was as large as 200 m for the 'purple' station transmission, 197 m for the 'green', and 66 m for the 'red' one. Consequently, we conclude that the observed positioning errors were mainly caused by systematic deviations of the DNS rather than simplifications used in our methodology. Since such large errors can be corrected locally with some confidence, analogue sidescan profiles geo-referenced by DNS can be used as a significant source of information after digital image processing at appropriate map scales.

© 2006 Elsevier Ltd. All rights reserved.

Keywords: Sidescan sonar; Mosaicking; Analogue data; Geo-referencing; Decca navigation system

1. Introduction

Before the United States Geological Survey introduced a digital method of collecting sidescan

sonar imagery, only analogue profiles recorded as a print-out on wet-paper were available. Mosaicking of neighbouring profiles was a tedious manual procedure of assembling the images in the correct sequence and then photographing the resultant mosaic (Belderson et al., 1972; Werner and Newton, 1975; Flemming, 1976). By this simple method, complicated sediment patterns covering large areas

*Corresponding author. Tel.: +49 431 880 2866;
fax: +49 431 880 4432.

E-mail address: akubicki@gpi.uni-kiel.de (A. Kubicki).

IV CASE STUDY ON SORTED BEDFORMS

IV.1 CAN OLD ANALOGUE SIDESCAN SONAR DATA STILL BE USEFUL? AN EXAMPLE OF A SONOGRAPH MOSAIC GEO-CODED BY THE DECCA NAVIGATION SYSTEM

IV.1.1 Abstract

In the Baltic and the North Sea area the collection of sidescan sonar data began in the early 1970s. Although positioning systems at that time were much less accurate than today, such analogue data archives are a valuable source of comparison for estimating spatial and temporal changes in sediment patterns. This paper describes how geographic information systems (GIS) and remote sensing methods are being applied for more accurate positioning and geometric correction of analogue sidescan sonar profiles geo-referenced by the DECCA navigation system (DNS). A 20 km² area in the North Sea, where even after 25 years a complicated sediment pattern has only changed slightly, was selected for the comparison. Data from two sidescan sonar surveys, one from 1977 and the other from 2002, were available. The 2002 data, acquired with a positioning accuracy of estimated 25 m, were mosaicked using modern digital processing techniques. This dataset was used to estimate positioning errors in the analogue sidescan sonar profiles of 1977. After the application of a geo-referencing method of 'rubber sheeting' based on an irregular network of ground control points to generate a mosaic of the analogue profiles, positioning errors of 211 m in the E–W and 98 m in the N–S directions were obtained. The positioning error of the DNS calculated from equations provided by the DECCA Navigator Company for this area, was as large as 200 m for the 'purple' station transmission, 197 m for the 'green', and 66 m for the 'red' one. Consequently, we conclude that the observed positioning errors were mainly caused by systematic deviations of the DNS rather than simplifications used in our methodology. Since such large errors can be corrected locally with some confidence, analogue sidescan profiles geo-referenced by DNS can be used as a significant source of information after digital image processing at appropriate map scales.

IV.1.2 Introduction

Before the United States Geological Survey introduced a digital method of collecting sidescan sonar imagery, only analogue profiles recorded as a print-out on wet-paper were available. Mosaicking of neighbouring profiles was a tedious manual procedure of assembling the images in the correct sequence and then photographing the resultant mosaic (BELDERSON ET AL., 1972; WERNER AND NEWTON, 1975; FLEMMING, 1976). By this simple method, complicated sediment patterns covering large areas could be viewed, even though quantitative geometric and acoustic correction methods of sonographs were not yet available. Although successful manual correction methods for scale distortions were applied (i.e. PRIOR AND COLEMAN, 1980; FLEMMING, 1982), accurate sea-floor mosaics could only be assembled after the collection of digital data combined with digital processing techniques (i.e. KLEIN, 1982; CHAVEZ ET AL., 2002). As a result, analogue data cannot be per se treated as a source for accurate mapping purposes due to inherent spatial inaccuracy. However, after the application of GIS and remote sensing methods for the geometric correction of analogue data, sonographs can be successfully used for comparative purposes in sediment-transport related studies (i.e. sorted bedforms appearance, movement of sandwaves over time). There are several factors though which have to be taken into account when assessing the usefulness of data for a particular purpose. These factors are mostly related to contemporary positioning technology, such as navigation system accuracy, or the time and position notation quality in contemporary data collection.

IV.1.3 Study area

The study area is located in the German Bight, south-eastern North Sea (Fig.IV.1), approximately 80 km W of the North Frisian Islands of Sylt and Amrum in water depths between 26 and 37 m below mean sea level. A 4 m deep depression is the most visible morphological feature of the area. It is elongated in a NW–SE axis and its bottom is the deepest point of the investigated site.

The present-day seafloor (Fig.IV.1) is characterized by patches of fine sand, coarse sand and gravel arranged in strips and furrows (DIESING ET AL., 2006; WERNER, 2004). Such

features are ubiquitous on sediment-starved continental margins. They are termed “sorted bedforms” by MURRAY AND THIELER (2004).

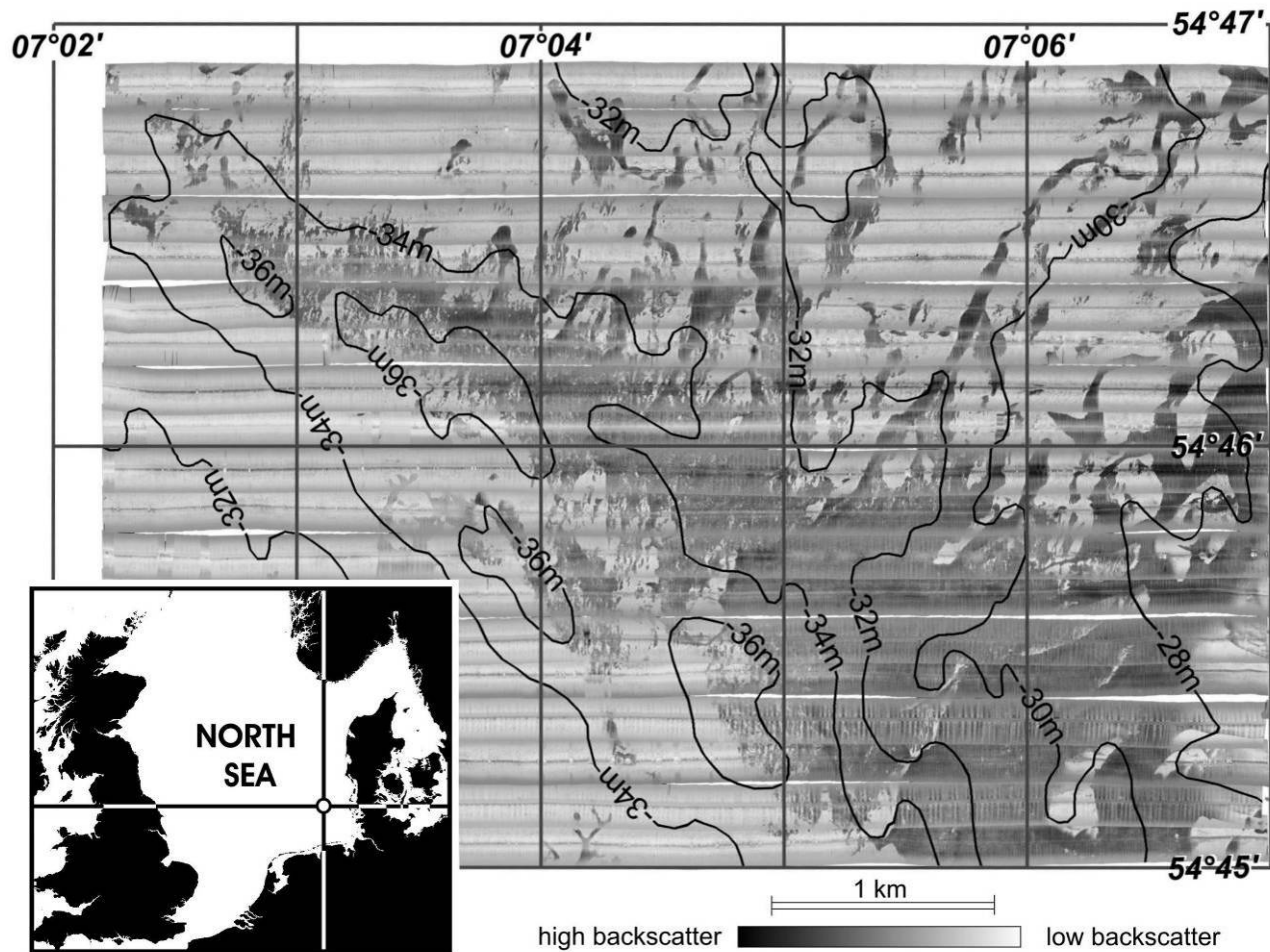


Figure IV.1. Sidescan sonar mosaic showing the area of interest. Coarse sediment strips (dark) occur together with fine sand areas (light). The mosaic was obtained from data collected in 2002. Contour lines represent water depth.

IV.1.4 Methods

IV.1.4.1 Analogue profile description

Analogue sidescan sonar profiles collected in 1977 were gathered with an EG&G dual channel sidescan sonar with a frequency of 105 kHz and a range of 152 m (500 ft). The sonar data were recorded on wet paper with a resolution of 1/250 of a range (ANON, 1971), which is 60 cm in our case. The event lines were marking the moment of position reading on the profiles. For every event mark the position coded in DECCA as well as the time of the reading

were logged in a profile protocol. Although positions were recorded every few minutes, it is not certain that these corresponded to precise full minute periods. The time notations in hours and minutes (HH:MM) are not particularly accurate. For example, a research vessel surveying at a speed of 4 knots would cover a distance of 120 m between HH:MM:00 and HH:MM:59. Along each profile at least four and a maximum of seven positions were fixed.

The speed of the vessel was usually recorded three times along one profile, but the speed difference between two neighbouring notations could be up to 1 knot. Thus, no geometric correction of varying vessel-speed was implemented. The length of the sidescan sonar layback is also missing in the protocol records, thus requiring estimation of this factor. Sonographs show the influence of pitch and roll of the sonar fish visible as enlightened triangles (several metres large) in the near-range and single pings unnaturally stretched up to ca. 20 m width in the far-range. The survey was carried out during the night of 18–19 July 1977. The track lines were set out almost parallel to each other.

IV.1.4.2 The DECCA Navigation System

The DECCA navigation system (DNS) is a hyperbolic radio navigation system similar to Loran-C, which was used in about 50 countries worldwide until the satellite navigation system GPS (Global Positioning System) became available. Positioning by DNS was based on the measurement of the phase differences between continuous signals being sent from a DECCA chain consisting of one Master and three Slave (called red, green and purple) radio beacons. The beacons transmitted the signal in the band between 70 and 130 kHz and, after receiving the readings of two pairs of hyperbolas, it was possible to locate the transmitted position on the navigation chart (HAIGH, 1960). Therefore, if the position of the Master and Slave stations, the frequency of their transmissions and the reading of the DECCA receivers are available, it is possible to project radio co-ordinates into any desired geographical ellipsoid, even retrospectively.

The accuracy of this conversion, however, is affected by several factors. The key one is the precision of the positioning by the DNS. The accuracy of this navigation system depended on the atmospheric conditions at the time the radio waves were transmitted. Inside the troposphere, radio wave propagation is significantly affected by meteorological

phenomena. Thus, radio waves attenuate, scatter and refract, causing a reduction in the positioning accuracy with growing distance from a radio beacon. Depending on the season and the time of day, the positioning accuracy of the DECCA system was assumed to be approximately 15m close to the radio beacon, and as much as four nautical miles at the outer range limit. As an example, the positioning error of the 'red' beacon, in the present case, is illustrated in Fig.IV.2. For any point on a DECCA navigation chart the values of position accuracy can be calculated from the following equations (ANON, 1976):

Standard deviation for the red chain:

$$\sigma^2_R = 16 \sigma^2_{am} + 9 \sigma^2_{br} + 16 \sigma^2_{Sm1} + (0.012)^2 \quad (IV.1)$$

Standard deviation for the green chain:

$$\sigma^2_G = 9 \sigma^2_{am} + 9 \sigma^2_{Sm2} + 4 \sigma^2_{cg} + (0.009)^2 \quad (IV.2)$$

Standard deviation for the purple chain:

$$\sigma^2_P = 25 \sigma^2_{am} + 25 \sigma^2_{Sm3} + 36 \sigma^2_{dp} + (0.015)^2 \quad (IV.3)$$

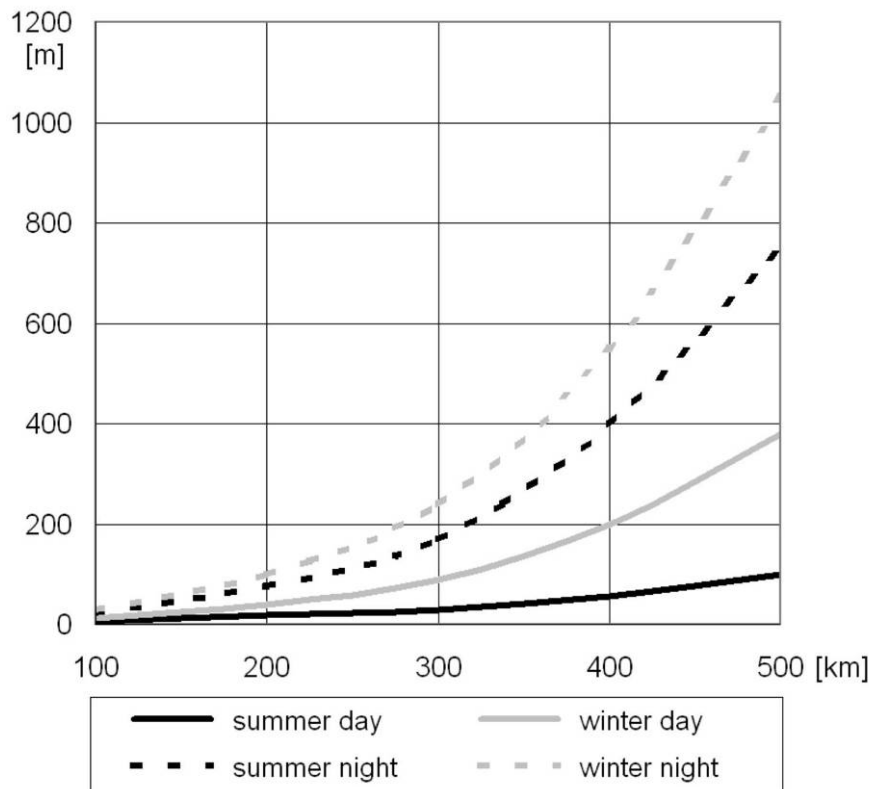


Figure IV.2. Dependence of the positioning error of the 'red' DECCA beacon on distance from the transmitting station and the time of the measurements (ANON, 1976). The most accurate measurements are obtained during summer days, the least accurate ones during winter nights.

where standard deviation values are given in empirically determined transmission cycles (by Decca Navigator Company) over different distances: σ_{am}^2 - Master station to the receiver, $\sigma_{br, cg, dp}^2$ - Red, Green, Purple station to the receiver, $\sigma_{Sm1, Sm2, Sm3}^2$ - Slave stations to Master

In addition, the values have to be adjusted to the time of day and year of the measurement (ANON, 1976). An example of a final standard deviation computation is presented in Tab.IV.1. It represents the point located in the geometric centre of the study area dealt with in this paper.

Table IV.1. Standard deviation values of the DECCA positioning error for all transmission stations in the geometric centre of the study area ($\varphi = 54^{\circ}45.95'$; $\lambda = 7^{\circ}4.63'$) calculated from equations IV.1, IV.2, and IV.3.

Station	Red	Green	Purple
σ^2	66 m	197 m	200 m

IV.1.4.3 Analogue data processing

The proper transformation of raw sidescan sonar data into images includes acoustic and geometric corrections (FLEMMING, 1976, 1982; JOHNSON AND HELFERTY, 1990; BLONDEL AND MURTON, 1997; FISH AND CARR, 2001). Acoustic correction means that a backscatter signal is compensated in order to account for spreading and absorption loss, noise, and acquisition failures. For this kind of image enhancement, appropriate algorithms have been developed for digital sidescan data, whereas analogue records were electronically enhanced by manipulations such as time-varying gain settings, variable paper feed rates and, in later years, also water column removal (e.g. KLEIN, 1982). However, image processing of scanned analogue records is more problematical, because backscatter pixels registered by an office scanner during analogue to digital format conversion, sonograph resolution and pixel position differ to the ones originally obtained from the transducer. Image processing of scanned sonographs used in our study, does therefore not improve the quality of the images. The correct identification of pixel intensity is actually less important in our case, where grain-size distributions are known. However, where such data is not available, a correction of the digitised records should be attempted.

During standard geometric correction, the spatial position of pixels recorded by the transducer is recalculated in order to obtain a geo-referenced map of the sea-floor, free from distortions produced during data collection. Perpendicular to the track, a slant-range correction (also referred to as beam angle correction) is usually performed in combination with the removal of the water column, whereas along the track variations in vessel speed are corrected (BLONDEL AND MURTON, 1997). The correction of the geometry in either direction can be performed with tools provided by modern geographic information systems (GIS). The creation of geo-referenced images is a crucial element of the mapping process in GIS during which real-world co-ordinates are assigned to every pixel of the scanned analogue profile. A modern system software-GPS-receiver automatically assigns co-ordinates during data collection, whereas in case of older analogue profiles geo-referencing has to be performed manually. Such manual geo-referencing was initially rather complex because the computation power of personal computers was insufficient to handle large sidescan sonar image files, comprising hundreds of megabytes. Such limits do not exist nowadays.

IV.1.4.4 Geo-referencing procedure

In the case discussed here, the universal transverse mercator (UTM) projection was selected as the geographic environment for the unification of the available data. It simplified all the calculations due to the application of metres as a unit of distance. Ground control points (GCPs), the positions of which were logged in DECCA co-ordinates, formed the basis of the geo-referencing procedure. The conversion of DECCA track co-ordination points into latitude/longitude values was performed by the DECCA 1.0.1 software released by the Hydrographic Service of the Netherlands. Such GCPs were then recalculated into UTM co-ordinates. These are located along the track lines and are labelled '1' in Fig.IV.3a. Sidescan sonar position was assumed to be the same as the ship's one, so no sidescan sonar layback was applied at this stage. Additional GCPs had to be computed perpendicular to the tracks in order to describe the swath. Since the position of the vessel was recorded at several minute intervals, it is not possible to reconstruct the correct heading angle for each ping. In order to compute the most probable ship path, a Matlab script was created. It compares the previous and the next position of the vessel and then computes the average heading. Including the

heading angle, two GCPs located at both outer ends of the swath are calculated (labelled '2' in Fig.IV.3a). The entire profile can thus be geo-referenced with such sets of GCPs.

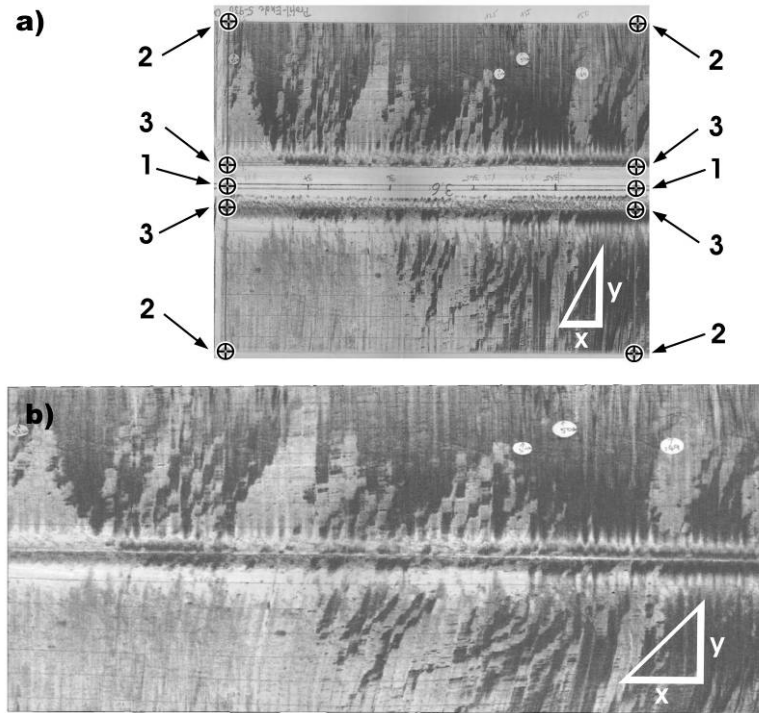


Figure IV.3. Geo-referencing procedure scheme: (a) GCPs selection 1- ship's path, 2-edge of the range, 3-first bottom reflection; (b) result of geo-referencing by the Rubber Sheeting method. Length of x and y correspond to 100 m in each case.

There are several remote sensing methods of georeferencing using GCPs. One of these methods is 'Rubber Sheeting', also known as 'Rubber Bending', a procedure of adjusting all the pixels between known GCPs by stretching, shrinking or re-orienting their interconnecting lines (McDONNELL AND KEMP, 1995) (Fig.IV.3). At first, a triangulated irregular network (TIN) covering all GCPs is formed and the image area covered by each triangle is then geo-referenced. By this procedure, performed by ERDAS Imagine software, the along-track geometry is partially corrected. Denser GCP distributions, of course, assure better isometric corrections. The Rubber Sheeting method is also suitable for the elimination of the water column from the sonograph. For this, it is sufficient to select two additional GCPs for every track position, each corresponding to the first bottom return on the respective channel (see Fig.IV.3a points labelled '3'). To each of the bottom return GCPs, real-world coordinates are assigned, which are, for example, created 10 cm away from the transducer. The water

column is thus compressed into a 20 cm thin, negligible stripe in a 380 m-wide profile (Fig.IV.3b).

In many cases such a water column removal can substitute for a slant-range correction. However, its efficiency depends on the sea-bottom morphology. In areas with complicated bathymetry it is vital to identify the bottom track line properly and morphological complexity may require many GCPs along the track. However, uncertainties influenced by sea-bottom relief also exist in the across-track direction. Most software packages compute slant-range correction as if the seabed were flat, thereby simplifying geometry calculations. This is also justified by the argument that not every survey collects and relates sidescan sonar data to swath bathymetry data. In the present study sufficient bathymetry data were not available. Application of the Pythagorean theory for the complex web of GCPs involved is still under study and thus a full and proper across-track geometry correction was not performed. Instead, a simplified stretching of the sidescan sonar image was carried out by the application of Rubber Sheeting as shown in Fig.IV.4c.

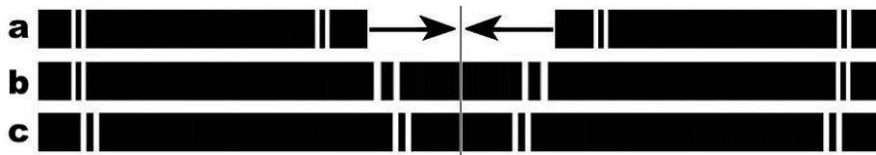


Figure IV.4. Slant-range correction. (a) Channels before correction; (b) proper correction; (c) simplified stretching.

Since areas situated closer to a transducer are more compressed on the sonograph, these need more stretching than areas lying further away (Fig.IV.4b). However, rubber sheeting uniformly stretches the entire record section illustrated in Fig.IV.4c. Thus, an additional positioning error comprising several metres across track is introduced. Its exact value, however, is difficult to estimate because it depends on both the distance from the transducer and the bottom morphology (BLONDEL AND MURTON, 1997).

IV.1.5 Results

Profiles geo-referenced by the procedures described above, were compared with a sidescan sonar mosaic from 2002 using a Klein 595 Hydroscan Sonar with a frequency of

384 kHz and a positioning accuracy of approximately 25 m (DIESING ET AL., 2006). For the spatial comparison of the two images, stable reference points are required. Such points can often be identified on both images, for example large boulders on the seabed. In the present case, large boulders (tens of centimetres in diameter) occur in the area, but most of them are not recognisable on the analogue profiles from 1977 due to poor resolution and quality of sonographs. Nevertheless, within the complicated sediment pattern it was possible to recognise numerous shapes which had remained virtually unchanged over the interim 25 years (Fig.IV.5). In the mosaics of 2002 as well as in the profiles of 1977, the borders between the two main sediment types are surprisingly similar and visible either as gentle transition zones or high-contrast lines.

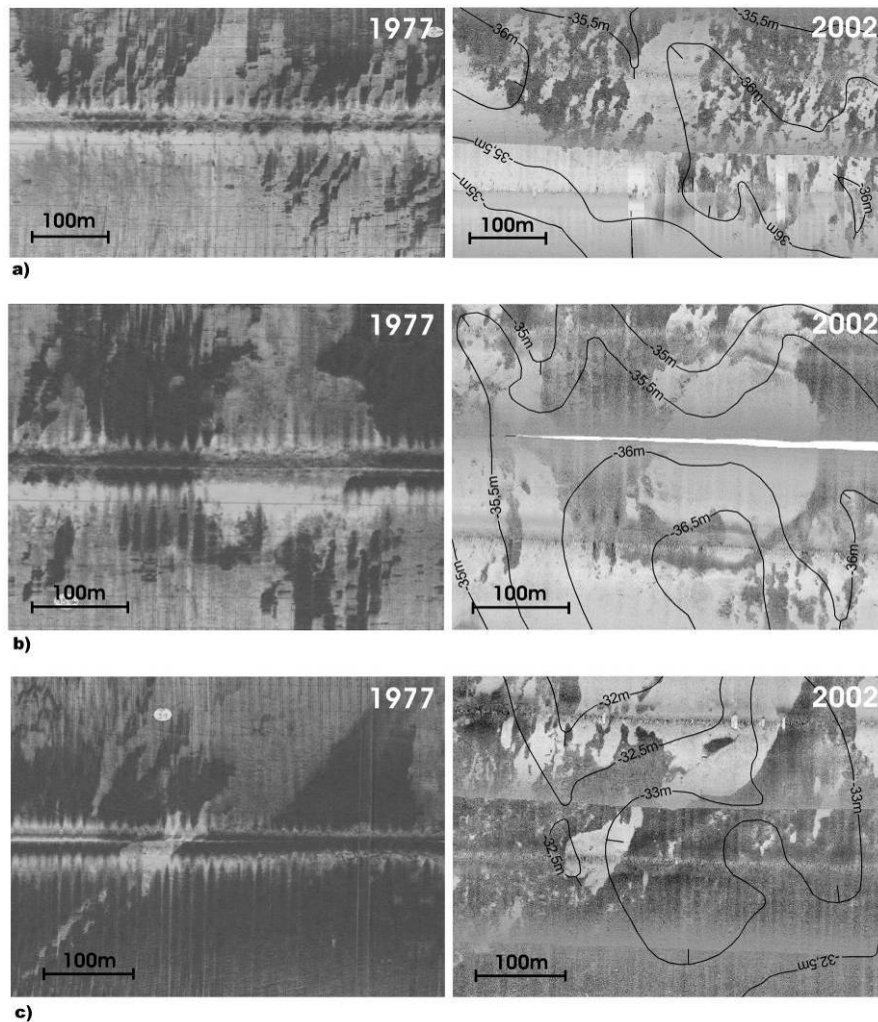


Figure IV.5. Comparison of sediment patterns on selected profile sections from 1977 and 2002. Contour lines represent water depth.

A software tool for identifying contours was used to identify high-contrast borders. The bold lines in Fig.IV.6 show such borders at a resolution of 100 steps (8-bit greyscale) between neighbouring pixels. The high similarity of the border lines observed in several places allowed the determination of apparently stable reference points with a 10-m precision for a spatial comparison of the sonographs. On the basis of such reference points, the profiles from 1977 were adjusted. In addition, the empirical positioning accuracy achieved in the geo-referencing process of the analogue sidescan sonar images could be calculated. The mosaic of the 1977 profiles compiled in this way is presented in Fig.IV.7.

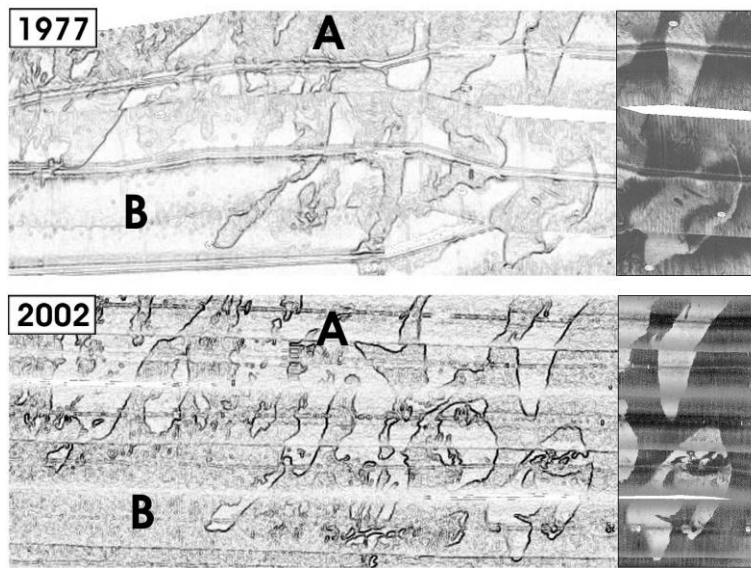


Figure IV.6. Results of a search for high contrast borders between sediment types in 1977 and 2002 images. An impression of the change in grayscale is a result of different qualities of the images processed by the same tool. In 1977 greater detail caused by roll and pitch artefacts was recorded in the ‘northern’ A type sediment, whereas in 2002 this influence was more prominent in the ‘southern’ B type sediment (see original sonographs examples).

IV.1.6 Discussion

The usefulness of the method described in this paper can be assessed by comparing the potential positioning errors with the observed positioning errors. In Tab.IV.2, the possible sources of inaccuracy are summarised. Unpredictable errors, such as human errors during position notation are excluded here. As it turns out, the probable error in the W–E direction is much higher than along the meridians, which is related to the data-recording direction.

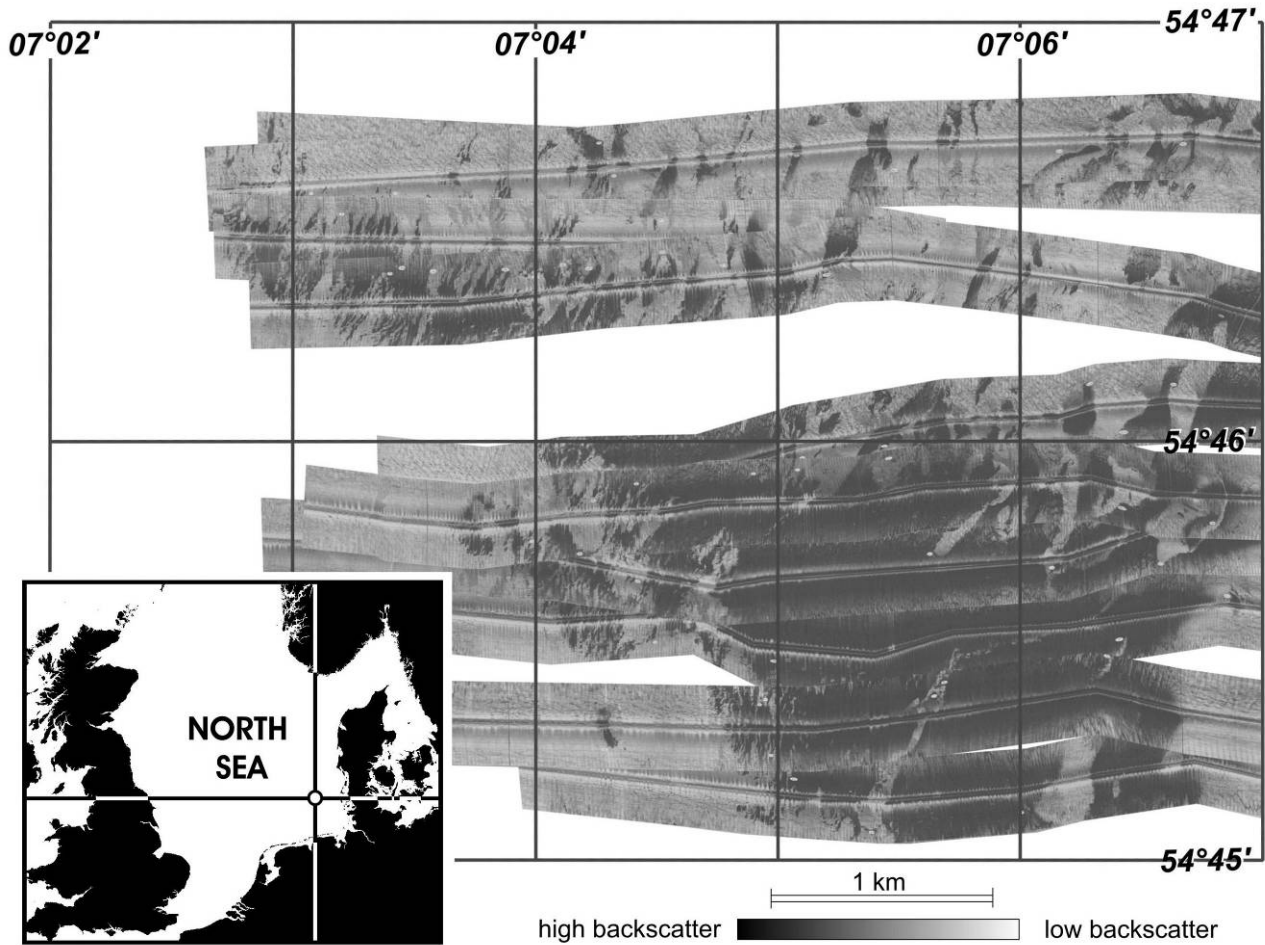


Figure IV.7. Ten analogue sidescan sonar profiles from 1977 were processed in this study. The resultant mosaic contains some blank areas indicating a lack of data, but the overall sediment pattern is clearly visible.

The layback distance plays an important role in data positioning. However, it is difficult to estimate it without acoustic transponders locating the transducer. At a depth of 30 m a sidescan sonar is towed about 50–120 m behind the GPS receiver, depending on vessel speed and local hydrodynamics. To provide an example, a 100-m layback was applied to test the relationship between layback and positioning error. The calculation of the layback effect also included a possible deviation in the heading angle of the ship. Since no current data were available, the assumption was made that the sidescan exactly followed the ship's track. For comparison, the raw, uncorrected positioning points converted from DECCA co-ordinates were plotted together with their equivalents after layback application (Fig.IV.8).

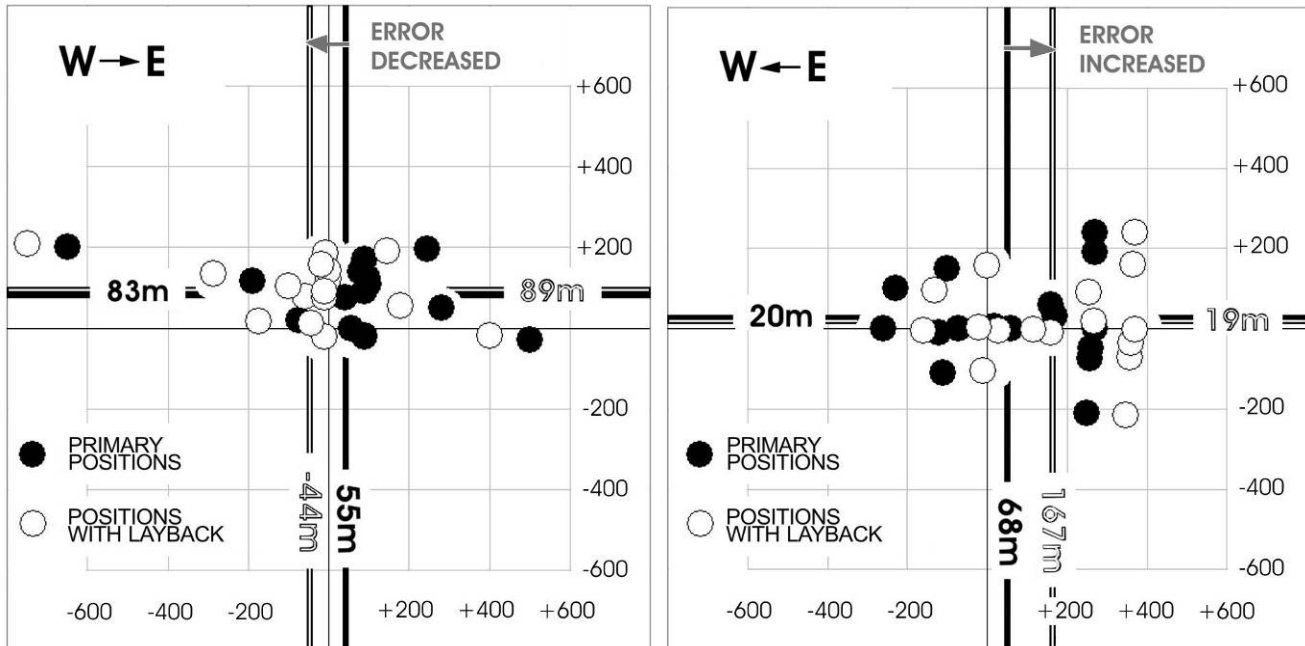


Figure IV.8. Positioning errors with and without layback application during eastward and westward measurements. Grid lines are given in metres and the axes are geographically aligned.

Two plots are presented in order to differentiate between eastwards and westwards measurements. For both plots, the grid lines are given in metres of positioning error and the plus (+) and minus (-) signs indicate the geographic direction of the error. Parallel lines showing algebraic means are also included in the plots of Fig.IV.8. While travelling eastwards, a large discrepancy in individual error positions is apparent, although the overall mean error is only 55 m East. In this case a layback application appeared advisable. However, while recording westwards, the mean error of 68 m East increased after adding the layback (Fig.IV.8). We thus conclude that the recalculation of positions by an assumed layback length does not increase the quality of positioning. Both plots show a shift of all errors towards the East and North, a feature we are unable to explain at this stage. It could have been caused by a south-westerly current, but the morphology of the area suggests that currents along a NW-SE axis are more probable.

The standard deviation for all GCPs positioning errors without layback application was equal to 164 m (211 m along the parallel and 98 m along the meridian). According to analogue map standards established in 1941 by the US Bureau of the Budget such a mistake is acceptable at map-scales smaller than 1:300,000. At such scales, old analogue profiles used in our study can thus be used as a primary source of data without selecting additional

GCPs based on the sediment pattern. The method presented in this paper is especially suitable for areas, where more stable reference points are available. Larger numbers of possible GCPs provides better spatial accuracy of the geo-referenced sonographs. In the areas characterised by uniform sediment, or significant sediment reworking, where no reference points can be selected, the method is also applicable, although the magnitude of error is indeterminate.

Table IV.2. . Possible sources of inaccuracy, magnitude of their error and error direction.

Source	Error	Direction
DECCA system accuracy	~200m	NWSE
Insufficient time notation	~120m	WE
Lack of layback application	~120m	WE
Accuracy of 2002 mosaic	~25m	NWSE
Pitching and rolling of the fish	~15m	NWSE
GCPs manual selection	~10m	NWSE
Simplified slant-range correction	~10m	NS

IV.1.7 Conclusions

Inaccurate, but meaningfully precise positioning appears to be the main source of the positioning error in the geo-referencing of analogue profiles, whereas the effects of other possible error sources (e.g. insufficient time notation, lack of layback application, accuracy of recent digital mosaics, pitching and rolling of the tow-fish, GCPs selection and simplified slant-range correction) are less important than the original navigation system inaccuracies.

The positioning accuracy derived by empirical comparison was, despite some simplifications, very similar to the one computed for the DECCA navigator system.

We therefore conclude that GIS and remote sensing methods can be successfully applied to analogue sidescan sonar archives. Analogue data is first converted into digital form and then geometrically corrected. However, applications for detailed mapping purposes are limited by the accuracy achieved by the navigation system used during data acquisition. Old analogue sidescan sonar data is therefore often unsuitable for accurate high-resolution mapping, although in some cases it can be an excellent source for temporal and spatial comparison of distinct seabed features.

In the present study, a positioning error of 164 m was determined. Such an error is acceptable at map-scales smaller than 1:300,000. However, in the majority of studies, sediment maps are produced at much larger scales. An alternative method, therefore, would be to select the map-scale in accordance with the aim of the study, keeping the positioning error in mind, or to improve the accuracy of positioning by finding stable reference points with known positions. The method presented here is therefore preferable for sidescan sonar images with a sufficient number of recognizable reference points, which can help in assessing the spatial error. For old sidescan sonar records from areas with a dearth of reference points this method is also applicable. All possible sources of error, however, should be listed and the error magnitude should be gradually reduced or eliminated before applying the georeferencing procedure.

Acknowledgements

We would like to thank Hans Gillissen of the Hydrographic Service of the Netherlands for the patient assistance in solving radio-navigation principles. Our colleagues Klaus Schwarzer, Patrycja Czerniak, Faustino Manso, Art Trembanis whose valuable remarks improved this paper, are greatly acknowledged. We also thank Veit Hühnerbach of National Oceanography Centre, Southampton and Burghard W. Flemming for a huge work and constructive comments. Data from the 2002 survey was obtained within the framework of a project funded by Bundesamt für Naturschutz and Bundesministerium für Umwelt, Naturschutz und Reaktorsicherheit (Grant no. 802 85 270).



Decadal scale stability of sorted bedforms, German Bight, southeastern North Sea

Markus Diesing^{a,*}, Adam Kubicki^a, Christian Winter^b, Klaus Schwarzer^a

^a*Institute of Geosciences, Christian-Albrechts-University, Olshausenstr. 40, D-24098 Kiel, Germany*

^b*Research Center Ocean Margins, University of Bremen, Leobener Str., D-28359 Bremen, Germany*

Received 27 June 2005; received in revised form 20 December 2005; accepted 13 February 2006
Available online 18 April 2006

Abstract

Complex, large-scale sorted bedforms have been investigated in the southeastern North Sea. We present a unique time series of sidescan sonar and multibeam backscatter data spanning 26 years (1977–2003). In the storm-dominated study area, sorted bedforms surrounded by fine sand plains, are widespread. Although, wave and current shear stresses indicate a frequent remobilisation of fine sediment and an episodic remobilisation of coarse sediment, it appears that existing patterns have remained essentially stable over a period of 26 years. Moreover, we observe the birth of new sorted bedforms. The observed patterns are interpreted as the product of a feedback-related sorting process consistent with a recent explanation of sorted bedform formation.

The observed sorted bedforms tend to be oriented perpendicular to the ambient tidal currents, indicating the importance of tidal flows in their shaping. Moreover, they are dominantly symmetric in cross-section, i.e. the boundaries between coarse and fine sediment are sharp. This finding is consistent with a reversing tidal current of almost equal strength during ebb and flood. Similar to subaqueous dunes, sorted bedforms might therefore be subdivided into symmetric and asymmetric types, depending on hydrodynamic forcing. However, the newly emerging sorted bedforms are asymmetric, with an orientation independent of tidal current flow but perpendicular to the direction from which the highest storm waves approach the study area. We thus conclude that extreme storm events may play a major role in the generation of sorted bedforms, whereas the quasi-continuous tidal currents form and maintain their final shape.

© 2006 Elsevier Ltd. All rights reserved.

Keywords: Inner shelf; Sorted bedforms; Rippled scour depressions; Backscatter; Shear stress; North Sea; German Bight

1. Introduction

The inner continental shelf (as defined by Wright, 1995) can be characterised as a realm where the seabed is frequently agitated by tidal flows and

storm-driven waves and currents. While subaqueous dunes and sand ridges are characteristic for sand-rich, tide-dominated environments, so-called rippled scour depressions (Cacchione et al., 1984) or sorted bedforms (Murray and Thieler, 2004), are ubiquitous where sand supply and tidal energy are low. Such bedforms have recently received increasing awareness. The term “rippled scour depression” (RSD) was first coined by Cacchione et al. (1984) to

*Corresponding author. Tel.: +49 431 880 4432;

fax: +49 431 880 7303.

E-mail address: md@gpi.uni-kiel.de (M. Diesing).

IV.2 DECADAL SCALE STABILITY OF SORTED BEDFORMS, GERMAN BIGHT, SOUTH-EASTERN NORTH SEA

IV.2.1 Abstract

Complex, large-scale sorted bedforms have been investigated in the southeastern North Sea. We present a unique time series of sidescan sonar and multibeam backscatter data spanning 26 years (1977–2003). In the storm-dominated study area, sorted bedforms surrounded by fine sand plains, are widespread. Although, wave and current shear stresses indicate a frequent remobilisation of fine sediment and an episodic remobilisation of coarse sediment, it appears that existing patterns have remained essentially stable over a period of 26 years. Moreover, we observe the birth of new sorted bedforms. The observed patterns are interpreted as the product of a feedback-related sorting process consistent with a recent explanation of sorted bedform formation.

The observed sorted bedforms tend to be oriented perpendicular to the ambient tidal currents, indicating the importance of tidal flows in their shaping. Moreover, they are dominantly symmetric in cross-section, i.e. the boundaries between coarse and fine sediment are sharp. This finding is consistent with a reversing tidal current of almost equal strength during ebb and flood. Similar to subaqueous dunes, sorted bedforms might therefore be subdivided into symmetric and asymmetric types, depending on hydrodynamic forcing. However, the newly emerging sorted bedforms are asymmetric, with an orientation independent of tidal current flow but perpendicular to the direction from which the highest storm waves approach the study area. We thus conclude that extreme storm events may play a major role in the generation of sorted bedforms, whereas the quasi-continuous tidal currents form and maintain their final shape.

IV.2.2 Introduction

The inner continental shelf (as defined by [WRIGHT, 1995](#)) can be characterised as a realm where the seabed is frequently agitated by tidal flows and storm-driven waves and currents. While subaqueous dunes and sand ridges are characteristic for sand-rich, tide-dominated environments, so-called rippled scour depressions ([CACCHIONE ET AL., 1984](#)) or

sorted bedforms (MURRAY AND THIELER, 2004), are ubiquitous where sand supply and tidal energy are low. Such bedforms have recently received increasing awareness. The term “rippled scour depression” (RSD) was first coined by CACCHIONE ET AL. (1984) to describe “channellike depressions of low, negative relief [y], containing large sand ripples and transecting the inner shelf generally normal to the bathymetric contours”. The term was subsequently more broadly applied to ubiquitous surficial sedimentary features of inner continental shelf environments on sediment-starved margins (see review in MURRAY AND THIELER, 2004). Such features have slight topographic depressions on the order of 1 m and are composed of coarse-to-very coarse sand, gravel and/or shell hash that is arranged into large wave-generated ripples, with wavelengths on the order of a metre. They are typically 100–200 m wide, and extend hundreds to thousands of metres in the cross-shore direction (MURRAY AND THIELER, 2004).

CACCHIONE ET AL. (1984) observed RSDs with sharp contacts between fine and coarse sediment and a coarse sediment domain centred in the topographic depression on the inner continental shelf off central California. They attributed the generation of RSDs to storm-generated downwelling flows parallel to the long (cross-shore) axis of the RSDs. In contrast to the results of CACCHIONE ET AL. (1984), a closer examination of similar bedforms off Wrightsville Beach, North Carolina (USA) revealed a distinct asymmetry: the coarse sediment domain is not centred on the bathymetric low, but instead occupies the bathymetric low and one flank, while the other flank is covered by finer sediments (THIELER ET AL., 2001). As the northern edges of the coarse sediment domains are sharp, while the southern edges appear “wispy”, THIELER ET AL. (2001) and MURRAY AND THIELER (2004) speculated that southward shore-parallel currents perpendicular to the axis of the bedforms were responsible for these observed patterns. This view of asymmetric bedforms as transverse rather than longitudinal is shared by several researchers (GOFF ET AL., 2005; GUTIERREZ ET AL., 2005). Because the observed bedforms are not simple depressions and the term RSD is associated with cross-shelf flows, MURRAY AND THIELER (2004) proposed the more neutral term “sorted bedform”. On the other hand, GOFF ET AL. (2005) pointed out that not all authors reported on the asymmetry of sorted bedforms (e.g. CACCHIONE ET AL., 1984; GREEN ET AL., 2004). They concluded that two distinct classes of bedforms might be lumped together, distinguished by their asymmetry.

MURRAY AND THIELER (2004) developed a model that explains the formation and maintenance of sorted bedforms. They suggested that wave motions interacting with large roughness elements (large wave-ripples), present on coarse sediment domains, generate near-bed turbulence that is greatly enhanced relative to that in fine sediment domains. This turbulence enhances entrainment and inhibits settling of fine material in an area dominated by coarse sediment. Thus, a feedback tending to produce accumulations of fine material separated by patches of coarse sediments is constituted. Direct field measurements performed on the inner shelf off Tairua Beach, New Zealand (GREEN ET AL., 2004), show that under high waves, the suspended-sediment load, originating from the surrounding fine sediment domain, will be high, but turbulence will also be more energetic on the coarse sediment domain, thus more effectively inhibiting deposition. Under low waves, deposition may be less inhibited on coarse sediment domains, but the suspended sediment load arriving from the surrounding fine sand domain will also be also lower. Consequently, the fine sand deposition rate on coarse sediment domains will be small, even though conditions are more favourable for settling.

The model of MURRAY AND THIELER (2004) predicts spatial stability of sorted bedform patterns, which was observed at time-scales of months to a few years on the inner shelves of off Tairua Beach (HUME ET AL., 2003) and the German Bight (WERNER, 2004). On the other hand, MURRAY AND THIELER (2004) and GOFF ET AL. (2005) observed shifts of the boundary between coarse and fine sediment domains on the order of tens of metres within months to a few years. In the case of Wrightsville Beach, such changes are attributable to storm events, such as hurricane Bonnie (MURRAY AND THIELER, 2004).

Although a general agreement concerning the mechanism responsible for maintaining sorted bedforms exists among researchers, there are still several open questions concerning their generation and long-term temporal stability and their relation to the ambient flow regime. Currently, more questions are raised than answered (GOFF ET AL., 2005). To contribute to this discussion, we investigate temporal changes of sorted bedform patterns on the inner shelf of the German Bight. To our knowledge, investigations of temporal changes of surficial sediment distribution patterns cover several months to a few years at most (e.g. THIELER ET AL., 1995; THIELER ET AL., 2001). Here, we present a unique time series of backscatter data covering 26 years between 1977 (WERNER, 2004) and 2003. We also investigate the relationships

between sorted bedform orientation and ambient inner shelf flow regime. We present a conceptual model for the formation and maintenance of sorted bedforms in the study area.

IV.2.3 Setting

The study area is situated in the German Bight (Fig.IV.9), approximately 80 km west of the North Frisian Islands Sylt and Amrum in water depths between 26 and 37 m below mean sea level.

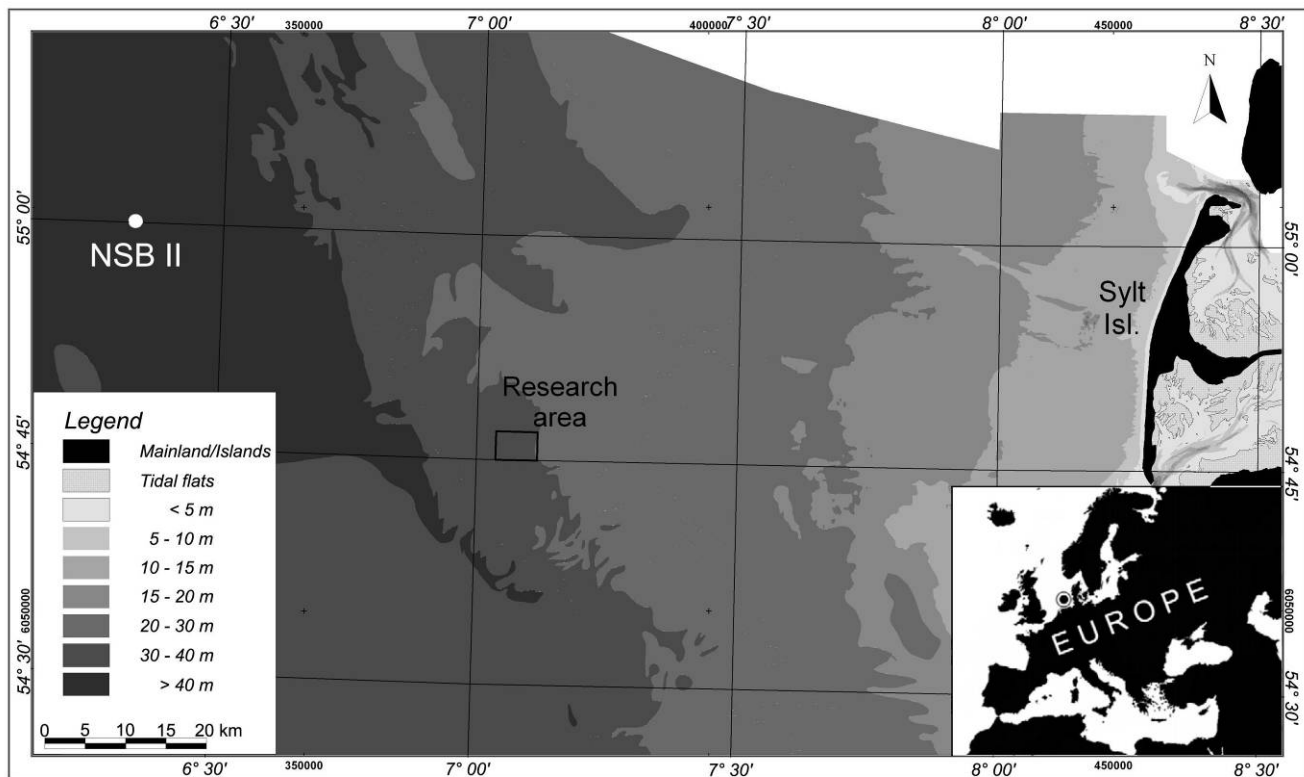


Figure IV.9. Overview of parts of the German Bight west of the North Frisian Islands. Location of the research area and wave gauge NSB II is indicated.

The German Bight was affected by glaciers during the Saalian, while periglacial conditions prevailed during the Weichselian glaciation. Tills and meltwater sands are overlain by Holocene fluvial deposits, which were partly eroded during the postglacial transgression. A transgressive gravel layer separates these units from Holocene marine sands (WINN AND WERNER, 1984). According to the sea-level curve of BEHRE (2003), the research area was

transgressed by the North Sea approximately 9000 cal. yr BP. The present-day seafloor is characterized by a patchy mosaic of fine sand plains and coarse sand, arranged in strips and furrows (WERNER, 2004), similar to sorted bedforms observed elsewhere.

While tides dominate the flow regime in the inner German Bight southeast of Helgoland Island, the research area can be characterised as a storm-dominated environment (VAN DER MOLEN, 2002), with a minor influence of tides. Long-term wave data are available online from “Nordseeboje II” (NSB II), located 55 km northwest of the study area in 42 m of water (see homepage of the German Federal Maritime and Hydrographic Agency: <http://www.bsh.de/en/Marine%20data/Observations/Sea%20state/index.jsp> for annual time series and wave statistics). Significant wave heights most frequently ranged between 0.5 and 1.0 m in 2003, but maximum values of up to 9 m were observed during storm events. Zero crossing periods between 4 and 5 s occurred most frequently. Waves dominantly approach from north–northwest (longest fetch), with a second-order maximum from the southwest direction (main wind direction). Swell waves (here defined as waves with periods longer than 10 s) are also significant during and after storm events, reaching maximum significant wave heights of up to 6 m.

The tidal system of the North Sea is characterized by semi-diurnal tides. In the research area, the mean astronomical tidal range is about 1.3 m. The tidal ellipse is aligned in a southeast–northwest direction. During spring tide, average current speeds are 34 cm/s during the flood phase (to the southeast) and 27 cm/s during the ebb phase (to the northwest) in 22 m of water. Neap tidal current speeds are somewhat lower, amounting to 27 and 24 cm/s, respectively (MITTELSTAEDT ET AL., 1983).

IV.2.4 Methods

For this study, data from two recent field surveys (May 2002 and 2003) are compared with archived data from 1977 (WERNER, 2004). The original size (approximately 5 km x 3.5 km) and location of the study area were established during this early survey. The area was remapped in 2002 and 2003. A comparison of these data sets therefore allows an investigation of the dynamics of sediment distribution patterns on annual and decadal time scales.

IV.2.4.1 Recent surveys

We employed a towed Klein 595 (Klein Associates Inc.) dual-frequency (100 and 384 kHz) sidescan sonar system and a hull-mounted Seabeam 1185 (Elac Nautik) 180 kHz multibeam swath bathymetry system, which also collects co-registered acoustic backscatter. The ship's tracklines were chosen to allow full coverage of the seafloor. The recorded spatial patterns of backscatter intensity are interpreted in terms of seafloor relief and sediment type. Validation of the data was achieved by grain-size analysis of sampled seafloor sediments. Additionally, single-beam echosounder data were collected routinely. Positioning was achieved by differential GPS, providing an accuracy of the vessel's (and therefore also of the multibeam's) position better than 5 m. The sidescan sonar was towed behind the vessel with about 40 m of cable out. This offset was accounted for by a constant value for each profile, when calculating the position of the towfish. The positioning error of the sidescan sonar is thus greater compared to the multibeam. Theoretically, it could be as high as the cable length. In practise, it is probably much smaller; a conservative estimate is 25 m.

The Klein 595 was run in the high-frequency mode in order to allow the highest-resolution imaging, with a range of 100 m. Sidescan sonar data were recorded in digital format employing the Isis software package (Triton Elics Int.). These data were processed and geo-referenced using the same software in order to create sidescan sonar mosaics of the study areas. The 126 individual beams of the Seabeam 1185 multibeam system allow a swath width of about seven times the water depth. Multibeam data were collected digitally with the HydroStar program (Elac Nautik). The post-processing of the raw data was conducted using the software HDPpost (Elac Nautik). The mosaic files were displayed in the geographic information systems Delph Map (Triton Elics Int.) and ArcView (ESRI). Backscatter strength is displayed as grey scale from light (high) to dark (low).

Single-beam bathymetry data were corrected for water-level changes by the German Federal Maritime and Hydrographic Agency (BSH, Hamburg). In order to achieve a spatial distribution of water depth, the data were gridded including variogram analysis.

IV.2.4.2 Archived data from past surveys

In this study, we also incorporated archived analogue sidescan sonar data, which were collected in 1977 by the former Geological–Paleontological Institute of Kiel University (WERNER, 2004). The data were gathered with an EG&G 272 towfish (105 kHz) and a wet paper recorder. Positioning was made with the hyperbolic radio navigation system DECCA, which accuracy is highly variable, depending on the distance to the radio station and the meteorological conditions. For the geometrical centre of the study area a positioning error computed from equations provided by system producers (ANON., 1976) was as large as 200 m. The ship's position given in DECCA coordinates was recorded every several minutes and marked on the analogue paper record.

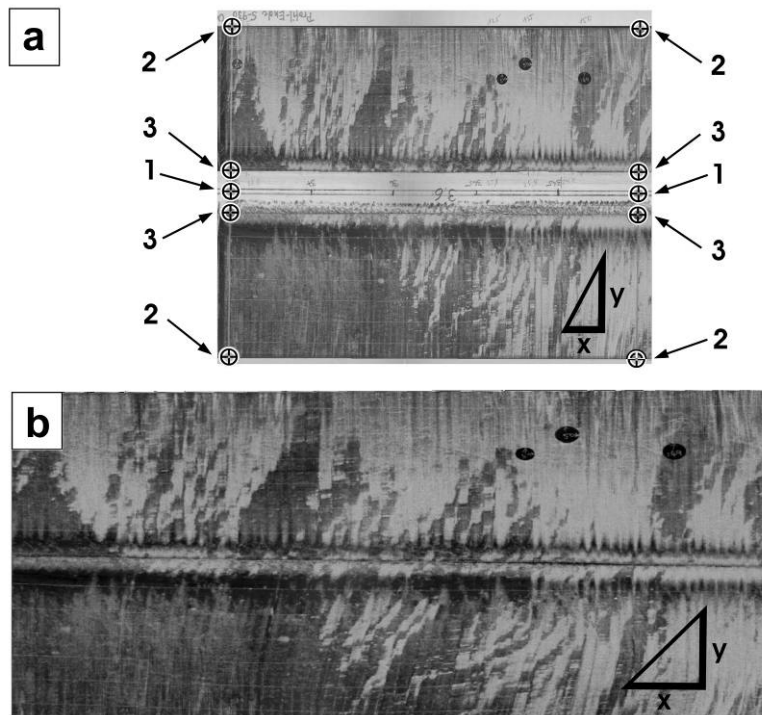


Figure IV.10. Geo-referencing procedure scheme: (a) Selection of ground control points: 1—sidescan sonar path, 2—edge of the range, 3—first bottom reflection and (b) result of geo-referencing with rubber sheeting method. Length of x and y is 100 m.

A sidescan sonar mosaic from these data was created in a process of conversion of analogue paper records into digital and geo-referenced data. Therefore, the analogue profiles were scanned into digital form. For every logged ship position four additional points were computed for the two sidescan sonar channels describing both swath and water column

extent (Fig.IV.10). The latter points were assigned lying on the centreline. After that, a geo-referencing method of 'rubber sheeting' was applied, in which the sonography was stretched or compressed between two neighbouring geo-referencing points (Fig.IV.10). In this way the entire water column visible in the sonographs was removed.

The result of geo-referencing based only on direct transformation of DECCA coordinates into UTM ones was unsatisfactory due to the positioning error, whose magnitude as well as the direction was different even for neighbouring points. Therefore, it was intended to fit the obtained image to stable ground control points (GCPs), like boulders, that were identifiable in both data sets. A significant amount of GCPs (six per profile at least) was necessary to fit the 1977 image. In the analogue paper records, selected boulders or groups of boulders were not numerous enough to perform this fitting. Therefore, a different approach was chosen to select reference points. A graphic tool processed both images in order to identify lines dividing areas of large grey-scale contrast. Consequently, sharp borders between two major sediment types were delineated, whereas gentle transition zones were omitted. Similarity of sharp borders layout in both images allowed selecting GCPs used for mosaic fitting. An error of 10m was assumed during their manual selection. A detailed description of the geo-referencing procedure as well as a study of positioning errors will be given in an upcoming publication (KUBICKI AND DIESING, 2006).

This procedure is admittedly not truly independent as it also uses sediment boundaries besides boulders to fit the data. We are therefore not able to resolve movements or oscillations of sediment boundaries in the range of metres or even a few decametres. The high similarity of sediment boundaries was nevertheless obvious, particularly when comparing individual analogue profiles with recent data prior to geo-referencing. Given the complicated and patchy nature of the surface sediment patterns present in the research area (as will be shown in the results section), it is highly unlikely that a largely different sediment distribution pattern would lead to the same results.

IV.2.4.3 Grain-size analysis

Eight seafloor samples were retrieved for ground-truthing. Samples were analysed for their particle size distributions. Therefore, they were first wet-sieved on a 63 µm sieve. The

weight-percentage of the mud fraction ($< 63 \mu\text{m}$) was calculated from the difference between non-sieved and sieved material. The remaining sediment was then dried and dry sieved afterwards, using sieves in steps of 0.25Φ . Grain-size distributions and statistical parameters were computed from the raw sieve data.

IV.2.4.4 Shear stress calculations

Time series of significant wave height H_s and the zero-crossing period T_z from the wave buoy NSB II (42 m water depth) were transformed by shoaling transformations according to Airy-wave theory, in order to account for shallower water depths in the study area (app. 34 m water depth). Given the relatively high water depths and the small depth change, this simple procedure is expected to yield reliable results. The calculation of bottom orbital velocities and shear stresses mainly followed the procedures outlined in SOULSBY (1997). The wave-induced bottom shear stress τ_w is linked with the bottom orbital velocity u_w via

$$\tau_w = 0.5 \cdot \rho \cdot f_w \cdot u_w^2, \quad (\text{IV.4})$$

where ρ is density of water and f_w is the wave friction factor (JONSSON, 1966). To calculate the friction factor via the roughness length z_0 , a flat bed was assumed, so that

$$z_0 = \frac{d_{50}}{12}, \quad (\text{IV.5})$$

where d_{50} is the median grain size of the bed sediment. The assumption of a flat bed is probably not realistic (see Section 5.1). Therefore, the bottom shear stresses might be underestimated, yielding a conservative estimate of the frequency of remobilization events. Critical shear stresses for the remobilization of bed sediment were calculated by the threshold Shields parameter

$$\theta_{cr} = \frac{\tau_{cr}}{g \cdot (\rho_s - \rho) \cdot d}, \quad (\text{IV.6})$$

where τ_{cr} is the threshold bed shear stress, g is acceleration due to gravity, ρ_s is grain density and d is grain diameter. The threshold Shields parameter is related to the dimensionless grain size d^* through the following (SOULSBY AND WHITEHOUSE, 1997):

$$\theta_{cr} = \frac{0.3}{1+1.2d_*} + 0.055(1 - \exp(-0.02d_*)), \quad (\text{IV.7})$$

$$d_* = \left(\frac{g((\rho_s/\rho) - 1)}{\nu^2} \right)^{\frac{1}{3}} d, \quad (\text{IV.8})$$

In theory, remobilisation takes place when the bottom shear stresses surpass the threshold bed shear stress.

Current-induced shear stresses were computed with a numerical model of the European continental shelf sea. An implicit finite difference numerical modelling system is used (ROELVINK AND VAN BANNING, 1994). The spherical grid covers the region between W13°/N48° and E13°/N62° with a resolution of 2.5 nautical miles (1/24°) in the latitudinal and 3.75 nautical miles (1/16°) in the longitudinal direction. For three-dimensional simulations, ten layers form the vertical sigma-coordinate grid.

The bathymetry was interpolated from the worldwide bathymetric and topography data from SMITH AND SANDWELL (1997) and digitised local nautical charts. At the lateral open boundaries the model is forced by water-level conditions from a global tidal model (EGBERT ET AL., 1994; EGBERT AND EROFEEVA, 2002). The harmonic open boundary conditions (10 astronomical constituents) were corrected for atmospheric pressure. At the water surface boundary, climate data (wind- and atmospheric pressure fields, e.g. from NOAA NCEP Re-analysis) were imposed to account for meteorological forcing.

The model has been calibrated and validated on the basis of water-level time-series from several tidal gauges throughout the model domain. Fig.IV.11 gives a comparison between measured and computed tidal harmonics for a station close to the study area. Although slightly under-predicting the amplitude of tidal harmonics, the relative and absolute amplitudes are reproduced by the numerical model. At this station, model simulations result in a variance

explained by 95% ($n = 19000$) and a mean squared error in water-level height of 0.05 m.

The shear stress at the bed induced by a turbulent flow is calculated by the quadratic friction law:

$$\tau_c = \frac{\rho g u_c^2}{C^2} \quad (\text{IV.9})$$

where u_c is the depth-averaged horizontal velocity and C the Chezy coefficient ($\text{m}^{0.5}/\text{s}$).

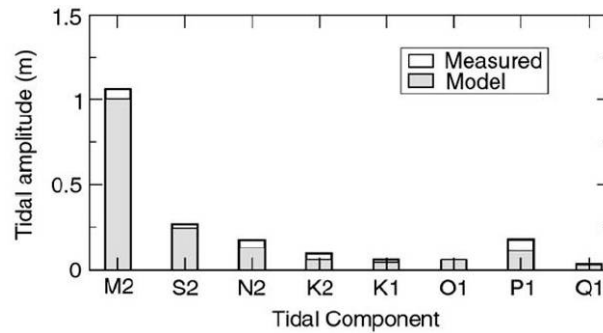


Figure IV.11. Water-level amplitudes of station Helgoland in the German Bight. Shown are results for the eight main tidal components as analysed from gauge records and numerical model simulations.

No improvements for the outcome of this study would be expected by the application of a fully coupled current and wave model. Such a model could not be validated with sufficient 3D-hydrodynamic data at the location of interest. Instead we prefer the application of a well-validated hydrodynamic model for currents and state-of-the-art wave measurements for waves. Moreover, it is our aim to investigate the relative importance of waves and currents for the remobilisation of bed sediment. We therefore treat wave- and current-induced shear stresses separately and make no attempt to compute combined shear stresses. Such an approach was already satisfactorily adopted by other authors (PALANQUES ET AL., 2002).

IV.2.5 Results

IV.2.5.1 Surficial geology

Sidescan sonar backscatter and single-beam bathymetry data sets gathered during a survey in May 2002 were merged to yield a three-dimensional representation of the seafloor in the study area (Fig.IV.12). Morphologically, the area is dominated by a northwest–southeast-trending elongate depression, which is cut into a relatively plain seafloor. The plains in the northeast and southwest are dominantly covered with well-to-moderately well-sorted fine sands (Tab.IV.3), which are also present on the southwestern flank of the depression (Figs.IV.12 and IV.13). Grain-size distributions peak around 2.85Φ , equivalent to $139\ \mu\text{m}$ (Tab.IV.3 and Fig.IV.14).

Table IV.3. Grain-size statistical measures of samples from ground-truth stations.

Sample	Median (Φ)	Folk-mean (Φ)	Folk-sorting (Φ)	First mode (Φ)
<i>Well-to-moderately well sorted fine sands</i>				
UR-04	2.88	2.92	0.39	2.88
UR-06	2.70	2.58	0.56	2.85
UR-07	2.60	2.54	0.48	2.80
UR-08	2.77	2.68	0.52	2.85
UR-33	2.83	2.83	0.38	2.85
<i>poorly sorted sandy gravels ("coarse sediment")</i>				
UR-05	-1.30	-1.05	1.49	-2.03
UR-34	-1.33	-1.32	1.13	-1.33
<i>Transitional sediment</i>				
UR-09	1.17	1.28	0.46	1.10

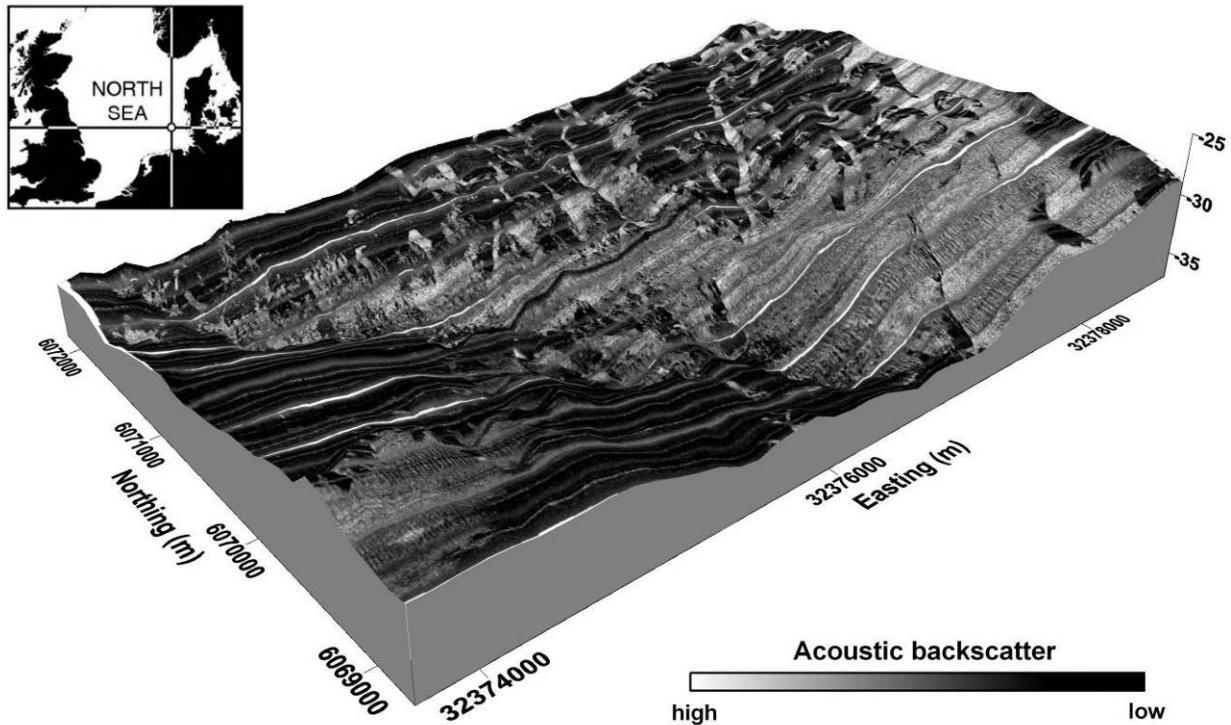


Figure IV.12. Overview of the research area showing relationships between surficial sediments indicated by sidescan sonar backscatter strength and bathymetry. View is from southwest. Vertical exaggeration: 75-fold.

The deepest parts and the northeastern flank of the depression are covered with coarse grained and poorly sorted lag deposits consisting of sand, gravel, and boulders. In some occasions, boulders are also present in the fine sand domains, where they protrude through a

thin layer of sand. A fourth class of sediments, poorly sorted sandy gravels (Tab.IV.3 and Fig.IV.14), can be observed, especially on the north-eastern plain. Here, the coarse sediments are organised into elongate bands of several tens of metres in width and hundreds to thousands of metres in length (Figs.IV.12 and IV.13). The bands are dominantly oriented in a north–northeast–south–southwest direction, but other directions are also observed. The coarse sediment bands are located in slight depressions on the seafloor. The described patterns are interpreted as sorted bedforms.

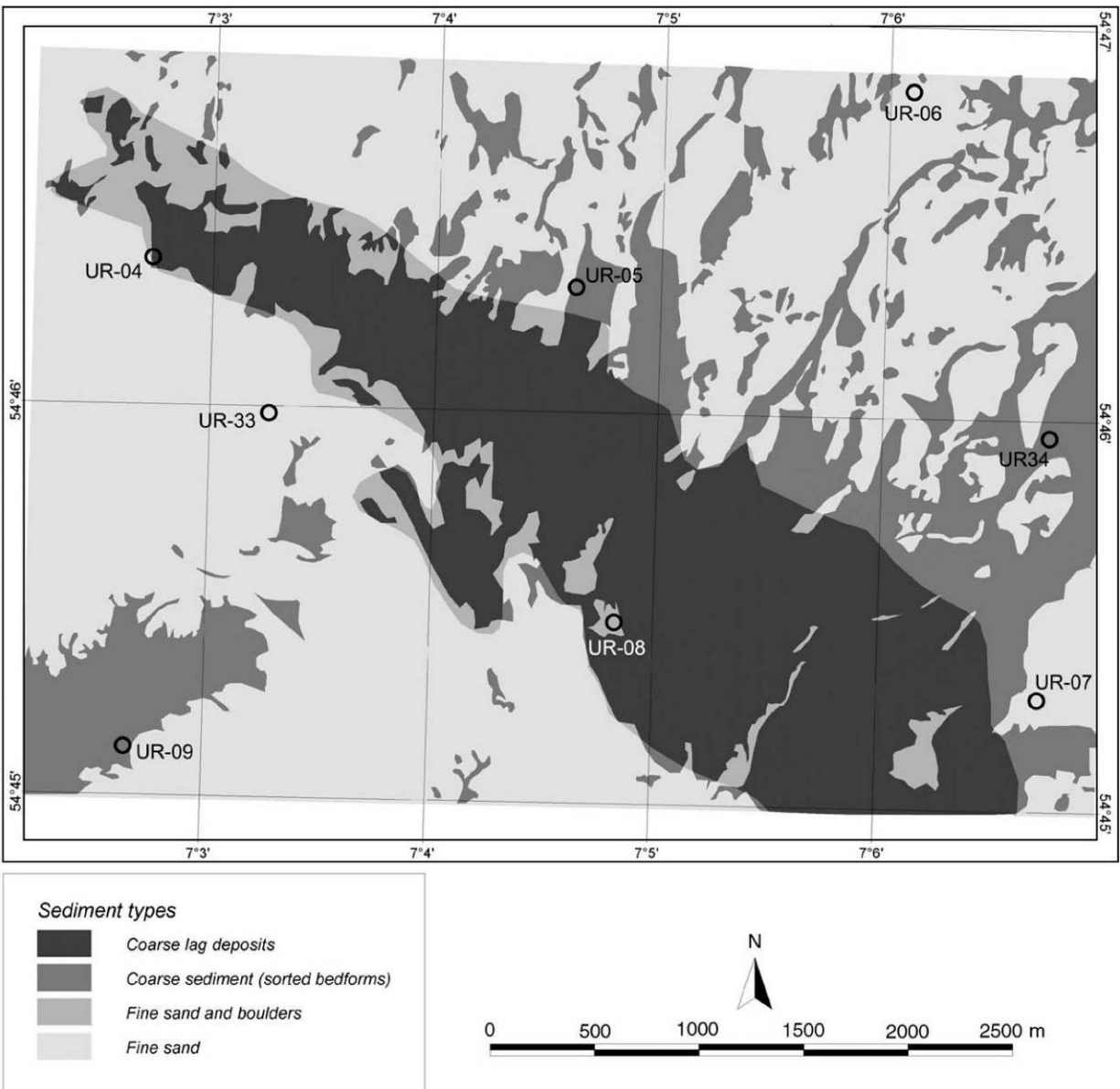


Figure IV.13. Sediment types within the research area. Interpretation is based on sidescan sonar backscatter strength and ground-truth sediment grab sample data. Positions of grab sampling stations are indicated.

Sorted bedforms are also present in the southwestern corner of the research area but they reveal a slightly lower backscatter when compared to “regular” sorted bedforms. The lower backscatter corresponds with a grain-size distribution intermediate between fine sands and coarse sediment (Fig.IV.14).

Ripples were observed within the lag deposit and sorted bedform areas. Ripple wavelengths varied between 0.7 and 1.4 m. Two distinct ripple crest orientations of 32° (north–northeast–south–southwest) and 137° (southeast–northwest) are discernable, whereby the former tends to be associated with larger wavelengths of 1.2 m on average, while the latter has average wavelengths of 0.85 m. Ripple marks are probably also present on the fine sand plains as was evidenced from video surveys in adjacent areas, but are below the resolution of the sidescan sonar.

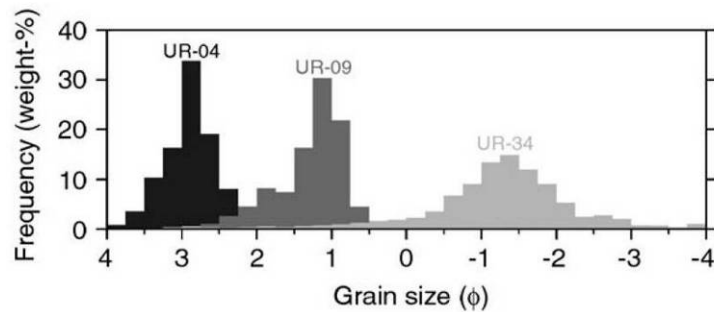


Figure IV.14. Representative grain-size distributions for fine sand (UR-04), coarse sediment (UR-34) and transitional sediment (UR-09).

Boundaries between fine sand and coarse sediment/ lag deposits are sharp in most instances. Gradual boundaries are present in the southeastern and southwestern corner of the study area and they tend to be located at the northeastern to southeastern boundaries of the coarse sediment patches.

IV.2.5.2 Re-mobilisation of surficial sediments

Wave- and current-induced shear stresses were calculated for the period between two surveys in May 2002 and 2003 at two sites, where seafloor samples were retrieved and investigated (Fig.IV.13): fine sand (UR-33, $d_{50} = 141 \mu\text{m}$, water depth: 34.5 m) and coarse sediment (UR-05, $d_{50} = 2.46 \text{ mm}$, water depth: 34 m). At the fine sand station (Fig.IV.15), the seabed sediment is remobilised by tidal- and wind-induced currents during approximately one-quarter of the time. Storm-wave-induced remobilization takes place during 31 events or approximately 9% of the time. At the coarse sediment station (Fig.IV.16), current induced shear stresses are not at all capable of remobilising the seafloor sediment. Remobilisation only takes place during 5 strong storm events, which comprise approximately 2% of the time between the surveys.

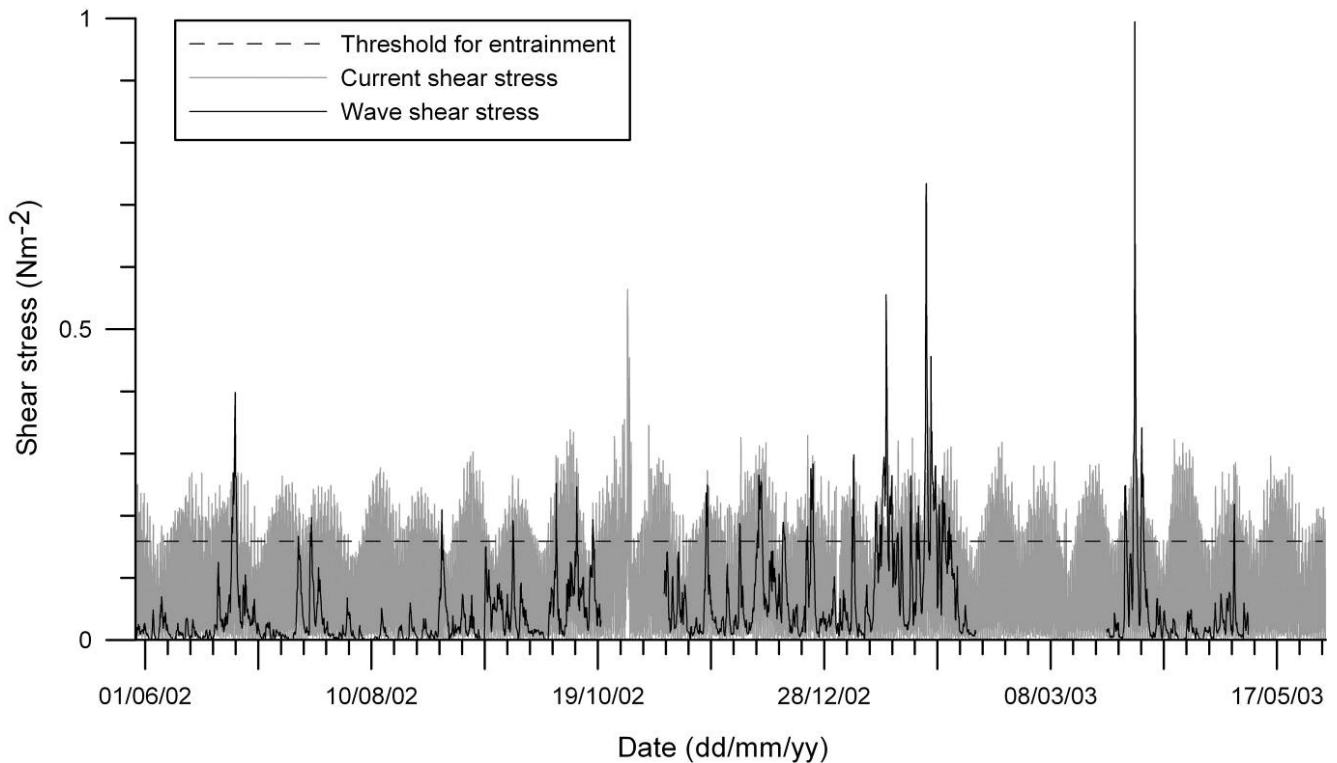


Figure IV.15. Current- and wave-induced shear stresses in relation to critical shear stresses for the remobilisation of seabed sediment at the fine sand station (UR-33, $d_{50} = 141 \mu\text{m}$, water depth 34.5 m).

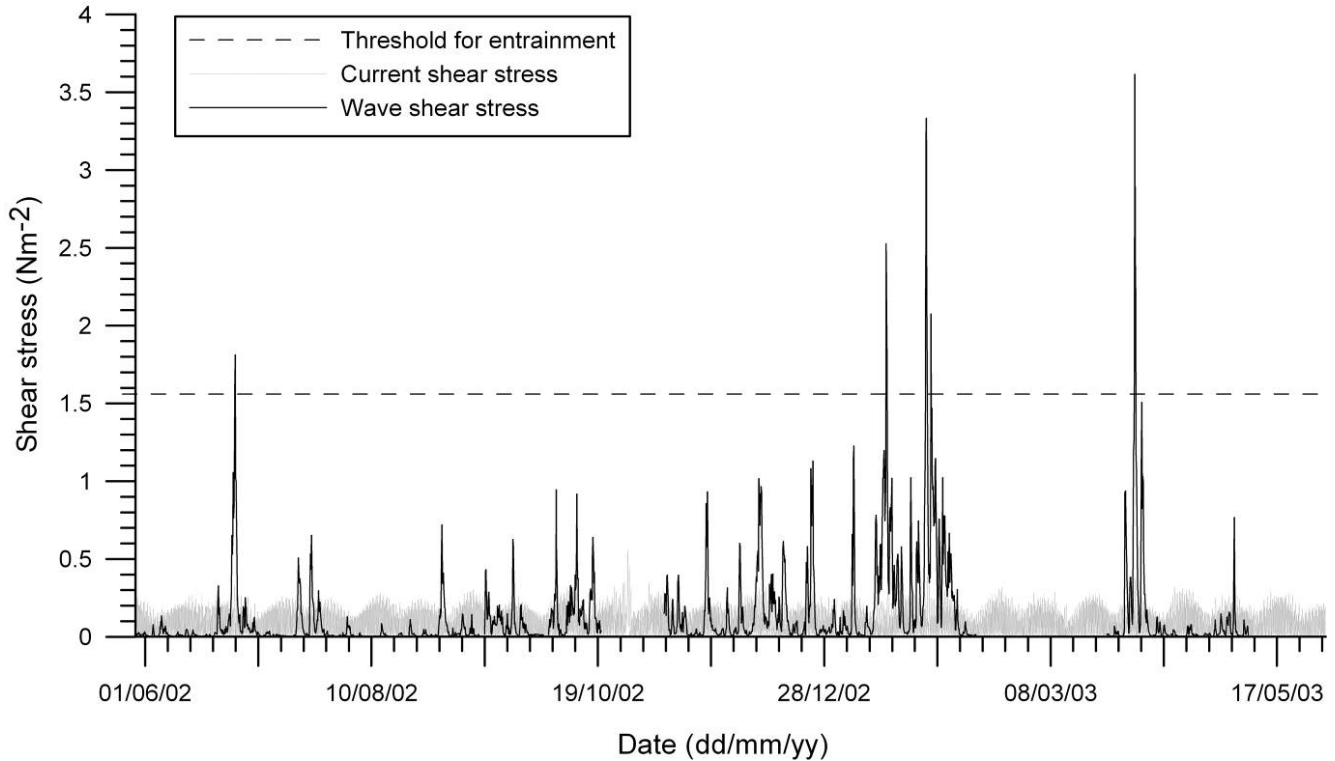


Figure IV.16. Current- and wave-induced shear stresses in relation to critical shear stresses for the remobilisation of seabed sediment at the coarse sediment station (UR-05, $d_{50} = 2.46$ mm, water depth 34 m).

IV.2.5.3 Temporal variability of sediment distribution patterns

The study area was surveyed in May 2003 with a multibeam echo sounder providing backscatter data. A comparison of the two backscatter images reveals a generally high stability of sediment distribution patterns (Fig.IV.17). In most instances, observed differences of the location of boundaries between coarse sediment and fine sand are within the range of the positioning error and therefore not significant.

We subsequently used archived analogue paper records of sidescan sonar data to investigate the longer-term (decadal scale) evolution of bedform patterns. When comparing the sediment distribution patterns of individual survey lines from 1977 with digital data from 2002, it appeared that slight differences were discernable, but the general picture looked very similar. Three typical examples are shown in Fig.IV.18. This is also in line with findings of WERNER (2004), who compared distribution patterns from three successive years (1977–1979) in the same area. These results gave us confidence to “reconstruct” a sidescan sonar mosaic of the 1977 analogue data. As stable geo-referencing points like large boulders were

not sufficiently numerous in the analogue records, we also used characteristic sediment patterns, as outlined in Section 4.2. This approach enabled us to work out a plausible picture of the sediment distribution patterns in 1977. Thus, it was easily possible to fit the 1977 patterns with the 2002 data, which would have been impossible if significant changes in the sediment patterns had occurred (Fig.IV.19).

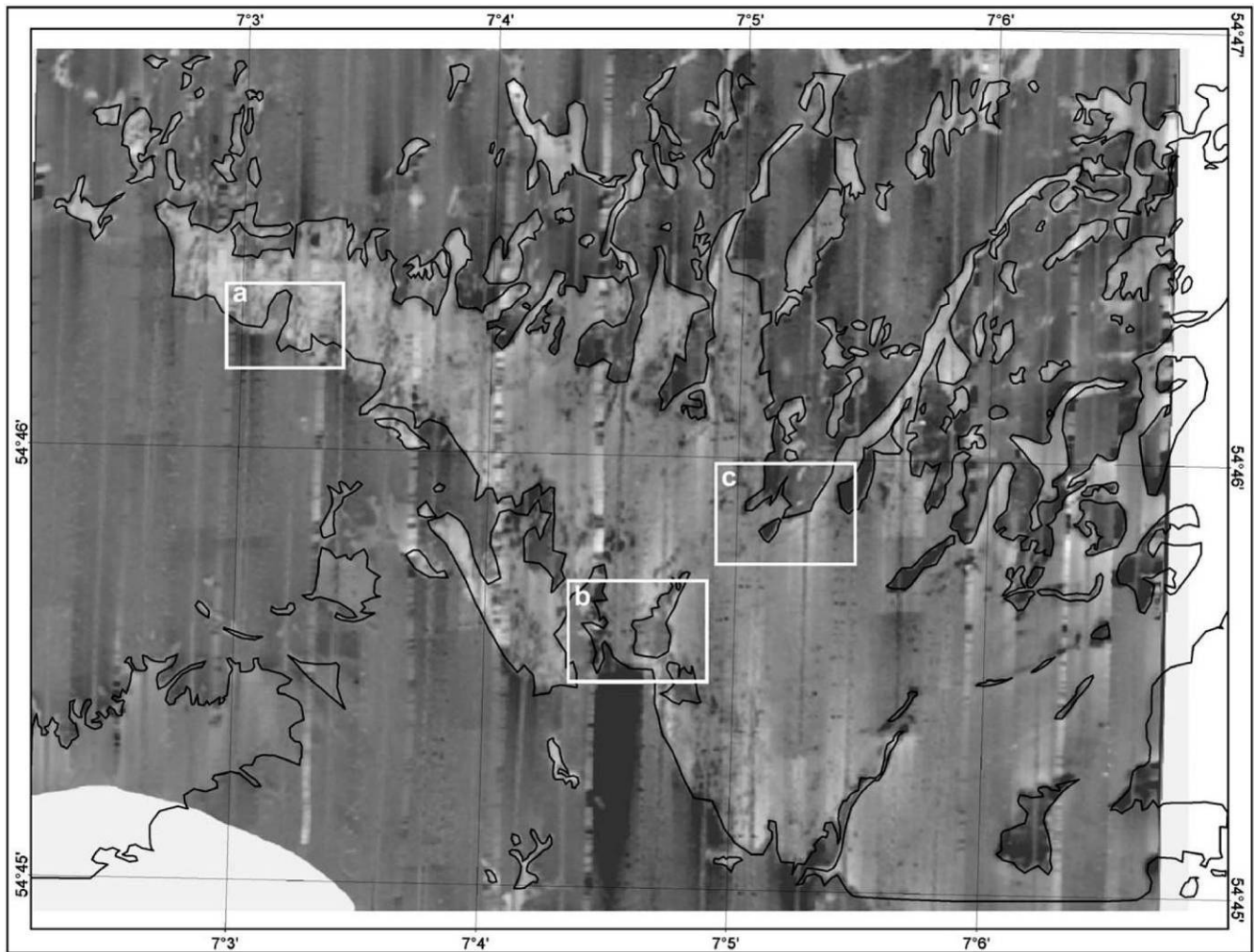


Figure IV.17. Multibeam backscatter map from May 2003. Outline of fine sand/coarse sediment boundary derived from data obtained in May 2002 is indicated by black line. White boxes indicate locations of close-ups shown in Fig.IV.18.

Taking into account the uncertainty of a few decametres introduced by the georeferencing method, the general sediment distribution patterns remained almost unchanged through a period of 25 years, except in the southwest-corner of the study area. Here, the seafloor was covered with fine sand in 1977, while in 2002, several coarse sediment patches

were present. These coarse sediments appear to have an intermediate backscatter and grain-size. The orientation of the largest new coarse sediment patch is approximately 60° (northeast) being perpendicular to the dominant direction of approaching waves.

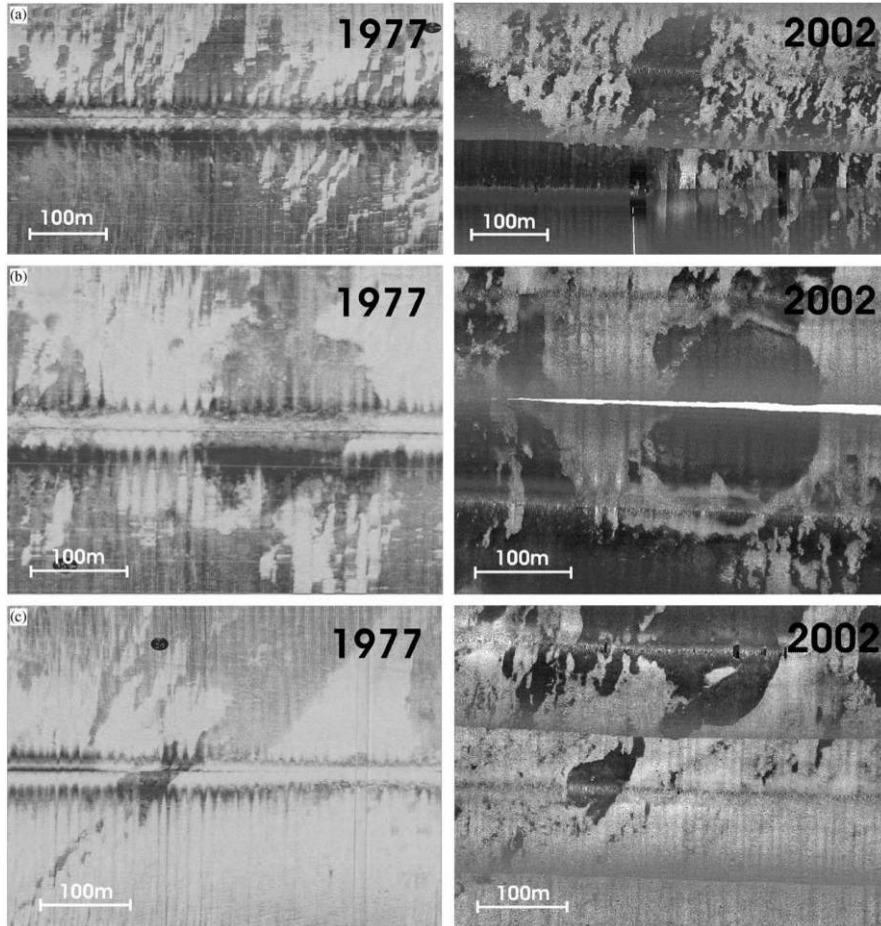


Figure IV.18. Comparison of sidescan sonar backscatter records from individual profile lines gathered in 1977 and 2002. A high level of seafloor morphologic stability is apparent.

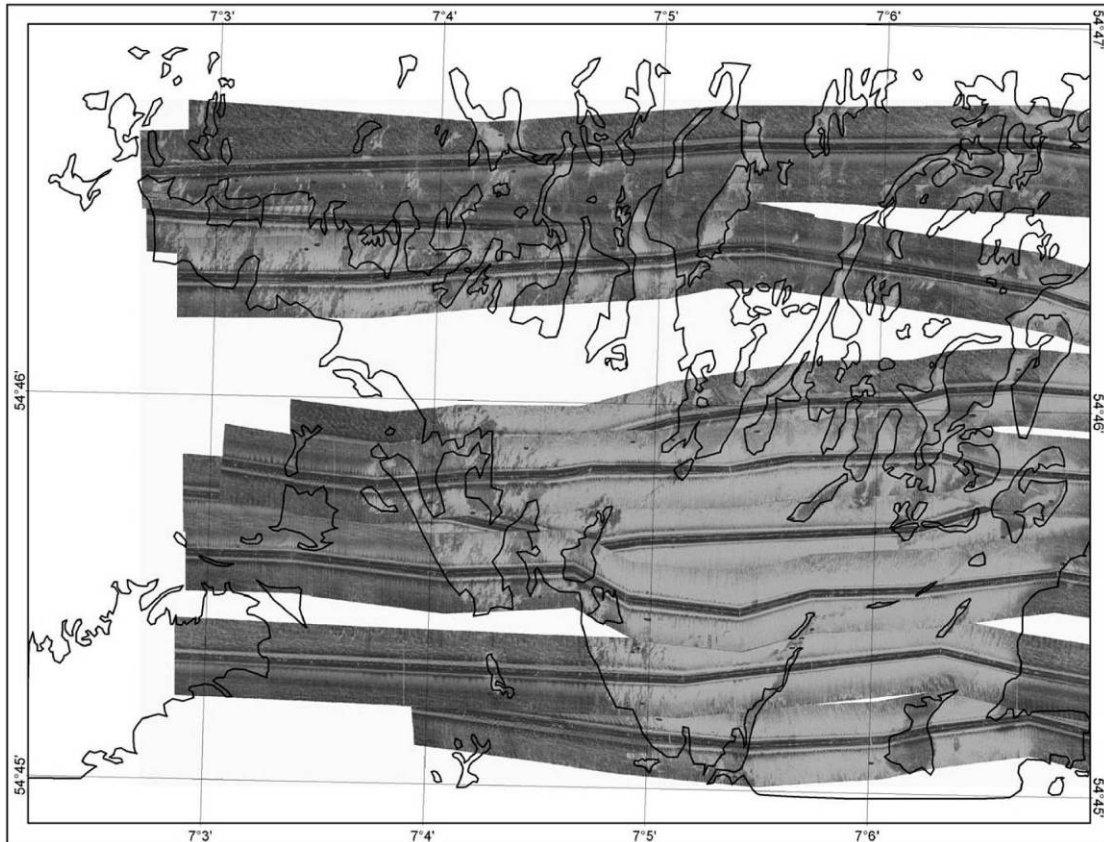


Figure IV.19. Reconstructed mosaic of geo-referenced analogue sidescan sonar backscatter data from 1977. Outline of fine sand/coarse sediment boundary derived from data obtained in May 2002 is indicated by black line.

IV.2.6 Discussion

Although wave and current conditions favour a frequent remobilisation of fine sands and an episodic remobilisation of sandy gravels, we observed no significant changes in the distribution of sorted bedform patterns on annual time-scales. Our results coincide with other studies which report on a high stability of sorted bedforms (HUME ET AL., 2003; THIELER ET AL., 2001; WERNER, 2004) or other sediment distribution patterns with high grain-size contrast (ANTHONY AND LETH, 2002; SCHWARZER ET AL., 2003; TAUBER AND EMEIS, 2005). Our results also support the hypothesis for the maintenance of sorted bedforms (MURRAY AND THIELER, 2004).

Moreover, we have shown that sorted bedform patterns on the inner shelf of the German Bight are generally stable on time-scales of several decades. GOFF ET AL. (2005) observed movements of sorted bedform boundaries in the range of tens of metres over a time

span of months. However, they reasoned that the boundaries oscillated, rather than migrating in one direction. Moreover, the general bathymetry of the sorted bedforms appeared quite stable over a span of nearly four decades. Although we cannot resolve oscillations and we lack bathymetric data from 1977, it is reasonable to assume that the same applies to the German Bight field site. Sorted bedforms might therefore be viewed as stable features on time-scales of at least decades, regarding bathymetric expression and general sediment distribution patterns, while the boundaries oscillate in the range of tens of metres. Further stratigraphic evidence for this hypothesis is reported by [THIELER ET AL. \(2001\)](#). From several vibracores taken in a profile line perpendicular to a sorted bedform, the authors inferred periodic infilling with fine sand. According to [GOFF ET AL. \(2005\)](#), such oscillations can be attributed to small-scale ripple migration forced by wave orbital velocity skewness. Another explanation could be reversing tidal currents of unequal strength. Nevertheless, systematic movements of sorted bedforms seem to occur under extraordinary conditions such as hurricanes as shown by [MURRAY AND THIELER \(2004\)](#).

Our long-term comparisons also indicate the formation or “birth” of new sorted bedforms in an area which was previously covered with fine sand. Due to their appearance (intermediate backscatter/ grain size), it seems that these emerging patterns are still in a transient state and have not reached maturity, i.e. the process of sorting is still underway. Sediment core and seismic data indicate that the thickness of fine sand amounts to a few metres within this area ([WINN AND WERNER, 1984](#)). It is therefore not very likely that the formation of the sorted bedforms was initiated by the excavation of buried coarse material, such as the transgressive gravel layer or Saalian till which is present in the research area. Moreover, we observed intermediate backscatter/grain-size, which can be explained by a continuous sorting process, but is in conflict with a hypothesis of excavation of coarse material. Other mechanisms should therefore be responsible for the formation of these sorted bedforms. Measurements from the inner shelf off Tairua Beach ([GREEN ET AL., 2004](#)) indicate that coarse sand entrained from sorted bedforms can escape onto surrounding fine sand plains under high waves. This escaping coarse sand may seed the growth of new sorted bedforms and might be the case in the study area of the German Bight. If so, coarse sand was transported at least several hundreds of metres away from existing sorted bedforms and almost ten metres upslope. On the other hand, the widespread occurrence of lag deposits

indicates that inherited geology (like coarse-grained underlying strata) cannot be a priori ruled out in the formation of sorted bedform patterns.

The observed sorted bedforms, especially in the northeastern part of the study area, tend to have an orientation of 30° (north-northeast–south–southwest) and are in most cases symmetric with sharp coarse-fine sediment boundaries. This symmetry of sorted bedforms can be explained in two ways: (1) the patterns are interpreted as longitudinal in origin, induced by flows parallel to the axis of the bedforms. This explanation is in conflict with the observed tidal currents, which flow to the east–southeast (120°) during the flood phase and west–northwest (300°) during the ebb phase. It would therefore imply that the sorted bedforms were initially formed in a completely different environmental setting, e.g. during a phase when the sea-level was lower than present. Reconstructions of paleo-shorelines (BEHRE, 2003) indicate a north–northwest–south–southeast trend of the shoreline approximately 9000 years ago, when the sea-level was 30 m lower than present. Shore-normal storm-induced flows could then have been capable of forming the observed patterns as proposed by CACCHIONE ET AL. (1984). However, this would suggest that the sorted bedforms are 9000 years old, which seems highly unlikely; (2) more likely, the sorted bedforms are flow-transverse in orientation, as indicated by the orientation perpendicular to the tidal flows, and are shaped and maintained by reversing tidal currents. Similar to sand waves (ALLEN, 1982), sorted bedforms might be subdivided into transverse-asymmetric and transverse-symmetric types, depending on the flow field. A reversing tidal current of almost equal strength during ebb and flood (as present in the research area) would favour the formation of symmetric sorted bedforms, while unidirectional currents, like persistent coast-parallel flows, form asymmetric sorted bedforms as observed by MURRAY AND THIELER (2004) and GOFF ET AL. (2005). However, the newly emerging sorted bedforms are asymmetric, with an orientation independent of tidal current flow but perpendicular to the direction from which the highest storm waves approach the study area. We thus conclude that extreme storm events play a major role in the generation of sorted bedforms in the study area, whereas tidal currents form and maintain their final shape.

This conclusion is also in line with the results of our shear stress estimations. The movement of fine sand can be regarded as the main process in shaping the boundaries of sorted bedforms. Our data indicate a frequent remobilisation of fine sands, which can be

regarded as quasi-continuous on time scales of several decades. On the other hand, the emergence of new sorted bedforms might be linked with the escape of coarse material from existing sorted bedforms under high waves, thereby seeding the growth of new sorted bedforms (GREEN ET AL., 2004). According to our shear stress estimations, such strong storm events capable of remobilizing coarse material only occur episodically.

In addition to the newly emerging sorted bedforms, asymmetric sorted bedforms are observed in the shallowest regions of the study area with water depths of less than 30 m. Moreover, farther to the east, southeast and south, beyond the boundaries of the study area, where water depths are generally less than 30 m, asymmetric sorted bedforms are widespread, as indicated in Fig.IV.12 of WERNER (2004). These bedforms are aligned dominantly in a north–northeast–south–southwest-direction and the sharp boundaries face seaward to the west–northwest. These observations indicate that whether sorted bedforms are symmetric or asymmetric might also be controlled by depth-dependent factors. In the absence of detailed hydrodynamic data, we can only speculate that especially under storm conditions increased asymmetry of wave orbital velocities in shallower water might account for the observed patterns. A similar explanation was given by NEWTON ET AL. (1973) in the case of the Spanish Sahara continental shelf.

IV.2.7 Conclusions

Based on the comparison of backscatter maps spanning 26 years between 1977 and 2003 we conclude that existing sorted bedforms in the southeastern German Bight are stable on time scales of at least decades. Moreover, we observe the formation of new sorted bedforms. Our observations confirm the hypothesis of sorted bedform formation through a feedback-related sorting process (MURRAY AND THIELER, 2004). Due to their geometric characteristics (orientation, symmetry), it appears that most observed sorted bedforms in the study area are shaped and maintained by tidal flows. However, the initial formation of new sorted bedforms seems to be related to exceptional storm waves.

Acknowledgements

This work was funded by Bundesamt für Naturschutz and Bundesministerium für Umwelt, Naturschutz und Reaktorsicherheit (grant number 802 85 270). Fieldwork was assisted by the captain and crew of R/V Littorina

(Leibniz Institute for Marine Sciences, Kiel). Wave data from NSB II were kindly provided by Ralf Berger (BSH, Hamburg). Bathymetric data were corrected for waterlevel variations by BSH, Hamburg. We thank all persons and institutions mentioned above. We are especially grateful to Frieder Werner for numerous valuable discussions and comments on an earlier draft of the manuscript and two anonymous reviewers for their constructive comments and suggestions.

V GENERAL DISCUSSION AND CONCLUSIONS

Sidescan sonar data play a significant role in morphodynamics investigations on shelf seas. Sonographs carry important information on shelf sediment and, properly interpreted, they can be the key source of seabed dynamics studies. The characteristics of individual sidescan sonar system, however, influences greatly a quality of performed work (see Section IV.1). In the presented case studies sidescan sonar systems without towfish position control were used, what led to additional estimations of spatial error and to several assumptions of spatial confidence. This difficulty does not exist for modern sidescan sonar systems, as stressed in section I.2.1.

A major issue in morphodynamics studies is the frequency of repetitive surveying of investigated area, which should be controlled by a rate of morphological changes. In the case of sand dunes migration, the frequency of several months is commonly practiced (section I.5.1). For refilling marine extraction pits a monitoring rate of half a year was found appropriate (section III), whereas a one year span of imaging sorted bedforms still did not reveal significant dynamics (section IV.2).

The seabed dynamics can be investigated by numerous methods. Except enhanced sidescan sonar systems none of the models can collect information on water-depth, swath morphology, sub-bottom architecture, or associated hydrodynamic conditions, which are all important data for estimating rates of changes (see sections I.4 and I.5). Therefore a combination of devices is usually applied, which guarantees better overview of a topic and in some of the cases is unavoidable (see the combination of sub-bottom profiler and sidescan sonar in a study of fluid mud dynamics by [SCHROTTKE ET AL., 2006](#)).

The combination of methods seems to be dependant on accessibility of devices rather than on the need for particular data. A very good example is introduced in the case study on sand dunes migration (Section II), where sidescan sonar data are accompanied by a single-beam echosounder, shallow seismics and sediment sampling data. Here, sidescan sonar was used even though its role was limited to crests delineation and thus sand-bodies orientation. Height of sand dunes as well as water depth values applied to [YALIN \(1964\)](#) equation, were registered by the echosounder. A 3-dimensional morphology of dunes was deduced from the sonographs, but it is hard to assume that a nadir point of the echosounder crossed a dune in

the place of maximum dune height. In such a small-scale study, problems with correct dunes height estimation are certainly minor, however, where the precision is essential, a much better device for sand dunes mapping appears to be a modern multibeam echosounder, which collects simultaneously swath bathymetry and backscatter (PRASTON AND EDWARDS, 1996).

Multibeam echosounders are applied for already longer than 30 years (see WHITE, 1971), but early versions were not perfectly designed for undistorted image collection (e.g. MITCHELL, 1996), nor precise backscatter mapping (e.g. MITCHELL AND HUGHES CLARKE, 1994; SHAW ET AL., 1997). Technological development of these devices, however, resulted in a high horizontal and vertical accuracy of the latest models (ERNSTSEN ET AL., 2006b) and implementation of 300 kHz wavelengths to record backscatter (FERRINI AND FLOOD, 2006). Such systems become gradually equal to sidescan sonars, however in this study (Section III), an earlier multibeam model (180 kHz) was utilised.

In the case study on refilling extraction pits (Section III) multibeam echosounder was successfully applied for overall comparison of morphological changes within pits. The accuracy of pits depths measurement appeared to be much beyond the estimation based on acoustic shadow in the sonographs. The multibeam resolution, however, did not allow to identify slumps edges. Furthermore, its co-registered backscatter could not resolve a screened sand fraction. The resolution of sonographs became thus a significant advantage of sidescan sonar application for this large-scale study.

For a middle-scale investigation, the resolution of a multibeam data set proved to be sufficient for spatial evaluation of backscatter (see Section IV.2). Two sidescan sonar mosaics were successfully compared to a multibeam backscatter map and only a relatively short time-span between surveys excluded multibeam as a helpful source of material for this particular study. The long-term stability of sorted bedforms and the birth of new units were observed in sidescan sonar images due to their availability.

Newer and more precise sidescan sonar systems appear on the market, but majority of scientific investigations is executed in wavelengths 100-500 kHz (see sections I.4 and I.5). Such working frequencies appear to be a limit of cost-efficient surveys. As it is presented in this work, sonographs registered in wavelengths 105-384 kHz appeared to be an ideal tool for morphodynamics studies in any scales. And thus, a technological superiority of dual-purpose

multibeam echosounders will probably cause gradual substitution of sidescan sonar systems in sedimentological researches.

On the other hand, surf-zone studies or target recognition activities demand an application of higher frequency systems (section I.3 and [QUINN ET AL., 2005](#)). In marine archaeology studies there exists a cost-efficient limit of 1.2 MHz. Operators of such sonar systems have to keep towfish steady below 2 m of altitude to obtain desired good-quality sonographs (www.marinesonic.com). This certainly restricts towed systems for deeper-water studies, but mounting even 2.4-MHz systems on unmanned vehicles ([WILCOX AND FLETCHER, 2003](#)) opens more possibilities for sidescan sonar applications in offshore very-large-scale research (e.g. offshore ripplemarks dynamics).

VI LITERATURE CITED

- ACKERS, P. AND WHITE, W.R., 1973: Sediment Transport: New Approach and Analysis. *Journal of the Hydraulic Division, Proceedings Am. Soc. Civil Engineers*, 99 (HY11), 2041-2060.
- ADAMS, C.E.JR, WELLS, J.T., COLEMAN, J.M., 1986: Transverse Bedforms on the Amazon Shelf. *Continental Shelf Research*, 6 (1/2), 175-187.
- ALLEN, J.R.L., 1962: Asymmetrical Ripple Marks and the Origin of Cross-stratification. *Nature*, 194, 167-169.
- ALLEN, J.R.L., 1968: Current Ripples. North-Holland. Amsterdam, 433 pp.
- ALLEN, J.R.L., 1982: Sedimentary Structures, Their Character and Physical Basis. Developments in Sedimentology, 30 A, 593 pp.
- AMOS, C.L. AND KING, E.L., 1984: Bedforms of the Canadian Eastern Seaboard: A Comparison with Global Occurrences. *Marine Geology*, 57, 167-208.
- ANON, 1976: Decca Navigator Principles and Performance of the System, The Decca Navigator Company Limited, New Malden.
- ANON, 2005: Tide Tables Vol. II. Marine Hydrometeorological Centre, Hanoi, 218 pp.
- ANTHONY, D. AND LETH, J.O, 2002: Large-scale Bedforms, Sediment Distribution and Sand Mobility in the Eastern North Sea off the Danish West Coast. *Marine Geology*, 182, 247-263.
- ASHLEY, G.M., 1990: Classification of Large-scale Subaqueous Bedforms: a New Look at an Old Problem. *Journal of Sedimentary Petrology*, 60(1), 160-172.
- AUBREY, D.G., TWICHELL, D.C., PFIRMAN, S.L., 1982: Holocene Sedimentation in the Shallow Nearshore Zone off Nauset Inlet, Cape Cod, Massachusetts. *Marine Geology*, 47, 243-259.
- BAGNOLD, R.A., 1963: Beach and Near-shore Processes, I: Mechanics of Marine Sedimentation. In: Hill, M.N. (Ed.), *The Sea*. Interscience, New York, pp. 507-549.
- BALLARD, R.D., COLEMAN, D.F., ROSENBERG, G.D., 2000: Further Evidence of Abrupt Holocene Drowning of the Black Sea Shelf. *Marine Geology*, 170, 253-261.
- BALQUIN, Y. AND HOWA, H., 2002: Sediment Transport Pattern at the Barra Nova Inlet, South Portugal: a Conceptual Model. *Geo-Marine Letters*, 21, 226-235.
- BARRIE, J.V., LEWIS, C.F.M., FADER, G.B., KING, L.H., 1984: Seabed Processes on the Northeastern Grand Banks of Newfoundland; Modern Reworking of Relict Sediments. *Marine Geology*, 57, 209-227.
- BARTHOLOMÄ, A, 2006: Acoustic Bottom Detection and Seabed Classification in the German Bight, Southern North Sea. *Geo-Marine Letters*, 26, 177-184.
- BASSETTI, M.A., JOUET, G., DUFOIS, F., BERNÉ, S., RABINEAU, M., TAVIANI, M., 2006: Sand Bodies at the Shelf Edge in the Gulf of Lions (Western Mediterranean): Deglacial History and Modern Processes. *Marine Geology*, 234, 93-109.
- BEHRE, K.E., 2003: Eine Neue Meeresspiegelkurve für die Südliche Nordsee. Transgressionen und Regressionen in den Letzten 10.000 Jahren. Probleme der Küstenforschung im Südlichen Nordseegebiet, 28, 9-63.
- BELDERSON, R.H., KENYON, N.H., STRIDE, A.H., 1970: 10-km Wide Views of Mediterranean Deep Sea Floor. *Deep-Sea Research*, 17, 267-270.
- BELDERSON, R.H., KENYON, N.H., STRIDE, A.H., STRUBBS, A.R., 1972: Sonographs of the Seafloor, 185 pp., Elsevier, Amsterdam.
- BENDER, C.J. AND DEAN, R.G., 2003: Wave Field Modification by Bathymetric Anomalies and Resulting Shoreline Changes: a Review with Recent Results. *Coastal Engineering*, 49, 125-153.

- BERGEN, B.J., NELSON, W.G., MACKAY, J., DICKERSON, D., JAYARAMAN, S., 2005: Environmental Monitoring of Remedial Dredging at the New Bedford Harbor, MA, Superfund Site. *Environmental Monitoring and Assessment*, 111, 257-275.
- BESIO, G., BLONDEAUX, P., BROCCINI, M., VITTORI, G., 2003: Migrating Sand Waves. *Ocean Dynamics*, 53, 232-238.
- BEST, J.L., 1992: On the Entrainment of Sediment and Initiation of Bed Defects: Insight from Recent Developments within Turbulent Boundary Layer Research. *Sedimentology*, 39, 797-811.
- BIRCHENOUGH, S.N.R., BOYD, S.E., COGGAN, R.A., LIMPENNY, D.S., MEADOWS, W.J., REES, H.L., 2006: Lights, Camera and Acoustics: Assessing Macrobenthic Communities at a Dredged Material Disposal Site off the North East Coast of the UK. *Journal of Marine Systems*, 62, 204-216.
- BLACK, K.P. AND HEALY, T.R., 1986: The Sediment Threshold over Tidally Induced Megaripples. *Marine Geology*, 69, 219-234.
- BLONDEL, P. AND MURTON, B.J., 1997: Handbook of Seafloor Sonar Imagery; Wiley-Praxis Ser. in Remote Sensing, John Wiley & Sons, Chichester; 314 p.
- BLOTT, S.J., PYE, K., VAN DER WAL, D., NEAL, A., 2006: Long-term Morphological Change and its Causes in the Mersey Estuary, NW England. *Geomorphology*, 81, 185-206.
- BODUR, M.N. AND ERGIN, M., 1992: Holocene Sedimentation Patterns and Bedforms in the Wave-current-dominated Nearshore Waters of Eastern Mersin Bay (Eastern Mediterranean). *Marine Geology*, 108, 73-93.
- BOUMA, A.H., RAPPEPORT, M.L., ORLANDO, R.C., HAMPTON, M.A., 1980: Identification of Bedforms in Lower Cook Inlet, Alaska. *Sedimentary Geology*, 26, 157-177.
- BOYD, S.E., 2002: Guidelines for the Conduct of Benthic Studies at Aggregate Dredging Sites. UK Department for Transport, Local Government and the Regions, London and CEFAS Lowestoft, 117 p.
- BOYD, S.E. AND REES, H.L., 2003: An Examination of the Special Scale of Impact on the Marine Benthos Arising from Marine Aggregate Extraction in the Central English Channel. *Estuarine, Coastal and Shelf Science*, 57, 1-16.
- BOYD, S.E., LIMPENNY, D.S., REES, H.L., COOPER, K.M., CAMPBELL, S., 2003: Preliminary Observations of the Effects of Dredging Intensity on the Re-colonisation of Dredged Sediments off the Southeast Coast of England (Area 222). *Estuarine, Coastal and Shelf Science*, 57, 209-223.
- BOYD, S.E., COOPER, K.M., LIMPENNY, D.S., KILBRIDE, R., REES, H.L., DEARNALEY, M.P., STEVENSON, J., MEADOWS, W.J., MORRIS, C.D., 2004: Assessment of the Re-habilitation of the Seabed Following Marine Aggregate Extraction. Science Series Technical Report, CEFAS Lowestoft, 121, 154 p.
- BOYD, S.E., LIMPENNY, D.S., REES, H.L., COOPER, K.M., 2005: The Effects of Marine Sand and Gravel Extraction on the Macrobenthos at a Commercial Dredging Site (Results 6 Years Post-dredging). *ICES Journal of Marine Science*, 62, 145-162.
- BROWN, C.J., COOPER, K.M., MEADOWS, W.J., LIMPENNY, D.S., REES, H.L., 2002: Small-scale Mapping of Sea-bed Assemblages in the Eastern English Channel Using Sidescan Sonar and Remote Sampling Techniques. *Estuarine, Coastal and Shelf Science*, 54, 263-278.
- BROWN, C.J., MITCHELL, A., LIMPENNY, D.S., ROBERTSON, M.R., SERVICE, M., GOLDING, N., 2005: Mapping Seabed Habitats in the Firth of Lorn off the West Coast of Scotland: Evaluation and Comparison of Habitat Maps Produced Using the Acoustic Ground-discrimination System, RoxAnn, and Sidescan Sonar. *ICES Journal of Marine Science*, 62, 790-802.
- CACCHIONE, D.A., DRAKE, D.E., GRANT, W.D., TATE, G.B., 1984: Rippled Scour Depressions on the Inner Continental Shelf off Central California. *Journal of Sedimentary Petrology*, 54, 1280-1291.
- CASTON, G.F., 1981: Potential Gain and Loss of Sand by Some Sand Banks in the Southern Bight of the North Sea. *Marine Geology*, 41, 239-250.

- CATAÑO-LOPERA, Y.A. AND GARCÍA, M.H., 2006: Geometry and Migration Characteristics of Bedforms under Waves and Currents. Part 1: Sandwave Morphodynamics. *Coastal Engineering*, 53, 767-780.
- CHAVEZ, P.S.JR., ISBRECHT, J.A., GALANIS, P., GABEL, G.L., SIDES, S.C., SOLTESZ, D.L., ROSS, S.L., VELASCO, M.G., 2002: Processing, mosaicking and management of the Monterey Bay digital sidescan-sonar images. *Marine Geology*, 181, 305-315.
- CHEEN, C.S. AND WANG, J., 2003: Numerical Study of the Upper-Layer Circulation in the South China Sea. *Journal of Oceanography*, 59, 11-24.
- COCHRANE, G.R., LAFFERTY, K.D., 2002: Use of Acoustic Classification of Sidescan Sonar Data for Mapping Benthic Habitat in the Northern Channel Islands, California. *Continental Shelf Research*, 22, 683-690.
- COLEMAN, J.M., ROBERTS, H.H., MURRAY, S.P., SALAMA, M., 1981: Morphology and Dynamic Sedimentology of the Eastern Nile Delta Shelf. *Marine Geology*, 42, 301-326.
- COLLIER, J.S. AND BROWN, C.J., 2005: Correlation of Sidescan Backscatter with Grain Size Distribution of Surficial Seabed Sediments. *Marine Geology*, 214, 431-449.
- COLLIER, J.S. AND HUMBER, S.R., 2007: Time-lapse Side-scan Sonar Imaging of Bleached Coral Reefs: A Case Study from the Seychelles. *Remote Sensing of Environment*, in press, doi:10.1016/j.rse.2006.11.029
- COOPER, K., BOYD, S., ALDRIDGE, J., REES, H., 2007: Cumulative Impacts of Aggregate Extraction on Seabed Macro-invertebrate Communities in an Area off the East Coast of the United Kingdom. *Journal of Sea Research*, 57 (4), 288-302.
- COTTAZ, Y., BARTHES, V., BERNE, S., CROCHON, P., LERICOLAIS, G., ROBACH, F., 1989: Acoustic, Magnetic and Seismic Investigation of the Sea Floor off the Uraniferous District of Piriac, France. *Marine Geology*, 86, 201-220.
- DALRYMPLE, R.W., KNIGHT, R.J., LAMBIASE, J.J., 1978: Bedforms and Their Hydraulic Stability Relationships in a Tidal Environment, Bay of Fundy, Canada. *Nature*, 275, 100-104.
- DAVIS, R.A. AND HAYES, M.O., 1984: What is a Wave-dominated Coast? *Marine Geology*, 60, 313-329.
- DAVIS, K.S., SLOWEY, N.C., STENDER, I.H., FIEDLER, H., BRYANT, W.R., FECHNER, G., 1996: Acoustic Backscatter and Sediment Textural Properties of Inner Shelf Sands, Northeastern Gulf of Mexico. *Geo-Marine Letters*, 16, 273-278.
- DAVOULT, D. AND CLABAUT, P., 1988: Transition from the Sandy Bottom of the Bay of Wissant to the Hard Bottom Offshore and Associated Communities. *Journal of Research Oceanography*, 13, 32-35.
- DE GROOT, S.J., 1979: The Potential Environmental Impact of Marine Gravel Extraction in the North Sea. *Ocean Management*, 5, 233-249.
- DE GROOT, S.J., 1982: The Impact of Laying and Maintenance of Offshore Pipelines on the Marine Environment and the North Sea Fisheries. *Ocean Management*, 8 (1), 1-27.
- DESPREZ, M., 2000: Physical and Biological Impact of Marine Aggregate Extraction along the French Coast of the Eastern English Channel: Short- and Long-term Post-dredging Restoration. *ICES Journal of Marine Science*, 57, 1428-1438.
- DIESING, M., 2003: Die Regeneration von Materialentnahmestellen in der Suedwestlichen Ostsee unter Besonderer Beruecksichtigung der Rezenten Sedimentdynamik, Ph.D. thesis, University of Kiel, Germany, 158 p., unpublished.
- DIESING, M., KUBICKI, A., WINTER, C., SCHWARZER, K., 2006: Decadal Scale Stability of Sorted Bedforms, German Bight, Southeastern North Sea. *Continental Shelf Research*, 26, 902-916.
- DIESING, M., SCHWARZER, K., ZEILER, M., KLEIN, H., 2006: Comparison of Marine Sediment Extraction Sites by Means of Shoreface Zonation. *Journal of Coastal Research*, Special Issue 39, 783-788.
- DUCK, R.W., ROWAN, J.S., JENKINS, P.A., YOUNGS, I., 2001: A Multi-Method Study of Bedload Provenance and Transport Pathways in an Estuarine Channel. *Physics and Chemistry of the Earth (B)*, 26 (9), 747-752.

- EDWARDS, M.H., DAVIS, R.B., ANDERSON, R.M., 2003: Swath Mapping the Base of the Arctic Ice Canopy. *Cold Regions Science and Technology*, 36, 93-101.
- EGBERT, G., BENNETT, A., FOREMAN, M., 1994: TOPEX/Poseidon Tides Estimated Using a Global Inverse Model. *Journal of Geophysical Research*, 99(C12), 24821-24852.
- EGBERT, G. AND EROFEEVA, S., 2002: Efficient Inverse Modeling of Barotropic Ocean Tides. *Journal of Oceanic and Atmospheric Technology*, 19(2), 183-204.
- EHRHOLD, A., HAMON, D., GUILLAUMONT, B., 2006: The REBENT Monitoring Network, a Spatially Integrated, Acoustic Approach to Surveying Nearshore Macrobenthic Habitats: Application to the Bay of Concarneau (South Brittany, France). *ICES Journal of Marine Science*, 63, 1604-1615.
- EINSTEIN, H.A., 1950: The Bed Load Function for Sediment Transport in the Open Channel Flows. *Technical Bulletin*, U.S. Dept. of Agriculture Soil Conservation, 1026-1071.
- EITTREIM, S.L., ANIMA, R.J., STEVENSON, A.J., 2002: Seafloor Geology of the Monterey Bay Area Continental Shelf. *Marine Geology*, 181, 3-34.
- ENGELUND, F. AND HANSEN, E., 1967: A Monograph on Sediment Transport in Alluvial Streams. Teknisk Forlag, Copenhagen, 62 pp.
- ERDAS, Inc., 1997: ERDAS Field Guide, 4th ed. ERDAS, Inc., Atlanta, Georgia.
- ERGIN, M., BODUR, M.N., EDIGER, V., 1991: Distribution of Surficial Shelf Sediments in the Northeastern and Southwestern Parts of the Sea of Marmara: Strait and Canyon Regimes of the Dardanelles and Bosphorus. *Marine Geology*, 96, 313-340.
- ERNSTSEN, V.B., NOORMETS, R., WINTER, CH., HEBBELN, D., BARTHOLOMÄ, A., FLEMMING, B.W., BARTHOLDY, J., 2006a: Quantification of Dune Dynamics during a Tidal Cycle in an Inlet Channel of the Danish Wadden Sea. *Geo-Marine Letters*, 26(3), 151-163.
- ERNSTSEN, V.B., NOORMETS, R., HEBBELN, D., BARTHOLOMÄ, A., FLEMMING, B.W., 2006b: Precision of High-resolution Multibeam Echo Sounding Coupled with High-accuracy Positioning in a Shallow Water Coastal Environment. *Geo-Marine Letters*, 26(3), 141-149.
- FANG, W.D. AND FANG, G.H., 1998: The Recent Progress in the Study of the Southern South China Sea Circulation. *Advance in Earth Sciences*, 13(2), 166-172, (in Chinese with English abstract).
- FENSTER, M.S. AND FITZGERALD, D.M., 1996: Morphodynamics, Stratigraphy, and Sediment Transport Patterns of the Kennebec River Estuary, Maine, USA. *Sedimentary Geology*, 107, 99-120.
- FERENTINOS, G., PAPANICOLAOU, G., COLLINS, M.B., 1988: Sediment Transport Processes on an Active Submarine Fault Escarpment: Gulf of Corinth, Greece. *Marine Geology*, 83, 43-61.
- FERRINI, V.L. AND FLOOD, R.D., 2006: The Effects of Fine-scale Surface Roughness and Grain Size on 300 kHz Multibeam Backscatter Intensity in Sandy Marine Sedimentary Environments. *Marine Geology*, 228, 153-172.
- FIELD, M.E., NELSON, C.H., CACCHIONE, D.A., DRAKE D.E., 1981: Sand Waves on an Epicontinental Shelf: Northern Bering Sea. *Marine Geology*, 42, 233-258.
- FIGGE, K., ZEILER M., GRIEWATSCH, K., MITTELSTAEDT, E., KLEIN, H., SCHWARZER, K., DIESING, M., 2002: KFKI-Projekt Regenerierung von Materialentnahmestellen in Nord- und Ostsee. Final report, Bundesamt fuer Seeschiffahrt und Hydrographie, 94 p.
- FIGUEIREDO, A.G. JR., SANDERS, J.E., SWIFT, D.J.P., 1982: Storm-graded Layers on Inner Continental Shelves: Examples from Southern Brazil and the Atlantic Coast of the Central United States. *Sedimentary Geology*, 31, 171-190.
- FISH, J.P. AND CARR, H.A., 2001: Sound Reflections, Advanced Applications of Side Scan Sonar, Lower Cape Pub Co, 272p.
- FLEISCHER, P., SAWYER, W.B., FIEDLER, H., STENDER, I.H., 1996: Spatial and Temporal Variability of a Coarse-sand Anomaly on a Sandy Inner Shelf, Northeastern Gulf of Mexico. *Geo-Marine Letters*, 16, 266-272.

- FLEMMING, B.W., 1976: Side-scan Sonar: A Practical Guide, *International Hydrographic Review*, 53 (1), 5-82.
- FLEMMING, B.W., 1978: Underwater Sand Dunes along the Southeast African Continental Margin - Observations and Implications. *Marine Geology*, 26, 177-198.
- FLEMMING, B.W., 1980: Sand Transport and Bedform Patterns on the Continental Shelf between Durban and Port Elisabeth (Southeast African Continental Margin). *Sedimentary Geology*, 26, 179-205.
- FLEMMING, B.W., 1982: Causes and Effects of Sonograph Distortion and Some Graphical Methods for Their Manual Correction. In: Russel-Cargill, W.G.A. (Ed.), Recent Developments in Side-scan Techniques. Central Acoustics Laboratory, University of Cape Town, South Africa, p. 103-138.
- FLEMMING, B.W., 1988: Zur Klassifikation Subaquatischer, Strömungstransversaler Transportkörper. *Bochumer Geologische und Geotechnische Arbeiten*, 29, 44-47.
- FOLK, R.L., 1954: The Distinction between Grain Size and Mineral Composition in Sedimentary Nomenclature. *Journal of Geology*, 62, 344-359.
- GADD, P.E., LAVELLE, J.W., SWIFT, D.J.P., 1978: Estimates of Sand Transport on the New York Shelf Using Near-bottom Current Meter Observations. *Journal of Sedimentary Petrology*, 48, 239-252.
- GALLAGHER, E.L., 2003: A Note on Megaripples in the Surf Zone: Evidence for Their Relation to Steady Flow Dunes. *Marine Geology*, 193, 171-176.
- GAO, S. AND COLLINS, M., 1992: Net Sediment Transport Patterns Inferred from Grain-size Trends, Based upon Definition of Transport Vectors. *Sedimentary Geology*, 80, 47-60.
- GARDNER, W.D., RICHARDSON, M.J., CACCHIONE, D.A., 1989: Sedimentological Effects of Strong Southward Flow in the Straits of Florida. *Marine Geology*, 86, 155-180.
- GARNAUD, S., LESUEUR, P., GARLAN, T., 2005: Origin of Rippled Scour Depressions Associated with Cohesive Sediments in a Shoreface Setting (Eastern Bay of Seine, France). *Geo-Marine Letters*, 25, 34-42.
- GELLATLY, D.C., 1970: Cross-bedded Tidal Megaripples from King Sound (Northwestern Australia). *Sedimentary Geology*, 4, 186-191.
- GERKEMA, T., 2000: A Linear Stability Analysis of Tidally Generated Sand Waves, *Journal of Fluid Mechanics*, 417, 303-322.
- GILKINSON, K.D., FADER, G.B.J., GORDON, D.C.JR., CHARRON, R., MCKEOWN, D., RODDICK, D., KENCHINGTON, E.L.R., MACISAAC, K., BOURBONNAIS, C., VASS, P., LIU, Q., 2003: Immediate and Longer-term Impacts of Hydraulic Clam Dredging on an Offshore Sandy Seabed: Effects on Physical Habitat and Processes of Recovery. *Continental Shelf Research*, 23, 1315-1336.
- GILKINSON, K.D., GORDON, D.C.JR., MACISAAC, K.G., MCKEOWN, D.L., KENCHINGTON, E.L.R., BOURBONNAIS, C., VASS, W.P., 2005: Immediate Impacts and Recovery Trajectories of Macrofaunal Communities Following Hydraulic Clam Dredging on Banquereau, Eastern Canada. *ICES Journal of Marine Science*, 62, 925-947.
- GIOSAN, L., CONSTANTINESCU, S., CLIFT, P.D., TABREZ, A.R., DANISH, M., INAM, A., 2006: Recent Morphodynamics of the Indus Delta Shore and Shelf. *Continental Shelf Research*, 26, 1668-1684.
- GOFF, J.A., OLSON, H.C., DUNCAN, C.S., 2000: Correlation of Side-scan Backscatter Intensity with Grain-size Distribution of Shelf Sediments, New Jersey Margin. *Geo-Marine Letters*, 20, 43-49.
- GOFF, J.A., MAYER, L.A., TRAYKOVSKI, P., BUYNEVICH, I., WILKENS, R., RAYMOND, R., GLANG, G., EVANS, R.L., OLSON, H., JENKINS, C., 2005: Detailed Investigation of Sorted Bedforms, or "Rippled Scour Depressions," within the Martha's Vineyard Coastal Observatory, Massachusetts. *Continental Shelf Research*, 25, 461-484.
- GOSTIN, V.A., HAILS, J.R., BELPERIO, A.P., 1984: The Sedimentary Framework of Northern Spencer Gulf, South Australia. *Marine Geology*, 61, 111-138.
- GREEN, M.O., 1986: Side-Scan Sonar Mosaic of a Sand Ridge Field: Southern Mid-Atlantic Bight. *Geo-Marine Letters*, 6, 35-40.

- GREEN, M., VINCENT, C., TREMBANIS, A., 2004: Suspension of Coarse and Fine Sand on a Wave-dominated Shoreface, with Implications for the Development of Rippled Scour Depressions. *Continental Shelf Research*, 24(3), 317-335.
- GREENWOOD, D.B., DINGLER, J.R., SHERMAN, D.J., ANIMA, R.J., BAUER, B.O., 1985: Monitoring Bedforms under Waves Using High Resolution Remote Tracking Sonars. *Proceedings of the Canadian Coastal Conference, St John's: National Research Council of Canada, Associate committee for Research on Shoreline Erosion and Sedimentation*, Ottawa, 143-158.
- GUERRA-GARCIA, J.M., GARCIA-GOMEZ, J.C., 2006: Recolonization of Defaunated Sediments: Fine versus Gross Sand and Dredging versus Experimental Trays. *Estuarine, Coastal and Shelf Science*, 68, 328-342.
- GUTIERREZ, B.T., VOULGARIS, G., THIELER, E.R., 2005: Exploring the Persistence of Sorted Bedforms on the Inner-shelf of Wrightsville Beach, North Carolina. *Continental Shelf Research*, 25, 65-90.
- HAIGH J. D., 1960: The Services Textbook of Radio, Vol.7 – Radiolocation Techniques, 252-254, HMSO, London.
- HANEBUTH, T.J.J., STATTEGGER, K., GROOTES, P.M., 2000: Rapid Flooding of the Sunda Shelf; A Late-Glacial Sea-Level Record. *Science*, 288, 1033-1035.
- HARRIS, P.T., 1988a: Sediments, Bedforms and Bedload Transport Pathways on the Continental Shelf Adjacent to Torres Strait, Australia-Papua New Guinea. *Continental Shelf Research*, 8 (8), 979-1003.
- HARRIS, P.T., 1988b: Large-scale Bedforms as Indicators of Mutually Evasive Sand Transport and the Sequential Infilling of Wide-mouthed Estuaries. *Sedimentary Geology*, 57, 273-298.
- HARRIS, P.T., 1989: Sandwave Movement under Tidal and Wind-driven Currents in a Shallow Marine Environment: Adolphus Channel, Northeastern Australia. *Continental Shelf Research*, 9 (11), 981-1002.
- HARRIS, P.T. AND COLLINS, M.B., 1984: Side-Scan Sonar Investigation into Temporal Variation in Sand Wave Morphology: Helwick Sands, Bristol Channel. *Geo-Marine Letters*, 4, 91-97.
- HARRIS, P.T. AND COLLINS, M.B., 1985: Bedford Distributions and Sediment Transport Paths in the Bristol Channel and Severn Estuary, U.K. *Marine Geology*, 62, 153-166.
- HAY, A.E AND WILSON, D.J., 1994: Rotary Sidescan Images of Nearshore Bedform Evolution during a Storm. *Marine Geology*, 119, 57-65.
- HELCOM, 1999: Marine Sediment Extraction in the Baltic Sea - Status report. Baltic Sea Environment Proceedings, 76, 31 p.
- HENNINGS, I., PASENAU, H. AND WERNER, F., 1993: Sea Surface Signatures Related to Subaqueous Dunes Detected by Acoustic and Radar Sensors. *Continental Shelf Research*, 13 (8/9), 1023-1043.
- HENNINGS, I., LURIN, B., VERNEMMEN, C., VANHESSCHE, U., 2000: On the Behaviour of Tidal Current Directions Due to the Presence of Submarine Sand Waves. *Marine Geology*, 169, 57-68.
- HILTON, M.J. AND HESP, P., 1996: Determining the Limits of Beach-nearshore Sand Systems and the Impact of Offshore Coastal Sand Mining. *Journal of Coastal Research*, 12 (2), 496-519.
- HOBBS, C.H.III, 1986: Side-scan Sonar as a Tool for Mapping Spatial Variations in Sediment Type. *Geo-Marine Letters*, 5, 241-245.
- HOLME, N.A. AND WILSON, J.B., 1985: Faunas Associated with Longitudinal Furrows and Sand Ribbons in a Tide-swept Area in the English Channel. *Journal of the Marine Biological Association of the United Kingdom*, 65, 1051-1072.
- HU, J., KAWAMURA, H., HONG, H., QI, Y.O., 2000: A Review on the Currents in the South China Sea: Seasonal Circulation, South China Sea Warm Current and Kuroshio Intrusion. *Journal of Oceanography*, 56, 607-624.
- HULSCHER, S., 1996: Tidal-induced Large-scale Regular Bed Form Patterns in a Three-dimensional Shallow Water Model. *Journal of Geophysical Research*, 101 (C9), 20727-20744.

- HUMBORSTAD, O.B., NØTTESTAD, L., LØKKEBORG, S., RAPP, H.T., 2004: RoxAnn Bottom Classification System, Sidescan Sonar and Video-sledge: Spatial Resolution and Their Use in Assessing Trawling Impacts. *ICES Journal of Marine Science*, 61, 53-63.
- HUME, T., TREMBANIS, A., HILL, A., LIEFTING, R., STEPHENS, S., 2003: Spatially Variable, Temporally Stable, Sedimentary Facies on an Energetic Inner Shelf, Coastal Sediments 2003. World Scientific Publishing Corp. and East meets West Productions, Clearwater Beach, FL, pp. 1-14.
- HUNTER, R.E., DINGLER, J.R., ANIMA, R.J., RICHMOND, B.M., 1988: Coarse-sediment Bands on the Inner Shelf of Southern Monterey Bay, California. *Marine Geology*, 80, 81-98.
- ICES, 2001: Effects of Extraction of Marine Sediments on the Marine Ecosystem. WG-EXT. Copenhagen, International Council for the Exploration of the Sea (ICES), 247, 80 p.
- IHO – International Hydrographic Organisation, 1998: IHO Standards for Hydrographic Surveys, Special Publication 44, 4th Edition, 23 p.
- JAGODZIŃSKI, R., 2005: Petrography and Geochemistry of Surface Sediments from Sunda and Vietnamese Shelves (South China Sea). UAM University Press, Poznań, Poland, 144 pp.
- JOHNSON H.P. AND HELFERTY, M., 1990: The Geological Interpretation of Side-scan Sonar, *Reviews of Geophysics*, 28 (4), 357-380.
- JONSSON, I.G., 1966: Wave Boundary Layers and Friction Factors, Proceeding of the 10th International Coastal Engineering Conference. ASCE, Washington, DC, pp. 127-146.
- KARL, H.A., SCHWAB, W.C., WRIGHT, A.ST.C., DRAKE, D.E., CHIN, J.L., DANFORTH, W.W., UEBEL, E., 1994: Acoustic Mapping as an Environmental Management Tool: I. Detection of Barrels of Low-Level Radioactive Waste, Gulf of the Farallones National Marine Sanctuary, California. *Ocean & Coastal Management*, 22, 201-227.
- KEETON, K.A., SEARLE, R.C., 1996: Analysis of Simrad EM12 Multibeam Bathymetry and Acoustic Backscatter for Seafloor Mapping, *Marine Geophysics Researches*, 19, 63-688.
- KELLAND, N.C. AND HAILS, J.R., 1972: Bedrock Morphology and Structures within Overlying Sediments, Start Bay, Southwest England, Determined by Continuous Seismic Profiling, Side-scan Sonar, and Core Sampling. *Marine Geology*, 13, M19-M26.
- KENNY, A.J. AND REES, H.L., 1994: The Effects of Marine Gravel Extraction on the Macrobenthos: Early Post-dredging Recolonization. *Marine Pollution Bulletin*, 28 (7), 442-447.
- KENNY A.J. AND REES, H.L., 1996: The Effects of Marine Gravel Extraction on the Macrobenthos: Results 2 Years Post-Dredging. *Marine Pollution Bulletin*, 32 (8/9), 615-622.
- KENYON, N.H., 1970: Sand Ribbons of European Tidal Seas. *Marine Geology*, 9, 25-39.
- KLEIN, G.DEV., PARK, Y.A., CHANG, J.H. KIM, C.S., 1982: Sedimentology of a Subtidal, Tide-dominated Sand Body in the Yellow Sea, Southwest Korea. *Marine Geology*, 50, 221-240.
- KLEIN, H., 2003: Investigating Sediment Re-mobilisation Due to Wave Action by Means of ADCP Echo Intensity Data. Field Data from Tromper Wiek, Western Baltic Sea. *Estuarine, Coastal and Shelf Science*, 58, 467-474.
- KLEIN, H. AND MITTELSTAEDT, E., 2001: Strömungen und Seegangsverhältnisse vor Graal-Müritz und in der Tromper Wiek. *Berichte des Bundesamtes für Seeschifffahrt und Hydrographie*, 26, 162 p.
- KLEIN, M., 1982: A Modular Sonar System for Seabed Mapping. In: Russel-Cargill, W.G.A. (Ed.), *Recent Developments in Side-scan Techniques*. Central Acoustics Laboratory, University of Cape Town, South Africa, p. 11-44.
- KNAAPEN, M.A.F. AND HULSCHER, S.J.M.H., 2002: Regeneration of Sand Waves after Dredging. *Coastal Engineering*, 46, 277-289.
- KNAAPEN, M.A.F., VAN BERGEN HENEGOUW, C.N., HU, Y.Y., 2005: Quantifying Bedform Migration Using Multi-beam Sonar. *Geo-Marine Letters*, 25(5), 306-324.

- KNEBEL, H.J., 1986: Holocene Depositional History of a Large Glaciated Estuary, Penobscot Bay, Maine. *Marine Geology*, 73, 215-236.
- KNEBEL, H.J., 1989: Modern Sedimentary Environments in a Large Tidal Estuary, Delaware Bay. *Marine Geology*, 86, 119-136.
- KNEBEL, H.J., 1993: Sedimentary Environments within a Glaciated Estuarine-inner Shelf System: Boston Harbor and Massachusetts Bay. *Marine Geology*, 110, 7-30.
- KNEBEL, H.J., NEEDELL, S.W., O'HARA C.J., 1982: Modern Sedimentary Environments on the Rhode Island Shelf, off the Eastern United States. *Marine Geology*, 49, 241-256.
- KNEBEL, H.J., SIGNELL, R.P., RENDIGS, R.R., POPPE, L.J., LIST, J.H., 1999: Seafloor Environments in the Long Island Sound Estuarine System. *Marine Geology*, 155, 277-318.
- KNISKERN, T.A. AND KUEHL, S.A., 2003: Spatial and Temporal Variability of Seabed Disturbance in the York River Subestuary. *Estuarine, Coastal and Shelf Science*, 58, 37-55.
- KOMAR, P.D., 1976: The Transport of Cohesionless Sediments on Continental Shelves. In Stanley, D.J. and Swift, D.J.P., (Eds.), *Marine Sediment Transport and Environmental Management*. Wiley, New York, pp 107-125.
- KRAUSE, J.C., DIESING, M., ARLT, G.: The physical and biological impact of sand extraction: a case study of a dredging site in the Western Baltic Sea. *Journal of Coastal Research*, submitted for publication.
- KUBICKI, A. AND DIESING, M., 2006: Can Old Analogue Sidescan Sonar Data Still Be Useful? An Example of a Sonograph Mosaic Geo-coded by the DECCA Navigation System. *Continental Shelf Research*, 26, 1858-1867.
- KUIJPERS, A., WERNER, F., RUMOHR, J., 1993: Sandwaves and Other Large-scale Bedforms as Indicators of Non-tidal Surge Currents in the Skagerrak off Northern Denmark. *Marine Geology*, 111, 209-221.
- LANGHORNE, D.N., 1973: A Sandwave Field in the Outer Thames Estuary, Great Britain. *Marine Geology*, 14 (2), 129-143.
- LANGHORNE, D.N., 1981: An Evaluation of Bagnold's Dimensionless Coefficient of Proportionality Using Measurements of Sandwave Movement. *Marine Geology*, 43, 49-64.
- LANH, V.V. AND HOAN, D.V., 2002: The Southward Cold Current along the Coast of Central Vietnam. *Collection of Marine Research Works XII*, 19-32, Hanoi.
- LATHROP, R.G., COLE, M., SENYK, N., BUTMAN, B., 2006: Seafloor Habitat Mapping of the New York Bight Incorporating Sidescan Sonar Data. *Estuarine, Coastal and Shelf Science*, 68, 221-230.
- LEVITUS, S., 1982: Climatological Atlas of the World Oceans. *NOAA Professional Paper 13*, U.S. Government Printing Office, Washington D.C., 173 pp.
- LEWIS, K.B. AND BARNES P.M., 1999: Kaikoura Canyon, New Zealand: Active Conduit from Near-shore Sediment Zones to Trench-axis Channel. *Marine Geology*, 162, 39-69.
- LYKOUSIS, V., 2001: Subaqueous Bedforms on the Cyclades Plateau (NE Mediterranean) - Evidence of Cretan Deep Water Formation? *Continental Shelf Research*, 21, 495-507.
- MANIGHETTI, B. AND CARTER, L., 1999: Across-shelf Sediment Dispersal, Hauraki Gulf, New Zealand. *Marine Geology*, 160, 271-300.
- MANN R.G., SWIFT, D.J.P., PERRY, R., 1981: Size Classes of Flow-transverse Bedforms in a Subtidal Environment, Nantucket Shoals, North American Atlantic Shelf. *Geo-Marine Letters*, 1, 39-43.
- MARRINER, N. AND MORHANGE, C., 2006: Geoarchaeological Evidence for Dredging in Tyre's Ancient Harbour, Levant. *Quaternary Research*, 65, 164-171.
- MASSON, D.G., 2001: Sedimentary Processes Shaping the Eastern Slope of the Faeroe-Shetland Channel. *Continental Shelf Research*, 21, 825-857.
- MASSON, D.G., HOWE, J.A., STOKER, M.S., 2002: Bottom-current Sediment Waves, Sediment Drifts and Contourites in the Northern Rockall Trough. *Marine Geology*, 192, 215-237.

- MCCAVE, I. N., 1971: Sand Waves in the North Sea off the Coast of Holland. *Marine Geology*, 10, 199-225.
- MCDONNELL, R. AND KEMP, K., 1995: International GIS Dictionary, GeoInformation International, Cambridge, 111 p.
- MCKINNEY, T.F, STUBBLEFIELD, W.L., SWIFT, D.J.P, 1974: Large-scale Current Lineations on the Central New Jersey Shelf: Investigations by Side-scan Sonar. *Marine Geology*, 17, 79-102.
- MCLAREN, P. AND BOWLES, D., 1985: The Effects of Sediment Transport on Grainsize Distributions. *Journal of Sedimentary Petrology*, 55, 457-470.
- MIGNOTTE, M. AND COLLET, C., 2000: Markov Random Field and Fuzzy Logic Modeling in Sonar Imagery: Application to the Classification of Underwater Floor. *Computer Vision and Image Understanding*, 79, 4-24.
- MITCHELL, N.C., 1996: Processing and Analysis of Simrad Multibeam Sonar Data. *Marine Geophysical Researches*, 18, 729-739.
- MITCHELL, N.C. AND HUGHES CLARKE, J.E., 1994: Classification of Seafloor Geology Using Multibeam Sonar Data from the Scotian Shelf. *Marine Geology*, 121, 143-160.
- MITTELSTAEDT, E., LANGE, W., BROCKMANN, C., SOETJE, K.C., 1983: Die Strömungen in der Deutschen Bucht. Deutsches Hydrographisches Institut, 2347, 141 pp.
- MOHRHOLZ, V., 1998: Transport- und Vermischungsprozesse in der Pommerschen Bucht. - Meereswissenschaftliche Berichte, 33, 106 p.
- MORALES, J.A., DELGADO, I., GUTIERREZ-MAS, J.M., 2006: Sedimentary Characterization of Bed Types along the Guadiana Estuary (SW Europe) Before the Construction of the Alqueva Dam. *Estuarine, Coastal and Shelf Science*, 70, 117-131.
- MORELISSSEN, R., HULSCHER, S.J.M.H., KNAAPEN, M.A.F., NEMETH, A.A., BIJKER, R., 2003: Interacting Sand Waves and Pipelines: a Data-assimilation Based Mathematical Model. *Coastal Engineering*, 48 (3), 197-209.
- MORIMOTO, A., YOSHIMOTO, K., YANAGI, T., 2000: Characteristics of Sea Surface Circulation and Eddy Field in the South China Sea Revealed by Satellite Altimetric Data. *Journal of Oceanography*, 56(3), 331-344.
- MURRAY, A.B. AND THIELER, E.R., 2004: A New Hypothesis and Exploratory Model for the Formation of Large-scale Inner-shelf Sediment Sorting and "rippled scour depressions". *Continental Shelf Research*, 24, 295-315.
- NEMETH, A.A., HULSCHER, S.J.M.H., DEVRIEND, H.J., 2002: Modelling Sand Wave Migration in Shallow Shelf Seas. *Continental Shelf Research*, 22 (18-19), 2795-2806.
- NEMETH, A.A., HULSCHER, S.J.M.H., VAN DAMME, R.H.J., 2007: Modelling Offshore Sand Wave Evolution. *Continental Shelf Research*, 27, 713-728.
- NEWTON, R.S., SEIBOLD, E., WERNER, F., 1973: Facies Distribution Patterns on the Spanish Sahara Continental Shelf Mapped with Side-scan Sonar. "Meteor" *Forschungsergebnisse*, C15: 55-77.
- NEWTON, R.S. AND STEFANON, A., 1982: Side-scan Sonar and Subbottom Profiling in the Northern Adriatic Sea. *Marine Geology*, 46, 279-306.
- NGUYEN, B., (ED.), 2000: Surficial Sediment Map of Vietnamese Coastal Zone (0-30 m Water Depth). Project: Geological Investigation and Mineral Exploration of the Shallow Water (0-30 m) of Vietnam (1991-2001). Marine Geology and Mineral Centre, Hanoi, scale 1:500,000.
- NGUYEN, V.L., TA, T.K.O., TATEISHI, M. 2000: Late Holocene Depositional Environments and Coastal Evolution of the Mekong River Delta, Southern Vietnam. *Journal of Asian Earth Sciences*, 18(4), 427-439.
- NGUYEN, V.T., 1996: Characteristics of Quaternary Sediments of the Continental Shelf in a Part of Southern Vietnam. *Contributions of Marine Geology and Geophysics II*, 200-219, Science and Technics Publishing House, Hanoi (in Vietnamese with English abstract).
- NIEDERMEIER, A., HOJA, D., LEHNER, S., 2005: Topography and Morphodynamics in the German Bight Using SAR and Optical Remote Sensing Data. *Ocean Dynamics*, 55, 100-109.

- NIELSEN, A.F., HESP, P.A., LORD, D.B., 1991: Marine Dredging and Aggregate Extraction. - "Coastal Engineering - Climate for Change" Proceedings of the 10th Australasian Conference on Coastal and Ocean Engineering, Auckland, 2 - 6 Dec. 1991, 67-72.
- NINH, P.V., (ED.), 2003: South China Sea Monograph. Vol. II –Meteorology, Marine Hydrology and Hydrodynamics, Hanoi National University Publisher, Hanoi, 565 pp (in Vietnamese).
- NITSCHKE, F.O., BELL, R., CARBOTTE, S.M., RYAN, W.B.F., FLOOD, R., 2004: Process-related Classification of Acoustic Data from the Hudson River Estuary. *Marine Geology*, 209, 131-145.
- OJEDA G.Y., GAYES, P.T., VAN DOLAH, R.F., SCHWAB, W.C., 2004: Spatially Quantitative Seafloor Habitat Mapping: Example from the Northern South Carolina Inner Continental Shelf. *Estuarine, Coastal and Shelf Science*, 59, 399-416.
- OTAY, E.N., DEMIR, H., BÖRECKCI, O.S., WORK, P.A., 2002: Marine Sand Exploitation off the Turkish Black Sea Coast. Proceedings Littoral 2002 (Porto, Portugal, EUROCOAST/ EUCC), 467-476.
- OULASVIRTA, P. AND LEHTONEN, H., 1988: Effects of Sand Extraction on Herring Spawning and Fishing in the Gulf of Finland. *Marine Pollution Bulletin*, 19 (8), 383-386.
- PACE, N.G. AND GAO, H., 1988: Swath Seabed Classification, *IEEE Journal of Ocean Engineering*, 13, 83-90.
- PALANQUES, A., PUIG, P., GUILLEN, J., JIMENEZ, J., GRACIA, V., SANCHEZ-ARCILLA, A., MADSEN, O., 2002: Near-bottom Suspended Sediment Fluxes on the Microtidal Low-energy Ebro Continental Shelf (NW Mediterranean). *Continental Shelf Research*, 22 (2), 285-303.
- PARK, S.C. AND LEE, S.D., 1994: Depositional Patterns of Sand Ridges in Tide-dominated Shallow Water Environments: Yellow Sea Coast and South Sea of Korea. *Marine Geology*, 120, 89-103.
- PARSONS, B.S., VOGT, P.R., HAFLIDASON, H., JUNG, W.Y., 2005: Sidescan and Video Exploration of the Storegga Slide Headwall Region by Submarine NR-1. *Marine Geology*, 219, 195-205.
- PASQUALINI, V., PERGENT-MARTINI, C., CLABAUT, P., PERGENT, G., 1998: Mapping of *Posidonia oceanica* Using Aerial Photographs and Side Scan Sonar: Application off the Island of Corsica (France). *Estuarine, Coastal and Shelf Science*, 47, 359-367.
- PERILLO, G.M.E., LUDWICK, J.C., Geomorphology of a Sand Wave in Lower Chesapeake Bay, Virginia, U.S.A. *Geo-Marine Letters*, 4, 105-112.
- PINTO, B., PELLEGRINI, D., GABELLINI, M., AUSILI, A., 1995: Harbour and Coastal Sediment Chemistry and Toxicity: a Preliminary Assessment of Dredging Activities. *Journal of Aquatic Ecosystem Health*, 4, 249-255.
- POINER, I.R. AND KENNEDY, R., 1984: Complex Patterns of Change in the Macrobenthos of a Large Sandbank Following Dredging. *Marine Biology*, 78, 335-352.
- PRATSON, L.E. AND EDWARDS, M.H., 1996: Introduction to Advances in Seafloor Mapping Using Sidescan Sonar and Multibeam Bathymetry Data. *Marine Geophysical Researches*, 18, 601-605.
- PRIOR, D. B. AND COLEMAN, J., 1980: Sonograph Mosaics of Submarine Slope Instabilities, Mississippi River Delta, *Marine Geology*, 36, 227-239.
- QIAN, P.Y., QIU, J.W., KENNISH, R., REID, C.A., 2003: Recolonization of Benthic Infauna Subsequent to Capping of Contaminated Dredged Material in East Sha Chau, Hong Kong. *Estuarine, Coastal and Shelf Science*, 56, 819-831.
- QUINN, R., BREEN, C., FORSYTHE, W., 2002: Integrated Geophysical Surveys of The French Frigate *La Surveillante* (1797), Bantry Bay, Co. Cork, Ireland. *Journal of Archaeological Science*, 29, 413-422.
- QUINN, R., DEAN, M., LAWRENCE, M., LISCOE, S., BOLAND, D., 2005: Backscatter Responses and Resolution Considerations in Archaeological Side-scan Sonar Surveys: a Control Experiment. *Journal of Archaeological Science*, 32, 1252-1264.
- REED, T.B., HUSSONG, D., 1989: Digital Image Processing Techniques for Enhancement and Classification of SeaMARC II Side Scan Sonar Imagery. *Journal of Geophysical Research*, 94 (B6), 7469-7490.

- REYNAUD, J.Y., TESSIER, B., BERNE, S., CHAMLEY, H., DEBATIST, M., 1999: Tide and Wave Dynamics on a Sand Bank from the Deep Shelf of the Western Channel Approaches. *Marine Geology*, 161, 339-359.
- ROBINSON, J.E., NEWELL, R.C., SEIDERER, L.J., SIMPSON, N.M., 2005: Impacts of Aggregate Dredging on Sediment Composition and Associated Benthic Fauna at an Offshore Dredge Site in the Southern North Sea. *Marine Environmental Research*, 60, 51-68.
- ROELVINK, J. AND VAN BANNING, G., 1994: Design and Development of DELFT3D and Application to Coastal Morphodynamics. In: A. Verwey (Editor), Hydroinformatics '94. Proc. 1st International Conference. Balkema, Delft, pp. 451-456.
- ROGERS, J.N., KELLEY, J.T., BELKNAP, D.F., GONTZ, A., BARNHARDT, W.A., 2006: Shallow-water Pockmark Formation in Temperate Estuaries: A Consideration of Origins in the Western Gulf of Maine with Special Focus on Belfast Bay. *Marine Geology*, 225, 45-62.
- ROOPER, C.N. AND ZIMMERMANN, M., 2007: A Bottom-up Methodology for Integrating Underwater Video and Acoustic Mapping for Seafloor Substrate Classification. *Continental Shelf Research*, 27, 947-957.
- RUBIN, D.M. AND MCCULLOCH, D.S., 1980: Single and Superimposed Bedforms: a Synthesis of San Francisco Bay and Flume Observations. *Sedimentary Geology*, 26, 207-231.
- SALGE, U. AND WONG, H.K., 1988: Seismic Stratigraphy and Quaternary Sedimentation in the Skagerrak (Northeastern North Sea). *Marine Geology*, 81, 159-174.
- SANTORO, V.C., AMORE, E., CAVALLARO, L., DE LAURO, M., 2004: Evolution of Sand Waves in the Messina Strait, Italy. *Ocean Dynamics*, 54, 392-398.
- SARDA, R., PINEDO, S., GREMARE, A., TABOADA, S., 2000: Changes in the Dynamics of Shallow Sandy-bottom Assemblages Due to Sand Extraction in the Catalan Western Mediterranean Sea. *ICES Journal of Marine Science*, 57, 1446-1453.
- SCHIMANSKI, A. AND STATTEGGER, K., 2005: Deglacial and Holocene Evolution of the Vietnam Shelf: Stratigraphy, Sediments and Sea-level Change. *Marine Geology*, 214, 315-387.
- SCHROTTKE, K., BECKER, M., BARTHOLOMÄ, A., FLEMMING, B.W., HEBBELN, D., 2006: Fluid Mud Dynamics in the Weser Estuary Turbidity Zone Tracked by High-resolution Side-scan Sonar and Parametric Sub-bottom Profiler. *Geo-Marine Letters*, 26, 185-198.
- SCHUMACHER, W. AND BAYERL, K.A., 1999: The Shoreline Displacement Curve of Rügen Island (Southern Baltic Sea). *Quaternary International*, 56, 107-113.
- SCHWAB, W.C., RODRIGUEZ, R.W., DANFORTH, W.W., GOWEN, M.H., 1997: Sediment Distribution on a Storm-dominated Insular Shelf, Luquillo, Puerto Rico, U.S.A. *Journal of Coastal Research*, 12, 147-159.
- SCHWARZER, K., DIESING, M., TRIESCHMANN, B., 2000: Nearshore Facies of the Southern Shore of the Baltic Ice Lake - Example from Tromper Wiek (Rügen Island). *Baltica*, 13, 69-76, Vilnius.
- SCHWARZER, K., DIESING, M., LARSON, M., NIEDERMEYER, M., SCHUMACHER, R.O., FURMAŃCZYK, K., 2003: Coastline Evolution at Different Time Scales - Examples from the Pomeranian Bight, Southern Baltic Sea. *Marine Geology*, 194 (1-2), 79-101.
- SHAW, J., COURTNEY, R.C., CURRIE, J.R., 1997: Marine Geology of St. George's Bay, Newfoundland, as Interpreted from Multibeam Bathymetry and Back-scatter Data. *Geo-Marine Letters*, 17, 188-194.
- SHEPHERD, S.A. AND HAILS, J.R., 1984: The Dynamics of a Megaripple Field in Northern Spencer Gulf, South Australia. *Marine Geology*, 61, 249-263.
- SIMONINI, R., ANSALONI, I., BONVICINI PAGLIAI, A.M., CAVALLINI, F., IOTTI, M., MAURI, M., MONTANARI, G., PRETI, M., RINALDI, A., PREVEDELLI, D., 2005: The Effects of Sand Extraction on the Macrobenthos of a Relict Sands Area (Northern Adriatic Sea): Results 12 Months Post-extraction. *Marine Pollution Bulletin*, 50, 768-777.
- SMITH, R., BOYD, S.E., REES, H.L., DEARNALEY, M.P., STEVENSON, J.R., 2006: Effects of Dredging Activity on Epifaunal Communities - Surveys Following Cessation of Dredging. *Estuarine, Coastal and Shelf Science*, 70, 207-223.

- SMITH, W. AND SANDWELL, D., 1997: Global Sea Floor Topography from Satellite Altimetry and Ship Depth Soundings. *Science*, 277, 1956-1962.
- SOULSBY, R.L., 1997: Dynamics of Marine Sands: a Manual for Practical Applications. Thomas Telford Publications, London, 249 pp.
- SOULSBY, R.L. AND WHITEHOUSE, R.J.S., 1997: Threshold of Sediment Motion in Coastal Environments. In: Proceedings of the Pacific Coasts and Ports. Christchurch, New Zealand, pp 149-154.
- STERNBERG, R.W., 1971: Measurements of Incipient Motion of Sediment Particles in the Marine Environment. *Marine Geology*, 10, 113-119.
- STERNBERG, R.W. AND NOWELL, A.R.M., 1999: Continental Shelf Sedimentology: Scales of Investigation Define Future Research Opportunities. *Journal of Sea Research*, 41, 55-71.
- STRIDE, A.H., 1965: Preservation of Some Marine Current Bedding. *Nature*, 206, 498-499.
- STRIDE, A.H. AND CHESTERMAN, W.D., 1973: Sedimentation by Non-tidal Currents around Northern Denmark, *Marine Geology*, 15, M53-M58.
- STUBBLEFIELD, W.L., PERMENTER, R.W., SWIFT, D.J.P., 1977: Time and Space Variation in the Surficial Sediments of the New York Bight Apex. *Estuarine and Coastal Marine Science*, 5, 597-607.
- SWIFT, D.J.P., FIGUEIREDO, A.G., FREELAND, G.L., OERTEL, G.F., 1983: Hummocky Cross-stratification and Megaripples: a Geological Double Standard? *Journal of Sedimentary Petrology*, 53, 1295-1317.
- SZYMELFENIG, M., KOTWICKI, L., GRACA, B., 2006: Benthic Re-colonization in Post-dredging Pits in the Puck Bay (Southern Baltic Sea). *Estuarine, Coastal and Shelf Science*, 68, 489-498.
- TAMSETT, D., 1993: Sea-Bed Characterisation and Classification from the Power Spectra of Side-Scan Sonar Data. *Marine Geophysical Researches*, 15, 43-64.
- TANG, X. AND STEWART, W.K., 2000: Optical and Sonar Image Classification: Wavelet Packet Transform vs Fourier Transform. *Computer Vision and Image Understanding*, 79, 25-46.
- TAUBER, F. AND EMEIS, K.C., 2005: Sediment Mobility in the Pomeranian Bight (Baltic Sea): a Case Study Based on Sidescan-sonar Images and Hydrodynamic Modelling. *Geo-Marine Letters*, 25, 221-229.
- THIELER, E.R., BRILL, A.L., CLEARY, W.J., HOBBS, C.H.III, GAMMISCH, R.A., 1995: Geology of the Wrightsville Beach, North Carolina Shoreface: Implications for the Concept of Shoreface Profile of Equilibrium. *Marine Geology*, 126, 271-287.
- THIELER, E.R., PILKEY, O.H., CLEARY, W.J., SCHWAB, W.C., 2001: Modern Sedimentation on the Shoreface and Inner Continental Shelf at Wrightsville Beach, North Carolina, U.S.A. *Journal of Sedimentary Research*, 71(6), 958-970.
- THORNTON, E.B., SWAYNE, J.L., DINGLER, J.R., 1998: Small-scale Morphology across the Surf Zone. *Marine Geology*, 145, 173-196.
- THORNTON, E.B., SALLENGER, A., CONFRONTO SESTO, J.C., EGLEY, L., MCGEE, T., PARSONS, R., 2006: Sand Mining Impacts on Long-term Dune Erosion in Southern Monterey Bay. *Marine Geology*, 229, 45-58.
- THORPE, S.A. AND HALL, A.J., 1983: The Characteristics of Breaking Waves, Bubble Clouds, and Near-surface Currents Observed Using Side-scan Sonar. *Continental Shelf Research*, 1 (4), 353-384.
- TODD, B.J., FADER, G.B.J., COURTNEY, R.C., PICKRILL, R.A., 1999: Quaternary Geology and Surficial Sediment Processes, Browns Bank, Scotian Shelf, Based on Multibeam Bathymetry. *Marine Geology*, 162, 165-214.
- TOIMIL, L.J. AND REIMNITZ, E., 1979: A Herringbone Bedform Pattern of Possible Taylor-Görtler Type Flow Origin Seen in Sonographs. *Sedimentary Geology*, 22, 219-228.
- TONNON, P.K., VAN RIJN, L.C., WALSTRA, D.J.R., 2007: The Morphodynamic Modelling of Tidal Sand Waves on the Shoreface. *Coastal Engineering*, 54 (4), 279-296.
- TREVORROW, M.V., 2001: An Evaluation of a Steerable Sidescan Sonar for Surveys of Near-surface Fish. *Fisheries Research*, 50, 221-234.

- TWICHELL, D., BROOKS, G., GELFENBAUM, G., PASKEVICH, V., DONAHUE, B., 2003: Sand Ridges off Sarasota, Florida: A Complex Facies Boundary on a Low-energy Inner Shelf Environment. *Marine Geology*, 200, 243-262.
- VAN DALFSEN, J.A., ESSINK, K., TOXVIG MADSEN, H., BIRKLUND, J., ROMERO, J., MANZARENA, M., 2000: Differential Response of Macrozoobenthos to Marine Sand Extraction in the North Sea and the Western Mediterranean. *ICES Journal of Marine Science*, 57, 1439-1445.
- VAN DALFSEN, J.A. AND ESSINK, K., 2001: Benthic Community Response to Sand Dredging and Shoreface Nourishment in Dutch Coastal Waters. *Senckenbergiana maritima*, 31 (2), 329-332.
- VAN LANCKER, V., LANCKNEUS, J., HEARN, S., HOEKSTRA, P., LEVOY, F., MILES, J., MOERKERKE, G., MONFORT, O., WHITEHOUSE, R., 2004: Coastal and Nearshore Morphology, Bedforms and Sediment Transport Pathways at Teignmouth (UK). *Continental Shelf Research*, 24, 1171-1202.
- VAN VEEN, J., 1935: Sand Waves in the North Sea. *International Hydrographic Review*, 12, 21-29.
- VAN RIJN, L.C., 1984: Sediment Transport, Part III: Bed Forms and Alluvial Roughness, *Journal of Hydraulic Engineering, ASCE*, 110(12), 1733-1754.
- VAN DE MEENE, J.W.H., BOERSMA, J.R., TERWINDT, J.H.J., 1996: Sedimentary Structures of Combined Flow Deposits from the Shoreface-connected Ridges along the Central Dutch Coast. *Marine Geology*, 131, 151-175.
- VAN DER MOLEN, J., 2002: The Influence of Tides, Wind and Waves on the Net Sand Transport in the North Sea. *Continental Shelf Research*, 22(18-19), 2739-2762.
- VAN DER VEER, H.W., BERGMAN, M.J.N., BEUKEMA, J.J., 1985: Dredging Activities in the Dutch Wadden Sea: Effects on Macrobenthic Infauna. *Netherlands Journal of Sea Research*, 19 (2), 183-190.
- VIANA, A.R., FAUGERES, J.C., STOW, D.A.V., 1998: Bottom-current-controlled Sand Deposits - a Review of Modern Shallow- to Deep-water Environments. *Sedimentary Geology*, 115, 53-80.
- VINCENT, C.E. AND OSBORNE, P.D., 1993: Bedform Dimensions and Migration Rates under Shoaling and Breaking Waves. *Continental Shelf Research*, 13 (11), 1267-1280.
- VOULGARIS, G. AND COLLINS, M.B., 1991: Linear Features on Side-scan Sonar Images: An Algorithm for the Correction of Angular Distortion. *Marine Geology*, 96, 187-190.
- WALKER, C.D.T., 1978: Development of a Ground Speed Corrected Side Scan Sonar Display System. *Ultrasonics*, May, 108-110.
- WANG, N. AND GERRITSEN, F., 1995: Nearshore Circulation and Dredged Material Transport at Waikiki Beach. *Coastal Engineering*, 24, 315-341.
- WARWICK, R.M. AND DAVIES, J.R., 1977: The Distribution of Sublittoral Macrofauna Communities in the Bristol Channel in Relation to the Substrate. *Estuarine, Coastal and Shelf Science*, 5, 267-288.
- WERNER, F., 2004: Coarse Sand Patterns in the Southeastern German Bight and Their Hydrodynamic Relationships, *Meyniana*, 56, 117-148, Kiel.
- WERNER, F. AND NEWTON, R.S., 1975: The Pattern of Large-scale Bed Forms in the Langeland Belt (Baltic Sea). *Marine Geology*, 19, 25-59.
- WEVER, T.F., FIEDLER, H.M., FECHNER, G., ABEGG, F., STENDER, I.H., 1997: Side-scan and Acoustic Subbottom Characterization of the Sea Floor near the Dry Tortugas, Florida. *Geo-Marine Letters*, 17, 246-252.
- WEVER, T.F., ABEGG, F., FIEDLER, H.M., FECHNER, G., STENDER, H., 1998: Shallow Gas in the Muddy Sediments of Eckernförde Bay, Germany. *Continental Shelf Research*, 18, 1715-1739.
- WHIPP, E. AND HORNE, D.A., 1976: Digitising of Side-scan Sonar Signals. *Ultrasonics*, September, 201-204.
- WHITE, D. J., 1971: Bo'Sun, a Multibeam Sonar for Search and Survey, 3rd Annual Offshore Technology Conference, April 19-21, Houston, Paper 1457.

- WIENBERG, C. AND BARTHOLOMÄ, A., 2005: Acoustic Seabed Classification in a Coastal Environment (Outer Weser Estuary, German Bight) - a New Approach to Monitor Dredging and Dredge Spoil Disposal. *Continental Shelf Research*, 25, 1143-1156.
- WILCOX, T.E. AND FLETCHER, B., 2003: High Frequency Side Scan Sonar for Target Reacquisition and Identification. *Oceans 2003 Proceedings of IEEE*, 22-26 Sept., Vol.4, 1882-1887.
- WINN, K. AND WERNER, F., 1984: Ein Integriertes Akustisches Fernmeßsystem (IAFMS) zur Typisierung von Schichtfolgen im Meeresboden und Bestimmung ihrer Raumlage. *Berichte - Reports, Geol.-Paläont. Inst. Univ. Kiel*, 5, 132 pp.
- WOLANSKI, E., NGUYEN, N.H., LE, T.D., NGUYEN, H.N., NGUYEN, N.T., 1996: Fine-sediment Dynamics in the Mekong River Estuary, Vietnam. *Estuarine, Coastal and Shelf Science*, 43, 565-582.
- WORK, P.A., FEHRENBACHER, F., VOULGARIS, G., CHEN, J., 2003: Nearshore Dredging Impacts, Folly Island, SC, USA. *Proceedings of the International Conference on Coastal Sediments 2003*. CD-ROM Published by World Scientific Publishing Corp. and East Meets West Productions, Corpus Christi, Texas, USA. ISBN 981-238-422-7, 14 p.
- WRIGHT, L.D., 1995: *Morphodynamics of Inner Continental Shelves*. CRC Press, Boca Raton, 241 pp.
- WRIGHT, L.D., PRIOR, D.B., HOBBS, C.H., BYRNE, R.J., BOON, J.D., SCHAFFNER, L.C., GREEN, M.O., 1987: Spatial Variability of Bottom Types in the Lower Chesapeake Bay and Adjoining Estuaries and Inner Shelf. *Estuarine, Coastal and Shelf Science*, 24, 765-784.
- YALIN, M.S., 1963: An Expression for Bedload Transportation. *Journal of the Hydraulic Division, Proceedings Am. Soc. Civil Engineers*, 89(HY3), 221-250.
- YALIN, M.S., 1964: Geometrical Properties of Sand Waves, *Journal of the Hydraulic Division, Proceedings Am. Soc. Civil Engineers*, 90 (HY5), 105-119.
- YANG, C.S., 1986: Estimates of Sand Transport in the Oosterschelde Tidal Basin Using Current-velocity Measurements. *Marine Geology*, 72, 143-170.
- ZEILER, M., FIGGE, K., GRIEWATSCH, K., DIESING, M., SCHWARZER, K., 2004. Regenerierung von Materialentnahmestellen in Nord- und Ostsee, *Die Kueste*, 68, 67-98.

ABOUT THE AUTHOR

Adam Kubicki

Born on 11th December 1979 in Gdynia, Poland

Nationality: Polish



IX.1993 – V.1997 Waclaw Sierpinski High School No.6 in Gdynia, Poland
Graduated with A-level exams passed

X.1997 – I.2003 Marine Geography course at the University of Szczecin, Poland
Graduated with Master of Science (magister) degree
M.Sc. project: *“Three-dimensional topography model used in assessment of landscape attractiveness in the coastal zone between Dziwnowek and Pustkowo”* (in Polish)

X.2001 – IV.2003 Coastal Geosciences and Engineering course at
Christian Albrechts University of Kiel, Germany
Graduated with Master of Science degree
M.Sc. project *“Nearshore circulation systems and their role in coastal development in western Mecklenburg Bay”*

IV.2003 – VII.2006 PhD studies within the project Holocene Coastal Evolution, Sea-Level Fluctuations, Terrigenous Sedimentation and Sediment Dynamics on the Continental Shelf between the Mekong Delta and Nha Trang, SE Vietnam, financed by Deutsche Forschungsgemeinschaft (DFG)
Christian Albrechts University of Kiel, Germany